Reliability analysis of a steel fibre reinforced concrete tunnel lining

Afstudeercommissie:

Prof. drs. ir.	*J.K.*	*Vrijling*
Prof. ir.	*A.C.W.M.*	*Vrouwenvelder*
ir.	*K.J.*	*Bakker*
Dr. ir.	*R.A.*	*Vonk*
ir.	*K.*	*van Oosteren*

ing. M.G. Méndez Lorenzo
Faculteit der Civiele Techniek
Technische Universiteit Delft

All rights reserved. Use of disclosure of this data is subject to the restriction stated on the first page of this document.

All rights reserved. Use of disclosure of this data is subject to the restriction stated on the first page of this document.

Abstract

Space is a scarce commodity in the Netherlands. It is increasingly hard to realise new residences, office accommodations and traffic connections without putting too much of a burden on the (living) environment. Consequently, the utilisation of the subsoil can play an important role in this respect as it has potential for the construction of new infrastructure. For that reason the government, construction industry and science are working together in gaining expertise in underground works. The common tunnel driving technique consists of the building of the tunnel lining with prefab concrete ring segments in a discontinuous process. As this tunnel building method involves higher costs than the conventional 'cut and cover' method, recently the development of a new tunnel driving technique which is considered to be competitive with the conventional tunnel building methods has been started. A number of Dutch companies, united in ITM[1], are developing this new tunnel building method and the TBM[2] which is needed for the continuous building process through soft soil. The main difference with respect to the conventional driving method, is that the lining is continuous, made of Steel Fibre Reinforced Concrete (SFRC) and built by means of a continuous extrusion process. Furthermore, a specially designed TBM is needed to build the tunnel.

At the moment, there are no Dutch regulations giving criteria for the design of bored tunnels. These regulations are necessary to prove that the required safety and serviceability are guaranteed by the proposed design. The scope of the study presented in this report consists of a reliability analysis of a SFRC tunnel lining. This consists of the definition of the load and resistance factors that are considered necessary to make a design of a SFRC lining and the calculation of the failure probability of the tunnel in the ultimate limit state. The study carried out in this report is based on the ITM tunnel design case with a lining thickness of 0,40 m and a radius of 4,70 m.

The tunnel lining can fail by several mechanisms. The mechanism that is examined in this study, consists of the failure of the tunnel lining under strain of the soil stresses in the ultimate limit state. The analysis is executed with a level II probabilistic design method. The basis of this method is that the parameters used in the structural design are not specified constants, but stochastic variables. The most advanced method of this level is the so-called Approximate Full Distribution Approach (AFDA). This method is used for the reliability analysis executed in this report.

First of all, the reliability of the tunnel design is approached with a linear calculation model, i.e. with the analytical Duddeck model. The safety requirements are only met in some of the considered cases. The failure probability is the largest in case of deep clay profiles. In case of a lining of concrete without tensile strength, none of the reference cases meets the requirements. Addition of steel fibres gives a considerable increase of the safety. The model factor of the bending moments, the coefficient of lateral earth pressure, the soil stiffness and the compressive concrete strength have the largest impact on the cross-section forces.
The most remarkable conclusion drawn from the linear reliability analysis, is that the safety requirements are on the whole better met in case of more flexible and thinner linings. As this conclusion does not meet the expectations and as the use of a (simple) linear model has a real benefit, the impact of non-linear effects on the cross-section forces is examined in order to determine whether the assumption of linearity is likely to be acceptable within the limitations of the non-linear tunnel analysis. The non-linear elastic effects which have to be taken into account in a tunnel design are the plasticity of the soil, and the geometrical- and physical non-linearity. In this report, a study is carried out into the influence of the geometrical- and physical non-linear effects in tunnel tubes.

[1] ITM = Industrial Tunnel building Method
[2] TBM= Tunnel Boring Machine

All rights reserved. Use of disclosure of this data is subject to the restriction stated on the first page of this document.

The geometrical non-linear effect is examined because insufficient knowledge is available on the effects due to deformations of the tunnel-construction. These effects can influence the total mechanical behaviour of the lining. First a study of existing literature and a calculation of the geometrical non-linear effect according to this literature are carried out. Next, a calculation of the cross-section forces including the geometrical non-linear effect is executed for the ITM-tunnel lining. The results of both methods have been compared with each other. They showed a close resemblance. The conclusion drawn from this analysis is that the second order bending moments increase with approximately 10% in the short term and with 15% in the long term with respect to the bending moments according to the linear theory (i.e. in case of a tunnel radius of 4,70m). In case of slender constructions, the geometrical non-linear effect increases considerably.
The physical non-linear effect is caused by crack formation. When the lining cracks, the lining stiffness decreases and consequently the lining attracts smaller loads. This means that the physical non-linearity causes a contrary effect with regard to the geometrical non-linearity as it causes a decrease of the bending moments with decreasing lining thickness.
In this report, the physical non-linearity is only examined qualitatively by considering only one of the four reference cases presented in this report. The purpose is to give an indication of which of both the non-linear effects governs over the other. The physical non-linear effect causes a larger deviation of the linear bending moments than the geometrical non-linear effect, specially in case of larger loads. In case of slender tunnel linings, however, the geometrical non-linear effect starts governing the physical non-linear effect. The hoop forces are hardly influenced by the non-linear effects.
As the physical non-linear effect is only calculated for one reference case, the non-linear reliability analysis is also executed for only one case. By taking into account the non-linear effects, the safety of the lining results to be larger than the safety calculated with the linear model.
An important conclusion drawn from the non-linear reliability analysis is that the safety decreases with decreasing lining thickness. The latter refutes the conclusion drawn at the linear reliability analysis that the safety increases with decreasing lining thickness. Moreover, from the non-linear reliability analysis follows that it is not safe to use the (linear) analytical Duddeck method for the design of slender constructions.
The probabilistic influence coefficients α_{AFDA} computed with the non-linear AFDA calculation and which are needed for the computation of the safety factors, show a large resemblance with those calculated with the linear AFDA calculation. Consequently, the results of the linear AFDA calculation are used for the definition of the safety factors, as with the linear analysis all the reference cases have been examined.
The definition of the (partial) safety factors in case of soil retaining constructions, like tunnels, is rather difficult. The parameters of the calculation have to be divided into load- and resistance parameters in order to define the partial safety factors. The latter, however, is not unambiguous in case of soil retaining constructions. Dependent on the situation, certain parameters can have a contradictory effect with respect to the resistance of the construction and with respect to the loads. Consequently, it is not unambiguous to define an overall safety factor. The strategy has been to define a partial safety factor for each parameter used in the calculation of the lining. The calculated safety factors are small with values between 1,0 and 1,3. The higher factors correspond to the most uncertain parameters. Although the definition of an overall safety factor γ is not unambiguous, γ has been determined for the ITM nominal design case in order to able to make a comparison with the building codes. The calculated γ = 1,8 corresponds with the value given in the building codes.
In general, it can be concluded that the examination of the safety of a tunnel lining is very extensive and that still a lot of work is left to be done.

All rights reserved. Use of disclosure of this data is subject to the restriction stated on the first page of this document.

Preface

From November 1997 until May 1998, I have worked on this project to finish my study of civil engineering at the university of Delft.
The project consists of a reliability analysis of a steel fibre reinforced concrete lining as well as of an examination of the impact of non-linear effects on the mechanical behaviour of the lining.

It took me some time to find this project, nevertheless I worked on it with a lot of pleasure and I consider it as a very instructive part of my study.

By this way, I want to thank everybody who has assisted and advised me during the last six months.
Last but not least, I want to thank ITM for offering me the opportunity to do this study.

Rotterdam / Delft, may 1998

Maria Méndez Lorenzo

All rights reserved. Use of disclosure of this data is subject to the restriction stated on the first page of this document.

All rights reserved. Use of disclosure of this data is subject to the restriction stated on the first page of this document.

Contents

All rights reserved. Use of disclosure of this data is subject to the restriction stated on the first page of this document.

All rights reserved. Use of disclosure of this data is subject to the restriction stated on the first page of this document.

All rights reserved. Use of disclosure of this data is subject to the restriction stated on the first page of this document.

1. Introduction

In this chapter the problem definition and the scope of the study are described. Boundary conditions and starting points are summarised. The chapter is finished with a description of the structure of the report.

1.1 General

Space is a scarce commodity in the Netherlands. It is increasingly hard to realise new residences, office accommodations and traffic connections without putting too much of a burden on the environment. Consequently the utilisation of the subsoil could play an important role in this respect as it definitely has potential for the construction of new infrastructure. For that reason the government, construction industry and science are working together in gaining expertise in underground works.

With respect to tunnelling, several techniques can be distinguished:
- the so called 'cut and cover' method, i.e. the building of a tunnel in an open building pit,
- tunnel building method by means of sinking tunnel elements,
- tunnel driving technique.

The option to drive tunnels in the Netherlands has never been considered seriously until a few years ago due to the high groundwater level, the soft soil and the high costs involved. The available tunnel driving technique consists of the building of the lining with prefab concrete ring segments in a discontinuous building process. This tunnel building method involves higher costs than the traditional methods. That is why a few years ago the development of a new tunnel driving technique has been started. This method ought to be competitive with the traditional tunnel building methods. A number of Dutch companies, united in ITM[3], are developing the tunnel building method and the TBM[4], which is needed for the continuous building process. The lining is made of extruded steel fibre concrete.

At the moment there are no Dutch regulations giving a complete strategy for the design of bored tunnels. These regulations are necessary to prove that the required safety and serviceability are guaranteed by the proposed design.

The scope of this study is to determine the load and resistance factors needed to make a design of a Steel fibre Reinforced Concrete (SFRC) lining and to calculate the failure probability of the tunnel. Both will be calculated with a probabilistic analysis.

1.2 Problem definition

At the computation of the ITM tunnel, safety factors (material and load factors) have to be used to cover uncertainties in the design of the concrete lining, while at the moment there are no regulations specifying these safety factors. Furthermore there is a need to determine the safety of the tunnel in terms of a failure probability.

1.3 Scope

- Calculation of the failure probability of the cross-section of the tunnel lining for the load case combination of bending moment and hoop force (final phase).
- Definition of the safety factors (load- and resistance factors) for the calculation of an extruded steel fibre concrete lining in soft soil. These factors have to be determined for the final phase.

[3] Industrial Tunnel building Method (ITM)
[4] Tunnel Boring Machine (TBM)

All rights reserved. Use of disclosure of this data is subject to the restriction stated on the first page of this document.

1.4 Boundary conditions and starting points

1.4.1 Boundary conditions

Geometry of the tunnel (nominal case)

- coverage of the tunnel — 1 x tunnel diameter (shallow tunnel); 2 x tunnel diameter (deep tunnel)
- depth of the tunnel-axis — 22.5 m (deep tunnel), 13.5 m (shallow tunnel)
- length — 6.00 km
- distance between joints — 10.0 m
- internal diameter of the tunnel — 9.00 m
- thickness of the lining — 0.40 m
- radius — 4.70 m
- moment of inertia — 0.0053 m^4/m (= 1/12 . b . d^3_{lining})
- cross-sectional area of the lining — 0.40 m^2/m
- section modulus — 0.0266 m^3/m (= 1/6 . b . d^2_{lining})

Soil parameters

parameters		clay profile	sand profile
modulus of elasticity: E_g	[MPa]	4	25
dry volume weight: γ_{dry}	[kN/m^3]	16	18
wet volume weight: γ_{wet}	[kN/m^3]	16	20
angle of internal friction: φ	[^{0}]	17,5	32,5
coefficient of lateral effective pressure: $K_0 = 1 - \sin\varphi$	[-]	0,7	0,46
cohesion: c	[kPa]	5	-
bedding modulus: Kr shallow profile / deep profile	[kN/m]	20000 / 30000	110000 / 120000
Poisson's ratio: ν	[-]	0,3	0,3

table 1.1: soil parameters

remarks:

- the modulus of elasticity E_{oed} according to the oedometertest: $E_{oed} = \frac{(1-\upsilon)}{(1+\upsilon)\cdot(1-2\upsilon)} \cdot E_g$

  $E_{oed,\ clay}$ = 5.38 MPa ; $E_{oed,\ sand}$ = 33.65 Mpa

The margin in which the Dutch soil properties vary is to such an extent that it is necessary to limit the quantity of geotechnical profiles to make a lining design. In figure 1.1 the geotechnical profiles which cover the Dutch soil conditions are defined.

All rights reserved. Use of disclosure of this data is subject to the restriction stated on the first page of this document.

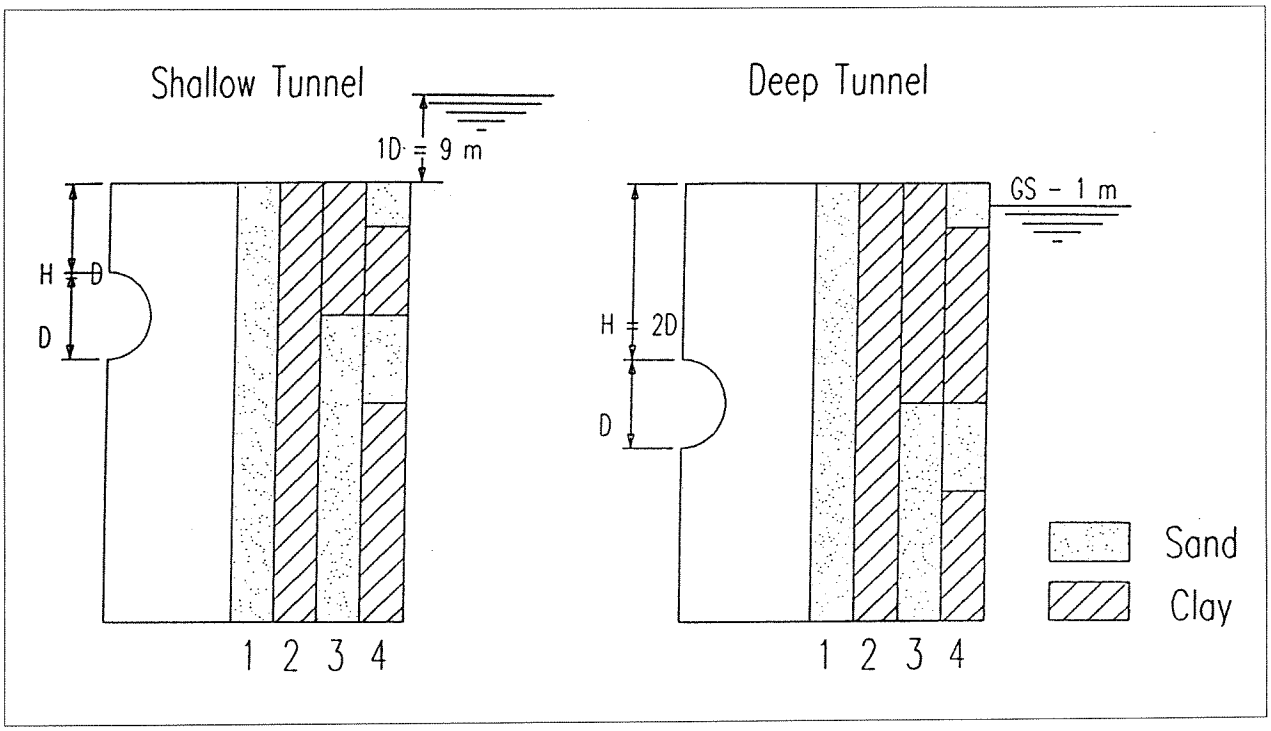

figure 1.1: geotechnical profiles

Concrete parameters

The applied steel fibre reinforced concrete has the following properties:

- concrete strength class: B15 (during extrusion) - B45,
- concrete strength class at the removal of the formwork: B25,
- the concrete is uncracked,
- amount of steel fibres in the lining: 50 kg/m^3,
- the concrete characteristics are based on the German regulations 'Merkblatt Bemessungsgrundlagen fur Stahlfaserbeton im Tunnelbau' [lit,2].

Calculations

- the boundary conditions of the calculation methods are presented in paragraph 6.3;
- the boundary conditions of the probabilistic analysis are presented in paragraph 4.4.2.

1.4.2 Starting points

- The soil is assumed to be elastic and homogenous.
- The properties of steel fibre concrete are determined from literature.
- The calculations are based on a single tunnel tube.
- Dynamic loads, variable actions and accidental loads are not taken into account.
- The reliability analysis is only executed for the cross-section of the tunnel in the final stage.

All rights reserved. Use of disclosure of this data is subject to the restriction stated on the first page of this document.

1.5 Structure of the report

This report consists of the following parts:

Introduction
Chapter 1 gives an introduction to the study executed in this report by means of a definition of the problem and a description of the scope of the study, the boundary conditions and the starting points.

Literature
The second part consists of chapters 2 to 6. In this part of the report a general description is given of topics which are needed in this study, i.e. a description of the available tunnel driving techniques, a review of the properties of steel fibre reinforced concrete and the definition of the safety factors and the failure probability. In chapter 6, the resistance and the strength of the tunnel lining are defined. Furthermore, a description is given of the available methods for the calculation of a tunnel lining.

Reliability analysis (linear approach)
The third part consists of chapter 7. A probabilistic analysis is executed based on a linear calculation model. The results of the analysis only partly meet the safety requirements. Consequently, it is decided to consider the impact of the non-linear effects on the results.

Analytical part
The fourth part consists of chapter 8 to 10. In chapter 8, a general description is given of the non-linear effects which play a part in the behaviour of the tunnel lining. Two of the non-linear effects are examined more thoroughly, i.e. the geometrical and the physical non-linearity. In chapter 9, the geometrical non-linear effect is determined according to literature and by means of a geometrical non-linear computation of the ITM tunnel lining. The geometrical non-linear effect resulted to be of such a magnitude that it can not be neglected, specially when slender constructions and the long term effect (creep of the concrete) are taken into account. In chapter 10, the physical non-linearity is examined in order to give an indication of the impact of this effect with regard to the geometrical non-linear effect. In general, it could be concluded that the impact of the physical non-linearity on the cross-section forces is larger than the impact of the geometrical non-linearity. However, in case of slender constructions or large cracks the effect of the geometrical non-linearity increases considerably with respect to the physical non-linearity.

Reliability analysis (non-linear approach)
The fifth part consists of chapter 11. A probabilistic analysis is executed taking into account the geometrical and the physical non-linearity. Considering the scope of this study, only one situation is considered, i.e. the geotechnical profile deep1 and a tunnel with a lining thickness of 0,40m. By taking into account the non-linear effects in the analysis, the safety of the tunnel lining resulted to be larger than the safety calculated with the linear model (remark: this statement is only valid for the situation of a lining thickness of 0,40m and a load which belongs to a deep tunnel in sand).

Safety factors
The sixth part consists of chapter 12. In this chapter the safety factors are computed. As the probabilistic influence coefficients (α_{AFDA}) of the non-linear reliability analysis showed a close resemblance with those of the linear reliability analysis, the computation of the safety factors is executed with the results of the linear analysis.

Finishing part
The report is finished with chapter 13. In this chapter conclusions are drawn and recommendations for further research are given.

All rights reserved. Use of disclosure of this data is subject to the restriction stated on the first page of this document.

2. Tunnel driving techniques

The most common tunnel driving techniques are described in this chapter, i.e. the conventional tunnel building method and the ECL[5] building method.

2.1 Introduction

Tunnel driving enables underground construction which causes no damage or nuisance above ground. Before starting the drive activities, a shaft has to be built at the beginning of the alignment of the future tunnel. The excavation is started in that shaft. Another shaft is built at the end of the alignment, where the TBM will arrive after finishing the construction of the tunnel. In the Netherlands these shafts are usually building pits, although they also are built as open or pneumatic caissons. The shafts serve as the site where several activities take place, like the assembly and dismantling of the TBM, the discharge of the excavated soil to the ground level, the supply of the tunnel lining segments, the supply and discharge of materials and equipment and the access of personnel.
In general, two tunnel driving techniques can be distinguished. Both the techniques use a specifically designed TBM. These techniques are described in the following paragraphs.

2.2 Conventional tunnel building method

The construction of the tunnel takes place in a steel tube, the so-called shield. This tunnelling shield consists of a cylinder with a cutting wheel in front and the completed tunnel in the back. The shield seals off the driven part to prevent ground and water form entering the tunnel. The tunnel rings can then be erected within the shield. One of the possible driving techniques is the so-called slurry shield method. The cutting wheel loosens the ground, after which this is mixed with a bentonite suspension, forming a slurry. The suspension ensures a stable cutting face which can then be excavated. In addition, the suspension makes it possible to pump out the excavated ground. The space between the ring segments and the soil, the so called tail void, is filled with grout simultaneously with the movement of the shield. The tail void arises because the diameter of the shield is larger than the diameter of the tunnel lining. Each time the TBM has driven a part, the tunnel lining is erected as a circle of prefabricated concrete segments. The TBM uses the ring as a 'push-off' to start driving the next part.
The bentonite suspension is not only used to ensure a stable cutting face, it is also the medium by which the excavated ground can be removed from the excavation chamber. In this chamber, situated behind the cutting wheel, a combination of ground and bentonite suspension form a slurry which can be pumped to the surface. There, the slurry is separated into a bentonite suspension and ground with the aid of cyclones and filters. Subsequently, the recycled bentonite suspension is pumped back to the cutting face, while the ground is transferred to a disposal area.

The process of excavation and tunnel construction is discontinuous; after driving a certain distance the excavation is stopped and the tunnel lining is built. After finishing the construction of one ring, the excavation is started again.

[5]ECL = Extruded Concrete Lining

All rights reserved. Use of disclosure of this data is subject to the restriction stated on the first page of this document.

2.3 Extruded Concrete Lining (ECL)

The main differences between the ECL building method and the conventional building method, are the building process of the tunnel lining and the TBM which has to be specifically designed. To build the tunnel lining, concrete is extruded[6] between the inner formwork and the soil (figure 2.1). The extrusion takes place by means of several injection points. These are regularly distributed over the cross-section as the concrete has to be distributed homogeneously over the circular space.

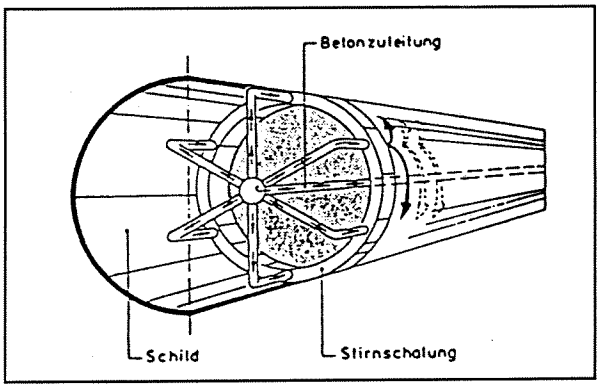

figure 2.1: supply of concrete by means of an extrusion process

The circular space, hatched in figure 2.2, is bounded by soil at the outside and at the inside by a removable steel formwork (Umsetzbare Stahlschalung).

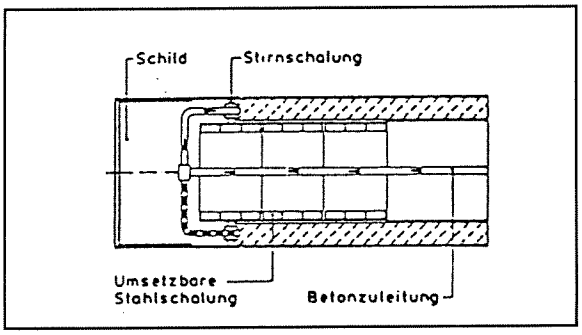

figure 2.2: schematic representation of the ECL-method

The steel formwork consists of steel rings which are composed of segments to enable the assembly and the removal of the formwork. The total length of the formwork depends on the hardening speed of the concrete and on the maximum driving speed. The shield thrusts itself forward against this inner formwork. The rest of the driving process is similar to the conventional technique. A cutting wheel is used to loosen the ground while the cutting face is stabilised by means of a bentonite suspension. The removal and separation of the slurry into a bentonite suspension and ground takes place in the same way as at the conventional technique.

[6] to extrude = to pump concrete under high pressure in a closed space

All rights reserved. Use of disclosure of this data is subject to the restriction stated on the first page of this document.

3. Industrial Tunnel building Method (ITM) project

This chapter deals with the purpose, the planning and the characteristics of the ITM project

3.1 Purpose

The purpose of the ITM project is the development of both a tunnel building method and a Tunnel Boring Machine (TBM) that are competitive with the conventional ones.
An important characteristic of this new tunnel building method is the lining that is built with extruded Steel fibre Reinforced Concrete (SFRC). The industrialisation of the method is based on simultaneous driving and construction of the tunnel in a continuous process.

3.2 The ITM joint venture

The ITM joint venture is formed by seven Dutch and one German company that have decided in 1994 to collaborate in the development of the Industrial Tunnel building Method:
- Heerema,
- IHC Holland N.V.,
- Koninklijke Begemann Groep N.V.,
- Fokker Space & Systems B.V.,
- Fugro Ingenieursbureau B.V.,
- Hoogovens Staalverwerking en Handel B.V. (HSH),
- Mebin B.V.,
- Wirth Maschinen- und Bohrgeräte-Fabrik GmbH.

3.3 Planning

The development of the ITM is divided into the following five phases:
phase A: feasibility study
phase B: concept design and testing
phase C: engineering: design of the TBM
phase D: construction of the TBM
phase E: assembly of the TBM

At the moment the project is in phase B.

3.4 Characteristics of the ITM

The characteristics of the ITM are summarised as follows:

- **Tunnel lining**
  - the lining is continuous in cross-sectional direction, this in contrast with the traditional segmented lining;
  - the lining is built by means of an extrusion process;
  - the lining is made of SFRC;
  - the lining is divided in sections in the longitudinal direction by means of mechanical[7] joints.

[7] mechanical joints: the term mechanical refers to the mechanical function of the joints, i.e. the prevention of crack formation and the guaranty of watertightness.

All rights reserved. Use of disclosure of this data is subject to the restriction stated on the first page of this document.

- **Joints**
  Crack formation is prevented by means of mechanical joints in longitudinal direction. These joints enable the concrete sections to make little displacements without cracking. Reduction of crack formation is important as it determines the watertightness of the tunnel lining.
- **Continuity**
  The building process of the conventional drilling methods is not continuous; drilling and building are alternated. At the ITM, the drilling- and building process takes place simultaneously; the process is continuous. The result is a high and effective construction speed.
- The method is optimised in such a way that the lining can be realised in soft soils.

In figure 3.1, the base concept of the TBM is schematised.

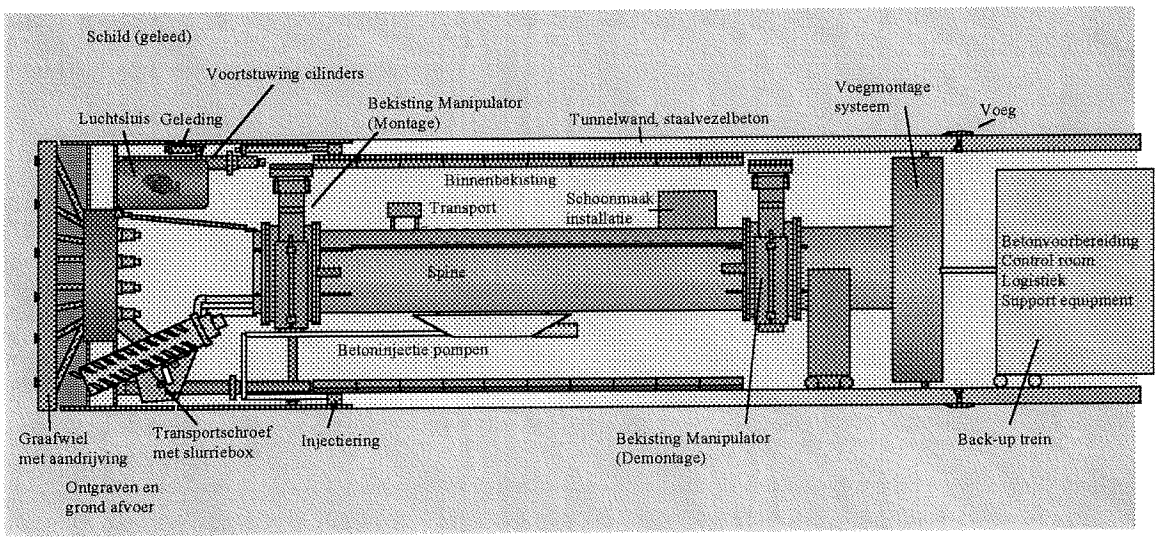

Copyright © ITM CV 1997

figure 3.1: tunnel lining production

All rights reserved. Use of disclosure of this data is subject to the restriction stated on the first page of this document.

4. Probabilistic analysis (general)

A probabilistic analysis is based on a statistical evaluation of experimental data or field observations. In case of lack of the latter, assumptions based on experience should be made. In this chapter a definition is given of safety and reliability and the possible limit states of a tunnel lining. A general review is given of probabilistic design methods. The procedure of the computation of the failure probability and the safety factors is described. Finally an abstract is given of the safety factors of the present building codes.

4.1 General

At the moment there are no Dutch regulations giving a complete strategy for the design of an extruded steel fibre concrete lining. These regulations are necessary to prove that the required safety and serviceability are guaranteed by the proposed design.
In general, (partial) safety factors are intended to take account of:

- unfavourable deviations from the representative values;
- inaccuracies in the action models and structural models;
- inaccuracies in the conversion factors.

In principle there are two ways to determine numerical values for (partial) safety factors:

1. on the basis of calibration to a long and successful history of building tradition;
2. on the basis of the statistical evaluation of experimental data and field observations; this should be done within the framework of a probabilistic reliability theory.

The value of the (partial) safety factors should depend on the degree of uncertainty in the actions, resistances, geometrical quantities and models, on the type of construction works and on the type of limit state.

4.2 Probabilistic design-methods

Safety is defined as the resistance or strength (R_Z) being larger than the loads (S): $R_Z > S$. To assure the fulfilment of this criterion a safety margin is introduced between the expected load and the pursued strength. There are four philosophies or design methods regarding the way of introducing a safety margin in the design [lit,14]:

1. level 0: deterministic,
2. level I: semi-probabilistic,
3. level II: quasi-probabilistic,
4. level III: probabilistic.

The first strategy (level 0) was common use up to 1990. Since 1990 many countries in Europe, including the Netherlands, have started to change their regulations by introducing a strategy based on design values for loads and material properties (level I). The design values in this strategy are derived from representative or characteristic values. The loads or the effects of the loads are multiplied with the partial factors for actions and the material properties are divided by the partial factors for the material properties. These partial factors should be determined in such a way, by means of a probabilistic analysis, that their application guarantees a maximum probability of failure equal to $\Phi(-\beta)$. Only at level II and III, the safety of using these factors is determined explicitly by means of a failure probability.

All rights reserved. Use of disclosure of this data is subject to the restriction stated on the first page of this document.

Level 0: deterministic design method
In this case 'safe' values are chosen for the basic variables causing the load. Usually the representative[8] or the characteristic[9] values of the strength parameters are used to determine the strength. The concept characteristic value is introduced because of the lack of statistical information. The safety margin is guaranteed by a safety-coefficient γ based on engineering experience.

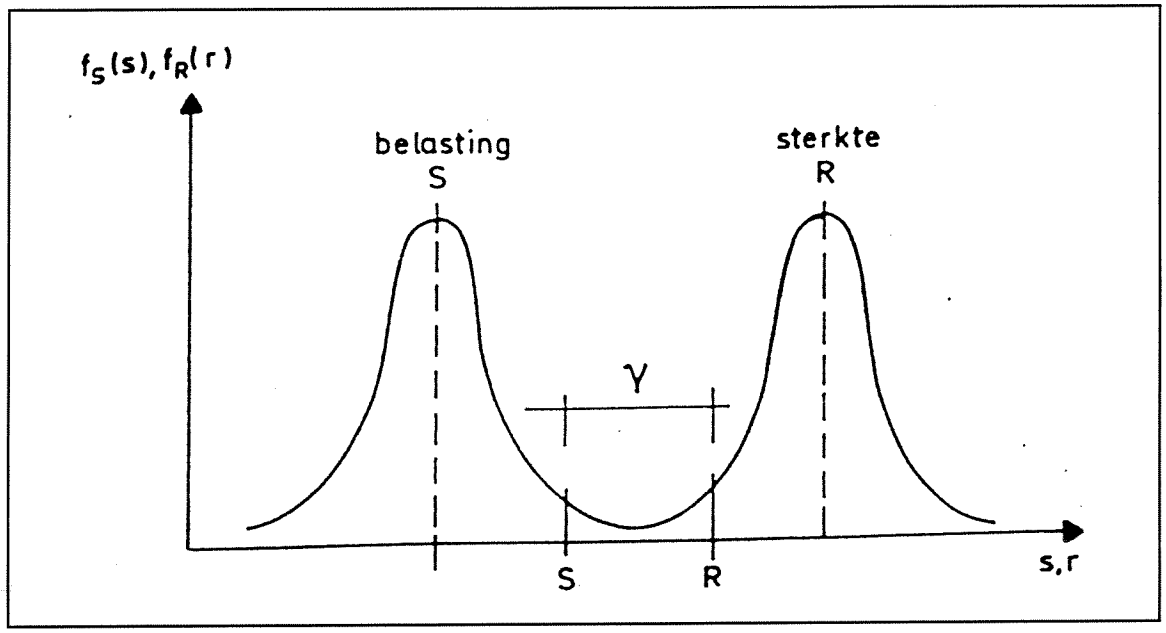

figure 4.1: dimensioning of a construction according to the Dutch regulations of 1974

Level I: semi-probabilistic design method
The representative or the characteristic values of the strength- and the load-parameters are used. The safety margin is guaranteed by partial safety factors:
$\gamma_S \cdot S \leq R_Z / \gamma_R$

with:
γ_S = partial factor for loads (includes model uncertainties and dimensional variations),
γ_R = partial factor for a material property (or resistance factor),
S = effect of an action (load),
R_Z = resistance or strength.

Level II: quasi-probabilistic design method
The basis of this method is that the parameters used in the structural design are not specified constants, but stochastic[10] variables. The exact magnitudes of this variables are not known with certainty in the design state. The most advanced method of this level is the Approximate Full Distribution Approach (AFDA) (see paragraph 4.4.2).
In the actual Dutch regulations [lit,6] a level II analysis is applied to determine the partial factors [lit,14].

[8] representative value = prescribed basis value for a load or material property
[9] characteristic value = an upper value with an intended probability of not being exceeded or a lower value with an intended probability of not falling below. In [lit, 27] the characteristic value for a variable load is defined as the load with a return period of fifty years and for the strength as the 5% exceedance value.
[10] stochastic variable = non-predictable variable

All rights reserved. Use of disclosure of this data is subject to the restriction stated on the first page of this document.

Level III: probabilistic design method
This is the most advanced design method. In this method all basic variables are specified by probability density functions (p.d.f.'s). With the help of theoretical models, p.d.f.'s of the strength and of the load are derived. These two p.d.f.'s form the basis in determining the failure probability of the mechanism. By checking this failure probability against the allowable failure probability of the total system, one can determine whether or not the safety is sufficient:

$P(S \leq R_Z) \leq \Phi(-\beta)$

with:
$P(\,)$ = probability,
$\Phi(\,)$ = distribution function of the normal distribution,
β = reliability index.

4.3 Limit States, reference period and safety class

The fundamental reliability requirement can be defined as follows:

The tunnel lining is not allowed to exceed:
- the defined ultimate or serviceability limit states,
- during the proposed reference period,
- with a defined amount of reliability.

Limit states, a reference period and reliability levels shall have to be specified in order to meet this requirement. Afterwards, the abstract failure probabilities have to be translated into a set of specified load cases in which the tunnel lining is not allowed to exceed the proposed limit states. This translation has to take into account the applied calculation models and their accuracy.

Limit states
Limit states are states beyond which a structure no longer satisfies the design performance requirements. In order to prove that the required safety and serviceability are met, limit states are formulated and analysed. The following limit states are distinguished:
- ultimate limit state: a state associated with collapse or other forms of structural failure.
- serviceability limit state: a state beyond which specified service requirements for a structure are no longer met.

A structure has a number of limit states equal to the number of failure mechanisms. In table 4.1, the limit states for the execution and final phase of the tunnel lining are summarised. These are only the most important limit states with respect to the calculation of the lining.

	execution phase	**final phase**
ultimate limit state	• structural failure of the lining in ring and longitudinal direction	• structural failure of the lining in ring and longitudinal direction during normal use • structural failure of the lining in ring and longitudinal direction due to accidents
serviceability limit state	• deformation of the lining in ring and longitudinal direction	• cracking of the lining in ring and longitudinal direction (consequences: corrosion, leakage) • deformations of the lining in ring and longitudinal direction

table 4.1 [lit,5]

All rights reserved. Use of disclosure of this data is subject to the restriction stated on the first page of this document.

Reference period
The reference period of the final phase, or in other words, the intended life of the tunnel shall be 100 years (for comparison: [lit,14], 5.2.1 gives a reference period of 50 years for buildings).
The reference period of the execution phase is taken equal to the duration of this phase with a minimum of 1 year ([lit,14], 5.2.2).

Safety class
The tunnel shall meet the requirements of safety class 3 of the present Dutch building codes ([lit,14], art. 5.3.4. and [lit,27], art. 5.1). Structures of safety class 3 are structures of which failure results in a high risk of loss of human lives or high costs. For safety class 3 a reliability index β of 3,6 for the ultimate limit state is prescribed ([lit,27], art. 5.1). Although fully equivalent to the failure probability itself, the use of the reliability index emphasises the formal and notional nature of the reliability analysis. The relationship between β and the probability of failure is presented in table 4.2:
a reliability index β = 3,6 corresponds with a probability of failure of approximately 10^{-4}.

P= $\phi(-\beta)$	10^{-1}	10^{-2}	10^{-3}	10^{-4}	10^{-5}	10^{-6}	10^{-7}
β	1,3	2,3	3,1	3,6	4,2	4,7	5,2

table 4.2: relation between the reliability index β and the probability of failure P = $\phi(-\beta)$ (valid for a *normal* distribution)

4.4 Calculation of the failure probability (general)

4.4.1 Definition of the reliability function

The failure of a construction is described by means of a reliability function Z which gives the relation between the load (S) and the resistance (R_Z) (see appendix 5):
$Z = R_Z - S$

$Z = Z(X_1, X_2,...,X_n)$ and X = stochastic variable
$Z > 0$: safe area
$Z = 0$: limit state
$Z < 0$: unsafe area, the construction fails
A reliability function has to be determined for each load case and limit state.

The check of reliability is based on the test of:
$P(Z(X_{d1}, X_{d2},...,X_{dn}) < 0) <$ acceptable failure probability, i.e. the chance that a limit state is exceeded.
This can be translated into the following equivalent requirement:
$Z(X_{d1}, X_{d2},...,X_{dn}) > 0$
with:
X_{di} = design point value of the variable X_i
The design point value is determined with a probabilistic analysis at level II (paragraph 4.4.2).

All rights reserved. Use of disclosure of this data is subject to the restriction stated on the first page of this document.

4.4.2 Approximate Full Distribution Approach (AFDA)(level II, class 3)

AFDA is a probabilistic analysis that operates at level II, class 3 (paragraph 4.2). Class 3 indicates that the distribution function of each basic variable of Z is taken into account.
With AFDA, failure probabilities are calculated based on Z. When Z is a non-linear function, AFDA replaces the curved Z-surface by a linearised surface. Z is linearised by means of the development of Taylor-series (see appendix 6) around the point of the failure boundary Z = 0 with the highest probability of occurrence. This point is the so-called design point and is defined as:

$X^*_i = \mu_i - \alpha_{AFDA,i}\ \beta\ \sigma_i$ in case of a normal distribution
$X^*_i = \mu_i\ .\ \exp(-\alpha_{AFDA,i}\ \beta\ V_i)$ in case of a lognormal distribution

with:
X^*_i = design point,
μ_i = mean value of X_i,
$\alpha_{AFDA,i}$ = probabilistic influence coefficient of X_i, which represents the impact of the variable X_i on the uncertainty of the whole failure mechanism ($\alpha_{AFDA,i} = f(\sigma_i)$),
β = reliability coefficient = μ_Z / σ_Z ,
σ_i = standard deviation of X_i,
V_i = variation coefficient: $V_i = \mu_i / \sigma_i$.

The correct failure probability is found by means of an iteration process (table 4.3) at which the following requirements have to be met:
- the design point values X_i^* have to be stable and
- the reliability index β has to be stable

so that:

$Z(X^*_1, X^*_2, ..., X^*_N) = 0$

In table 4.3 the iteration process of AFDA is given.

1. estimate a value for β
2. assume $X^*_i = \mu_{Xi}$ for all i
3. calculate $\delta Z/\delta Z(X_i)$ for all i in $X = X^*_i$ (vector)
4. calculate $\alpha_{AFDA,i}$ for all i
5. calculate the new values of X^*_i (vector)
6. repeat step 3 to 5 until a stable value for X^*_i is found
7. calculate $Z = (X^*_1, X^*_2, ..., X^*_N)$
8. adapt β, if necessary, so that Z = 0 and repeat step 3 to 5
9. determine the failure probability with $P_b = 1 - \phi_N(-\beta)$

table 4.3: iteration process of AFDA

In words

AFDA determines, by means of the iteration procedure of table 4.3, the failure probability in the point of the failure boundary Z = 0 with the highest probability of occurrence. The sensitivity of the solution Z=0 for a small variation in the magnitude of the variables X_i, is established by means of partial derivation $\delta Z/\delta Z(X_i)$ (point 3 of table 4.3). The amount of uncertainty of X_i is weighed by means of its standard deviation. The result is a contribution of each X_i to the total uncertainty, expressed by means of a coefficient $\alpha_{AFDA,i}$ (point 4 of table 4.3). When a stable value is found for the design point X^*_i, the mean value μ_Z and the standard deviation σ_Z are determined; with these parameters the reliability coefficient can be computed: $\beta = \mu_Z / \sigma_Z$. AFDA iterates until a stable value for β is found. To each value of β corresponds a failure probability (table 4.2, valid for a normal distribution).

All rights reserved. Use of disclosure of this data is subject to the restriction stated on the first page of this document.

Boundary conditions of the AFDA calculation

- the AFDA calculation is executed with a Turbo Pascal program;
- a failure probability of 0 means that the failure probability is smaller than 2.9 E-39; Turbo Pascal considers all the values smaller than this to be equal to zero;
- the Z-function, the start-values, the mean values and the standard deviations of the variables are used as input of the calculation (see appendix 10);
- the start-values are the mean values of the variables;
- AFDA iterates (see table 4.3) until two conditions are met:
  - a stable design point X^*_i is found;
  - a stable reliability index β is found.

4.5 Safety factors

The following safety factors are distinguished:

- the partial safety factors:
  - load factor,
  - resistance factor,
- the overall safety factor.

Load factor

$$\gamma_s = \frac{S_d}{S_k} \tag{4.1}$$

$S_d = \mu_S - \alpha \cdot \beta \cdot \sigma_S$ **normal distribution**

$S_d = \mu_s \cdot \exp(-\alpha \cdot \beta \cdot V)$ **lognormal distribution**

$S_k = \mu_S + k \cdot \sigma_s$

Resistance factor (or material factor)

$$\gamma_R = \frac{R_k}{R_d} \tag{4.2}$$

$R_d = \mu_R - \alpha \cdot \beta \cdot \sigma_R$ **normal distribution**

$R_d = \mu_R \cdot \exp(-\alpha \cdot \beta \cdot V)$ **lognormal distribution**

$R_k = \mu_R - k \cdot \sigma_R$

with:

γ_S = load factor,
γ_R = resistance factor (or material factor),
S_d = design point value of the load,
R_d = design point value of the material property,
S_k = characteristic value of the load,
R_k = characteristic value of the material property,
μ_S = mean value of the load,
μ_R = mean value of the material property,

All rights reserved. Use of disclosure of this data is subject to the restriction stated on the first page of this document.

α = influence coefficient (negative value in case of a *load* factor and a positive value in case of a *resistance* factor; in the following this factor will be referred to as α_{AFDA}),
β = reliability index,
σ_S = standard deviation of the load,
σ_R = standard deviation of the material property,
k = coefficient = 1,64.

Overall safety factor

The basic requirement of the reliability analysis with partial safety coefficients is:

$$S_k \cdot \gamma_s \le \frac{R_k}{\gamma_R} \qquad (4.3)$$

$$S_k \cdot (\gamma_s \cdot \gamma_R) \le R_K$$

with:
$\gamma_S \cdot \gamma_R = \gamma$ = overall safety factor

$$\gamma_{s(X,X_2,\ldots,X_n)} = \frac{S_d\left(X_{1d}, X_{2d}, \ldots, X_{nd}\right)}{S_k\left(X_{1k}, X_{2k}, \ldots X_{nk}\right)}$$

$$\gamma_{R(X,X_2,\ldots,X_n)} = \frac{R_k\left(X_{1k}, X_{2k}, \ldots, X_{nk}\right)}{R_d\left(X_{1d}, X_{2d}, \ldots X_{nd}\right)}$$

X_i = basic parameter of the reliability function,
$S_d (X_i)$ = design value of the load parameter X_i,
$S_k (X_i)$ = characteristic value of the load parameter X_i,
$R_d (X_i)$ = design value of the material parameter X_i,
$R_k (X_i)$ = characteristic value of the material parameter X_i.

Procedure in behalf of the computation of the overall safety factors [lit,15]

1. Calculate the partial safety factors γ_S and γ_R of each basic variable with equations 4.1 and 4.2
2. Check if the following safety requirement is met:

$$Z\left\{\gamma_{s,i} \cdot S_{kar}, \frac{R_{kar,j}}{\gamma_j}\right\} \ge 0$$

3. Calculate the overall safety factor γ
   The eventual overall safety factor is calculated as the average of the overall safety factors of some reference cases. The weighing procedure is based on the frequency that a certain reference case takes place. In general, γ is determined in such a manner that:

$$\sum_{i=1}^{n} p_i \cdot \left\{\beta_i(\gamma) - \beta_i^t\right\}^2 \qquad \text{is minimum}$$

   with:
   p_i = weight factor,
   $\beta_i(\gamma)$= reliability index that belongs to the overall factor γ,
   β_i^t = target value of the reliability index.

All rights reserved. Use of disclosure of this data is subject to the restriction stated on the first page of this document.

4.5.1 Aspects to take into account at the definition of the safety factors

The safety factors have to be determined in such a way that the desired safety level is achieved. At the definition of these factors the following aspects have to be taken into account:

- the safety level which corresponds to the limit state;
- the sensitivity of the limit state for a certain parameter;
- standard deviations, uncertainties and inaccuracies;
- the kind of fluctuations in time and in space.

Safety levels

In most of the actual building codes the definition of the safety levels is based on the calibration of the reliability index β with existing design-methods based on a large experience. This procedure is not or partially possible in the case of bored tunnels in soft soil. Furthermore, the safety level or reliability index β_{target} has to depend on the consequences of exceedance of the considered limit state; the safety levels of the ultimate limit state are higher than those of the serviceability state:

- ultimate limit state: $\beta = 3...5$
- serviceability state: $\beta = 0...2$

Sensitivity

A sensitivity analysis should be performed to determine the impact of each input-parameter of the calculation model on the safety of the tunnel lining. In this way the parameters which cause a certain limit state can be determined. The impact of variations in the magnitude of the parameters on the calculation results is determined by using alternatively a higher and a lower value of the variables as input of the model. When the safety of the tunnel lining is barely influenced by a parameter, the design value of this parameter will approximate the mean value.
In paragraph 6.3.2, a sensitivity analysis is executed of the parameters of the calculation of the tunnel lining.

Uncertainties and standard deviations

The quantification of uncertainties is an amplification of the sensitivity analysis. A large sensitivity is only detrimental when it coincides with big uncertainty. Uncertainties can be determined at several levels; the uncertainty of a single input-parameter or that of a whole calculation model.
The uncertainty of a calculation model can be specified explicitly by taking into account the deviation between 'the results of the model' and 'the reality', with the so called modelfactor or model uncertainty. This modelfactor can be used as stochastic variable in the probabilistic analysis.

Time and spatial variation

The following types of uncertainties can be distinguished:

- Uncertainties in time with respect to variables that remain constant in time or variables that vary in time. The unfavourable values don't have to coincide with each other necessarily. This can give a reduction in the safety factors.
- Uncertainties in space with respect to variables that remain constant in space or variables that vary from place to place. Volume and scale effects might have to be taken into account. When failure of a section is equal to failure of the whole construction then the length of the construction has to be taken into account. This means that a longer tunnel will have a larger failure probability or with other words, the acceptable failure probability per section will be smaller for a longer tunnel. The latter is the so-called length-effect. In this report the length-effect is not taken into account, although it is very important. At the definition of the characteristic length, the impact of the variation of the decisive parameters on the failure probability of the longitudinal section has to be taken into account. In this report the failure probability is determined per meter length of the tunnel.

All rights reserved. Use of disclosure of this data is subject to the restriction stated on the first page of this document.

4.5.2 Design value

For each load case has to be demonstrated that the tunnel lining, with its specified material properties, does not exceed the relevant limit states when it is loaded by the design values of the loads.

Design value of a load
Multiplication of the representative value of the load by a load factor:

$$X_d = \gamma_s \cdot X_{rep} \tag{4.4}$$

Design value of a material property
Division of the representative value of a material property by a resistance factor:

$$X_d = \frac{X_{rep}}{\gamma_R} \tag{4.5}$$

with:
γ_s = load factor,
γ_R = resistance factor,
X_{rep} = representative value.

The representative value X_{rep} can be:
- a characteristic value,
- a nominal value (e.g. in the case of geometrical properties): in some cases this value is equal to the mean value.

4.5.3 Safety factors based on the present building codes (ultimate limit state)

In this paragraph the safety factors of the present building codes are given. The purpose is to give a review of the actual safety factors. These factors will be compared with the calculated ones for the ITM tunnel lining (chapter 12).

4.5.3.1 Final phase

Former Dutch building codes [lit, 40]
In the former Dutch building codes the following overall safety factor is prescribed for the failure of a concrete section:

load factor:
- for the most unfavourable combination of actions: $\gamma_S = 1.7$
- for a favourable combination of actions:
  favourable permanent actions: $\gamma_S = 1.2$
  other permanent actions: $\gamma_S = 1.5$
  variable actions: $\gamma_S = 1.6$

resistance factor:
In case significant compressive forces dominate the failure of the cross section an extra resistance factor has to be used: $\gamma_R = 1.18$

overall safety factor: $\gamma = 1.7 * 1.18 = 2.0$

All rights reserved. Use of disclosure of this data is subject to the restriction stated on the first page of this document.

German regulations [lit,2]
In the German regulations for the design of tunnels of SFRC, two overall load factors are given dependent on the ductility[11] of the failure mode:

overall safety factor:

- more or less ductile failure: $\gamma = 1.75$
- more or less brittle[12] failure: $\gamma = 2.10$

Brittle failure is found when compressive failure dominates the failure mode and ductile failure is found when tensile failure dominates the failure mode. In detail the overall safety factor is given in figure 4.2 as function of the maximum strain found when the cross section fails.

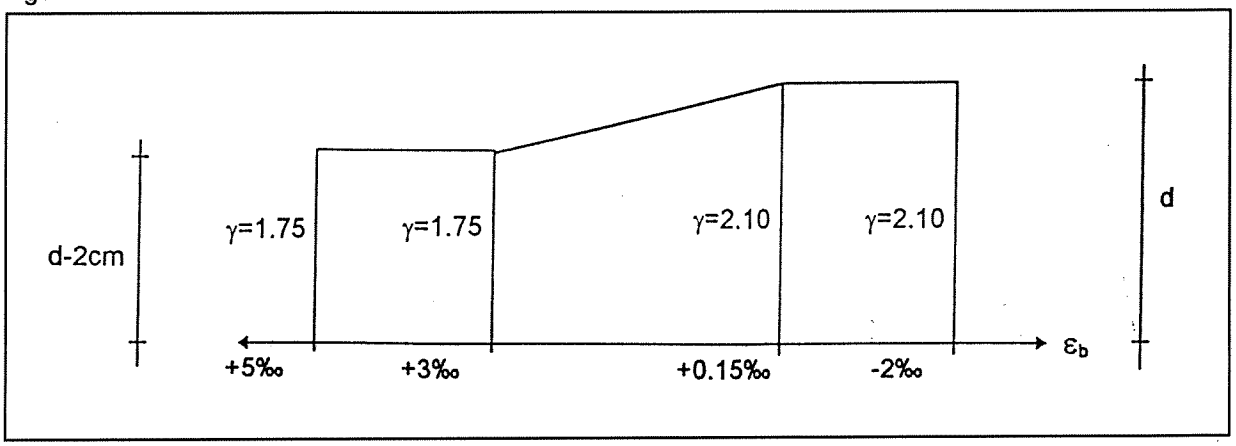

figure 4.2: overall safety factors as function of the maximum strain in the cross-section [lit,2]

Present Dutch tunnel design
In recent designs of conventional bored tunnels (2e-Heinenoord tunnel, Botlek tunnel, Sophia tunnel) [lit, 37, 38, 39] the following safety factors have been used:

- 2e-Heinenoord tunnel and Botlek tunnel:
  one overall safety factor is used, regardless the failure mode: $\gamma = 1.75$
- Sophia tunnel:
  more or less ductile failure: $\gamma = 1.75$
  more or less brittle failure: $\gamma = 2.10$

ITM design
The following remarks can be made about the applicability of the above mentioned overall load factors in the ITM design:

- The former Dutch building codes have not taken into account explicitly the applicability in a tunnel lining of SFRC. As mentioned above, in present Dutch bored tunnel design, the safety factors of the German regulations have been applied. Considering SFRC, the above mentioned overall safety factors are applicable under the condition that the concrete shows sufficient ductility and that overall collapse of the tunnel lining is caused by a ductile failure mode. For the ITM design, it is essential that the ductile character of the failure mode is shown explicitly.
- The German regulations seem to be directly applicable for Dutch circumstances. The regulations do not mention any limitations in soil conditions. This problem has to be encountered in the design calculations with the correct loads and boundary conditions.
- The safety factors used or prescribed for the present Dutch tunnel projects are applicable for the ITM design when it is shown that the failure mode of the ITM is ductile.

[11] ductility = the ability to absorb energy and thus to bear forces after crack formation. The antonym of ductility is brittleness.
[12] brittle = no bearing capacity is left after crack formation and consequently the construction collapses without warning. The antonym of brittleness is ductility.

All rights reserved. Use of disclosure of this data is subject to the restriction stated on the first page of this document.

The remarks above indicate that under the conditions:
- the ductility of the SFRC results in a ductile failure mode of the tunnel lining,
- great care is given to incorporating Dutch soil conditions in a conservative way in the design calculations,

the following overall safety factors may be applied for the ITM design:
γ = 1.75 in case of ductile failure of the cross section,
γ = 2.10 in case of brittle failure of the cross section.
In that case the same level of safety is achieved as guaranteed by the former Dutch building codes.

4.5.3.2 Execution phase

Former Dutch building codes [lit, 40]
In the former Dutch building codes the following overall safety factor is prescribed for the failure of a concrete section:

load factor:
- for the most unfavourable combination of actions: γ_S = 1.4
- for a favourable combination of actions:
  favourable permanent actions: γ_S = 1.1
  other permanent actions: γ_S = 1.3
  variable actions: γ_S = 1.4

This combination seems not to be relevant for a tunnel lining where the permanent actions dominate failure of the cross section.

resistance factor:
In case significant compressive forces dominate the failure of the cross section an extra resistance factor has to be used: γ_R = 1.18

overall safety factor: γ = 1.4 * 1.18 = 1.65

German regulations [lit,2]
In the German regulations for the design of tunnels of SFRC, two overall load factors are given dependent on the ductility of the failure mode:

overall safety factor:
- more or less ductile failure: γ = 2.10 / 1.15 = 1.8
- more or less brittle failure: γ = 1.75 / 1.15 = 1.5

Present Dutch tunnel design
Only for the Sophia tunnel [lit, 38] a safety factor for the construction is mentioned. The contract document states that the safety factor during construction should be equal to the safety factor for normal use: γ = 1.75 .

ITM design
For load cases during construction, regularly a lower safety factor can be used than for normal use because:
- consequences in terms of loss of human lives or money are smaller than in the final phase;
- repair can be an economic solution;
- the time span of execution is much smaller than the intended life span of the structure.

All rights reserved. Use of disclosure of this data is subject to the restriction stated on the first page of this document.

In case of the ECL, one has to be careful with the reduction of safety factors in the execution phase because:

- the loads are not better known or better controlled than in the final phase (this counts also for the special loading case of the ECL, where the loading caused by the soil is assumed to be equal to the hydrostatic concrete pressures);
- the structure is sensitive to deviations in loading, when compressive failure determines overall failure; this is possibly compensated by the fact that the lining is statically indeterminate;
- the consequences in terms of money can be significant;
- repair of serious damage may not be easy.

Therefore it is better to chose the overall load factors more closely to the somewhat conservative factors proposed by the German regulations:

- $\gamma = 1.5$ in case of ductile failure cross section,
- $\gamma = 1.8$ in case of brittle failure cross section.

4.5.3.3 Accidents

Former Dutch building codes [lit, 40]
The former Dutch building codes do not give an overall load factor in the case of accidents. The present Dutch building codes [lit, 14] prescribe the following safety factors:

load factor $\gamma_S = 1.0$

resistance factor

- explosions or collisions
  the resistance factor depends on whether the tensile strength or the compressive strength governs the overall structural failure:
  for tensile strength: $\gamma_R = 1.2$
  for compressive strength: $\gamma_R = 1.0$
- fire $\gamma_R = 1.0$

overall safety factor

- explosions/collisions: $\gamma = 1.2$
- fire: $\gamma = 1.0$

4.5.3.4 Overall safety factors (summary)

Execution phase

overall safety factor	ductile failure mode	brittle failure mode
Dutch regulations	1.4	1.7
DBV Merkblatt	1.5	1.8

table 4.4: overall safety factor (execution phase)

Final phase

overall safety factor	ductile failure mode	brittle failure mode
Dutch regulations	1.7	2.0
DBV Merkblatt	1.8	2.1

table 4.5: overall safety factor (final phase)

All rights reserved. Use of disclosure of this data is subject to the restriction stated on the first page of this document.

5. Steelfibre reinforced concrete

The development and application of SFRC has started in the seventies and still goes on. Among the range of applications, the most common one is in elastic founded floors. The first application of SFRC in tunnels has been in Germany in 1978. In the Netherlands, the first application in tunnels takes place with the building of the second 'Heinenoord' tunnel where some segments made of SFRC are used. The first paragraph of this chapter gives an introduction to the material SFRC. In the following paragraphs a review is given of the behaviour and the properties of SFRC.

5.1 Introduction

Concrete under tensile loading is a brittle construction material that has compressive strength and only limited tensile strength. That is why only the areas where tensile stresses are expected have to be reinforced, besides being the most cost-effective way of reinforcement.
There are a lot of materials that can be used as reinforcement, like steel, glass and synthetic fibres. Steel bars are applied most of the times. An alternative for this reinforcement with steel bars is the one with fibres. The ductility of SFRC is larger than that of plain concrete, but smaller than that of steel bars reinforced concrete.

5.2 The behaviour of steelfibres in concrete

The function of the fibres can be divided into a micro- and a macrofunction [lit,12, 22].

1. **Steelfibres reinforce the hardened cement paste (micro function)**
   The random distributed fibres reduce the width of the crack openings of the hardened cement paste in case of bending stresses. The growth of the micro cracks is counteracted by the fibres that transfer the tensile stresses (see figures 5.1 and 5.2). Under uni-axial tensile loading a large crack may arise.

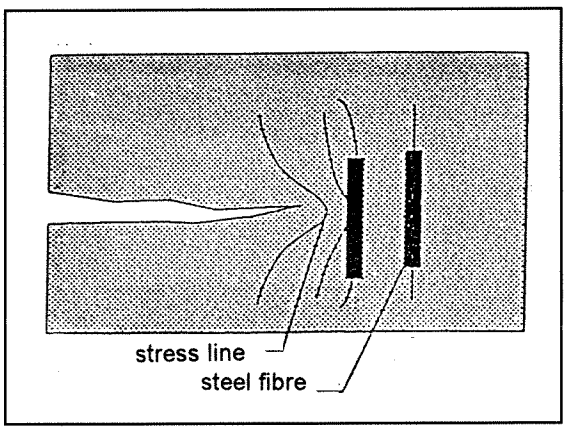

figure 5.1: The fibres reduce the concentration of stresses near the tip of the micro crack.

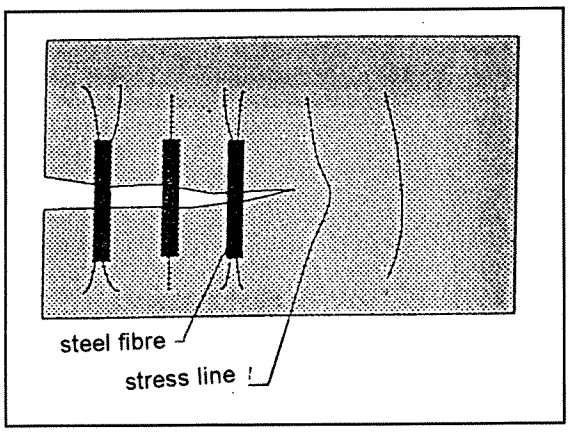

figure 5.2: Loadtransfer by means of fibres that cross the crack and pulling out of the fibres from the surrounding hardened cementpaste. In this case the tensile strength and the adherence ability are more important than the strain stiffness.

The residual tensile strength of the hardened cement paste increases after cracking by applying a certain (economic) quantity of fibres or in other words, the ductility increases.
The most economic and reasonable amount of steelfibres is 100 kg/m^3 or less. The conclusions of the reliability analysis of this report are based on this presumption.

All rights reserved. Use of disclosure of this data is subject to the restriction stated on the first page of this document.

2. **Steelfibres reinforce the concrete (macro function)**
   When a crack crosses a fibre, the attachment of the fibre to the concrete determines its effectiveness; i.e. the capacity of the fibre to carry over the forces to the concrete at both sides of the crack.
   The amount of attachment depends on the strength of the hardened cement paste, the quality of the surface, the anchorage and the shape of the fibre. When the fibre is less anchored or attached, the force that can be borne will also be less. However, the fibre can also break when it is anchored very well which results in brittle fracture of the concrete; this behaviour is unsafe and should be taken into account in the reliability analysis. The fibres have to be anchored to the cement paste at both sides of the crack in such a way that little deformation is possible without fracture of the fibre. This behaviour is called 'after crack behaviour'.

The fibres can collapse in two ways:
- the fibre is pulled out of the surrounding cement paste ;
- the fibre breaks.

5.3 Properties of steelfibre reinforced concrete

Compressive strength
The maximum compressive strength of concrete hardly changes by adding steelfibres.

Tensile strength
Direct tensile strength
The tensile strength after Crack formation increases by adding steelfibres. Cracks are assumed to arise when the tensile stresses exceed the tensile strength.
Steelfibre concrete can act in three ways when it is loaded by a tensile load [lit, 23]:
1. It fails due to brittle fracture because the fibres break as result of the increase of the stresses (see figure 5.3a). The strength of the fibre is too low.
2. It fails because the fibres are pulled out of the cement paste. The fibres aren't loaded until their ultimate tensile strength. As result of the skid of the fibres, failure is delayed. The strain increases and as result the concrete is more ductile then the case described under 1 (see figure 5.3.b): the 'after crack behaviour' improves.
3. The steelfibre concrete is able to bear an increasing tensile stress after Crack formation (see figure 5.3.c.). This behaviour is only possible in concrete with a high volume percentage of fibres (V_f = 15%) [lit, 23].

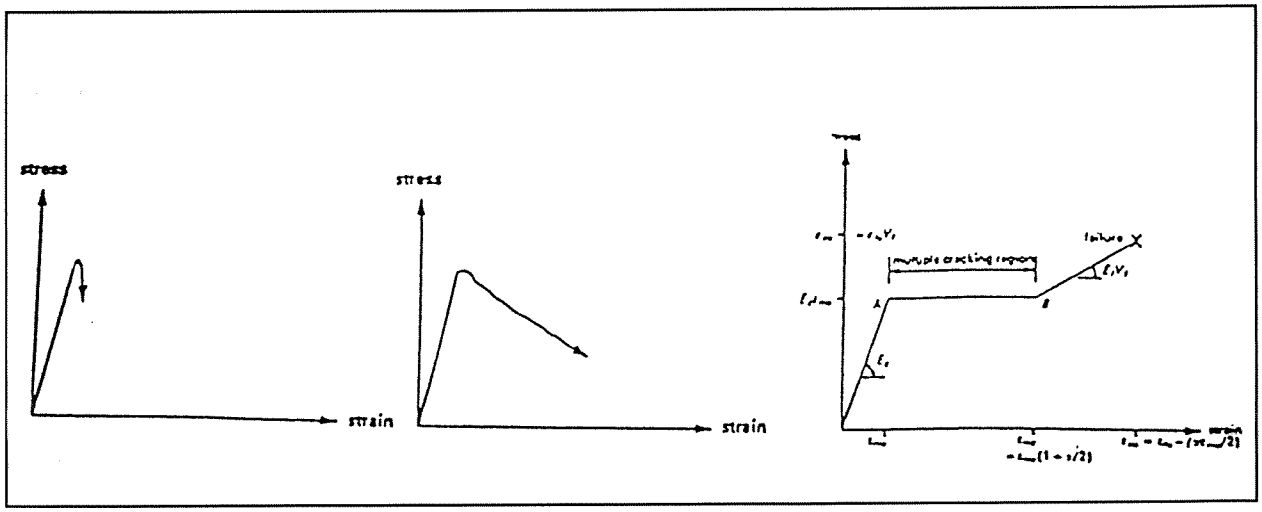

figure 5.3: possible ways of collapse of steelfibre concrete loaded by a tensile load [lit, 24]

All rights reserved. Use of disclosure of this data is subject to the restriction stated on the first page of this document.

Uni-axial tensile strength

The tensile strength of concrete under uni-axial tensile load increases by adding steelfibres [lit, 23].

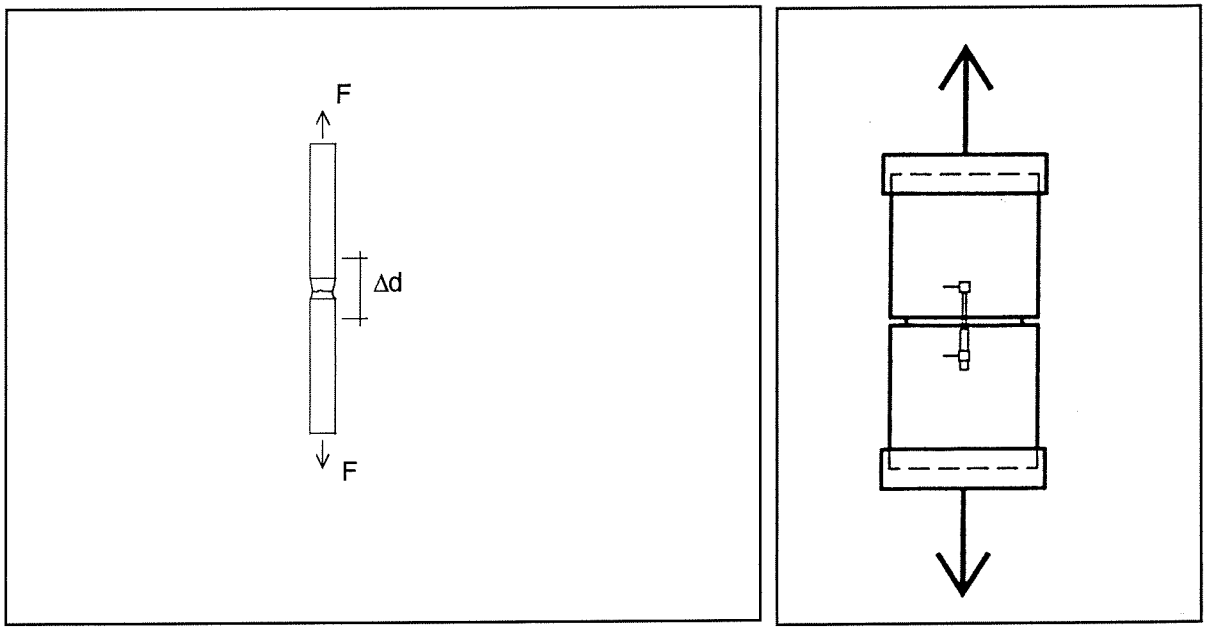

figure 5.4: uni-axial tensile test (Δd = elongation + crack opening)

The result of an uni-axial tensile test [lit, 25] is shown in figure 5.5. First of all, the material reacts linear elastic. When the maximum load is reached, the load-bearing capacity decreases quickly until a plateau is formed. This plateau depends on the continuous pulling out of fibres and the friction forces between the fibres and the concrete [lit, 9].

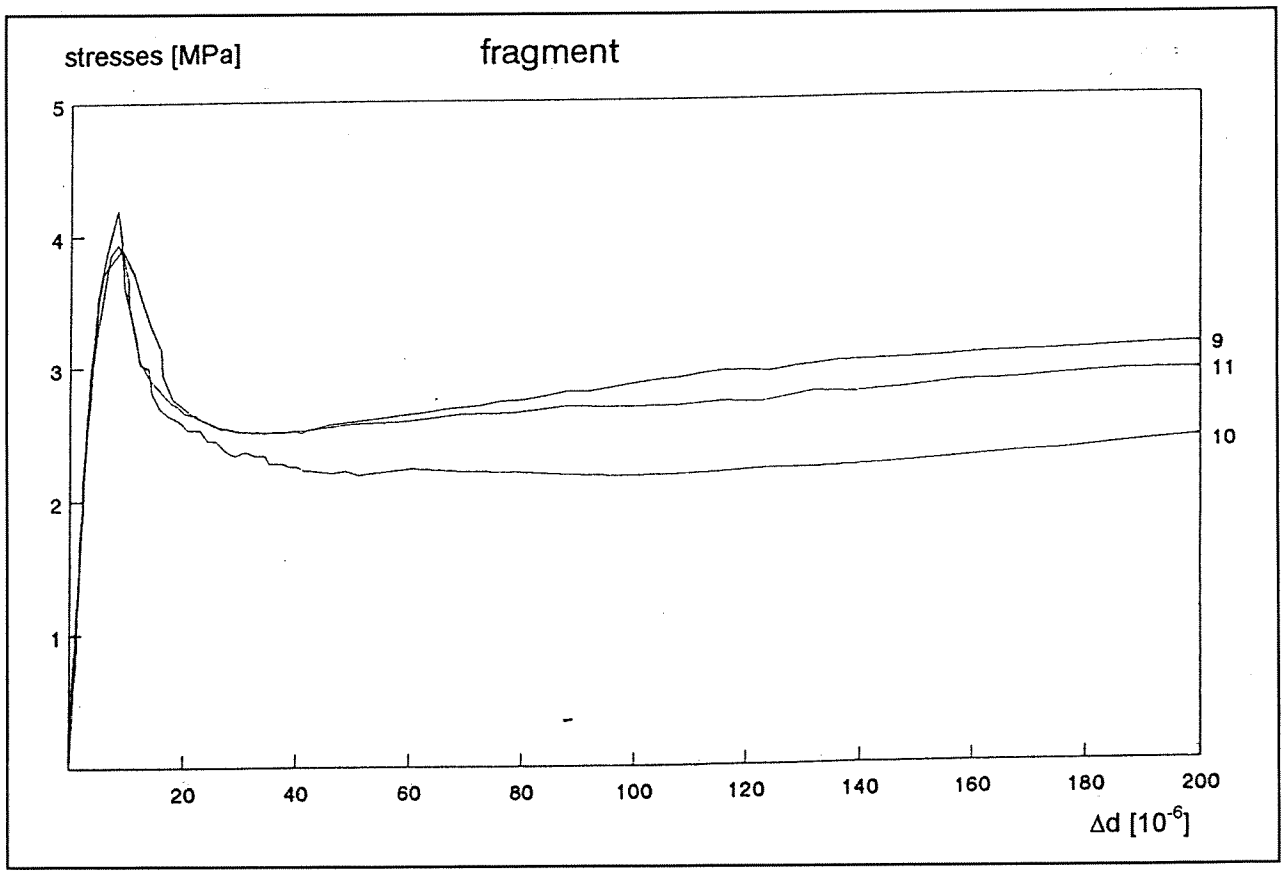

figure 5.5: results of an uni-axial tensile test of steelfibre concrete (the numbers 9,10 and 11 represent the sample number) [lit, 25]

All rights reserved. Use of disclosure of this data is subject to the restriction stated on the first page of this document.

Splitting tensile strength
Addition of fibres increases the splitting tensile strength [lit, 1]. The magnitude of the splitting tensile strength depends on the type of fibre, the Length/Diameter ratio (L/D) and the vol.% of fibres.

Flexural strength
The flexural strength increases more than the direct or splitting tensile strength. In the application of steelfibres in tunnels however, the flexural strength is of minor importance, because the cross-section is loaded by a compressive force, a shear force and a bending moment.

In comparison with plain concrete, steelfibres enhance the crack strength (point A in figure 5.6) and in a mayor way the flexural strength (point B of figure 5.6). The increase of the ductility or the fracture energy (area under the curve of figure 5.6) is considerable in comparison with the increase of the strength [lit, 1].

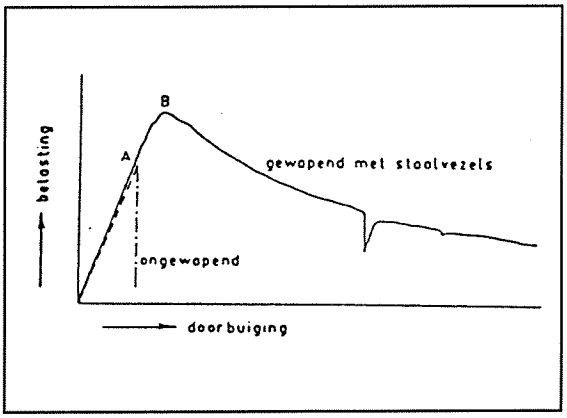

figure 5.6: load-bending curve

Shear strength
The shear strength increases with respect to plain concrete [lit, 1].

Modulus of elasticity
The modulus of elasticity (E_{lining}) hardly increases when fibres are added, specially when the fibres have not a preferred direction [lit,1].
Due to creep, E_{lining} is less in the long term. The values of E_{lining} in the short and in the long term are defined as follows:

$E_{lining,\ short\ term} = 22250 + 250 \cdot f'_{ck}$ [N/mm^2] [lit,14] (5.1)

$E_{lining,\ long\ term} = \frac{E_{lining,shortterm}}{1 + 0.75 \cdot \varphi}$ [N/mm^2] [lit,14] (5.2)

with:
φ = creep coefficient [-] (see table 5.1)

Possible reasons for a minor quality of SFRC:
- the concrete is not well mixed and the fibres tend to accumulate at one side;
- the fibres have such a shape that they cling together;
- gravel pockets are formed.

All rights reserved. Use of disclosure of this data is subject to the restriction stated on the first page of this document.

5.4 Time dependant deformations of steelfibre concrete

Shrinkage

The amount of shrinkage is not influenced by adding steelfibres. The growth and the width of the shrinkage-cracks however, do reduce with as result a finer crack pattern [lit,12]. The effect of the fibres on the behaviour of shrinkage [lit, 9] is shown in figure 5.7. A percentage of fibres higher than 100 kg/m^3 is not profitable for tunnel construction.

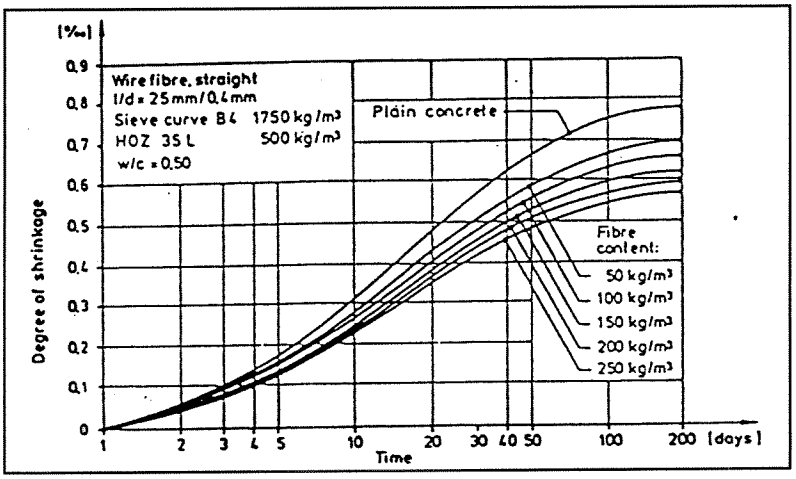

figure 5.7: effect of steelfibres on the shrink behaviour of concrete

Creep

The addition of fibres does not influence the behaviour of creep [lit,1].
The creep coefficient φ depends on the cube compressive strength f'_{ck} and the relative humidity (RH). In table 5.1, the value of φ is presented. (In fact these values belong to concrete without fibres, but as the addition of fibres does not influence the behaviour of creep, the same values can be used for SFRC).

f'_{ck} [N/mm^2]	φ: RH < 60% (dry air)	φ: 60% ≤ RH< 85% (open air)	φ: 85 ≤ RH < 100% (very humid)	φ: RH = 100% (in water)
15	4.2	3.1	2.3	1.7
25	3.6	2.7	2.0	1.4
35	3.2	2.4	1.8	1.2
45	2.8	2.1	1.5	1.1
55	2.4	1.8	1.3	0.9
65	2.2	1.6	1.2	0.8

table 5.1: creep coefficient φ [lit, 27] (RH = Relative Humidity)

5.5 Strength under dynamic loads

The addition of steelfibres gives a considerable increase of the strength under dynamic loads.

Fatigue strength

The fatigue strength increases by addition of steelfibres [lit,1].

Splitting resistance

Steelfibre concrete resists impact loads much better than plain concrete does, as result of its higher splitting resistance [lit,1,9]. The surface of steelfibre concrete has a high impact resistance because of the fibres which are close to the surface.

All rights reserved. Use of disclosure of this data is subject to the restriction stated on the first page of this document.

5.6 Water permeability

Watertightness is one of the most important requirements of a tunnel lining. The control of crack formation is an important aspect for the realisation of watertight concrete constructions. Cracking of the lining, specially cracks which cross the whole cross-section, must be prevented. The application of a steelfibre reinforcement is favourable for the watertightness because of the reduction of the growth and the width of the cracks.

5.7 Durability

With respect to the durability of the tunnel lining, relative high requirements have to be met, because the outside of the lining is not accessible for inspection and repair.

Physical - chemical resistance
Corrosion of uncracked SFRC only takes place at the surface [lit,1].
Cracks have a negative effect on the durability because they enable the entrance of water and oxygen [lit,16]. The fibres reduce the crack width and consequently the corrosion of SFRC will be less than that of steel bars reinforced concrete. However, the reduction of the cross-section area of the reinforcement is in proportion more severe for a certain amount of corrosion, because of the much smaller diameter of the steelfibres.

Mechanical durability
Laboratory tests have demonstrated that the wear resistance of concrete increases by adding steelfibres as the fibres reinforce the concrete until the surface [lit,9]. The resistance against spalling of pieces of concrete is considerably higher than in the case of plain concrete [lit,1].

From the above described phenomena, requirements are derived with respect to the composition and the density of the concrete, as well as for the presence of cracks in the lining.

5.8 Review of characteristics of steel fibre reinforced concrete

- Steelfibres are added to concrete to enhance the ductility of the concrete after crack formation and to reduce the crack width.
- Steelfibres can collapse in two ways:
  - by being pulled out of the surrounding cement paste,
  - by breaking.
- The following properties of plain concrete are improved by the addition of steelfibres:
  - the shear strength,
  - the ductility after crack formation,
  - the strength under dynamic loads, i.e. the fatigue strength and the splitting resistance,
  - the watertightness,
- The following properties of the concrete are not significantly influenced by the addition of steelfibres:
  - the compressive strength,
  - the modulus of elasticity,
  - shrinkage of the concrete,
  - creep of the concrete.
- Possible reasons for a minor quality of steelfibre reinforced concrete caused during the execution process:
  - the concrete is not well mixed and the fibres tend to accumulate at one side;
  - the fibres have such a shape that they cling together;
  - gravel pockets are formed.

All rights reserved. Use of disclosure of this data is subject to the restriction stated on the first page of this document.

6. The tunnel lining

The first paragraph of this chapter gives an introduction to the calculation of the tunnel lining by means of a description of the load cases which have to be considered at the calculation. Next, in paragraph 6.2, the loads which have to be taken into account at the calculation are described. There are several models available for the calculation of the lining. These are described in paragraph 6.3. As these models might deal in a different way with the safety aspect, they are compared with each other in paragraph 6.3.1 in order to establish the mutual relation. The analytical Duddeck method resulted to be the most conservative one and consequently it is chosen as model for the execution of the reliability analysis. Then in paragraph 6.3.2 a sensitivity analysis is executed in order to get insight in the impact of the input-parameters on the calculation results and to distinguish the important parameters. The wet volume weight of the soil, the lining thickness and the coefficient of lateral earth pressure resulted to have the largest impact on the cross-section forces. Further, in paragraph 6.4, the strength (or resistance) of the tunnel lining is described. Finally, in paragraph 6.5, the deformation of the lining in cross-sectional direction (the so-called ovalisation) and in longitudinal direction (the so-called beaming) are described.

6.1 Introduction

The following points have to be checked when a tunnel lining is dimensioned:
- stresses in cross-sectional direction (as result of the soil-stresses),
- stresses in longitudinal direction (the tunnel is prestressed by the thrust forces and stresses due to beaming[13]),
- deformations (beaming, ovalisation).

In this report only the cross-section is considered. The following two load cases have to be taken into account:

1. Load case: initial soil stresses (final phase)
The active soil stresses on the lining are taken equal to the primary stresses in the undisturbed ground. Hence, it is assumed that for the final stage (years after construction) the ground will eventually return to the same condition as before the tunnelling. The limit state 'failure of the lining' as result of soil- and waterpressures (the initial soil-stresses), is determined by calculating the decisive combination of hoop force and bending moment. The decisive combination consists of a maximum bending moment and a minimum hoop force at the top and the bottom of the tunnel. These points have the largest failure probability. The cross section forces in the lining are calculated analytically using the analytical Duddeck method (appendix 1).

2. Load case: prestressed soil initiated by hydrostatic concrete-pressure (execution phase)
The tunnel lining is built by extruding concrete between the inner formwork and the ground using overpressure. The distribution of the forces in the construction depends on the concrete pressure during the extrusion process. The overpressure with which the concrete is extruded will prestress the soil. The vertical and horizontal soil stresses will reach an equilibrium with the concrete pressure. As the fresh concrete can be considered as a liquid, the concrete pressure increases hydrostatically with the depth. The limit state 'failure of the lining' as result of concrete-pressure, can also be determined by calculating the decisive combination of hoop force and bending moment. This situation can be checked with PLAXIS.

The above mentioned load cases are only two of the possible load cases that can induce the failure of the tunnel. The load cases that cause failure of the tunnel and the subdivision into the possible (failure) mechanisms that bring about these load cases are described by S. van Kinderen[14] in ([lit, 36]). The reliability analysis of this report is limited to the first load case 'initial soil stresses (final phase)'.

[13] Beaming = deformation mechanism that takes place when the characteristics of the soil, wherein the tunnel is bedded, change over a short range.
[14] S. van Kinderen has determined the failure probability of a conventional bored tunnel.

All rights reserved. Use of disclosure of this data is subject to the restriction stated on the first page of this document.

6.2 Definition of the loads

6.2.1 Final phase

For normal use, the following loads or actions can be specified for an ITM tunnel lining:

Effective soil stresses
The effective soil stresses working on the lining can be derived from the initial effective soil stresses. The inhomogeneous layered structure of the ground, future excavations and embankments have to be taken into account when the initial effective soil stresses on the lining are calculated. Besides that the ground is a load on the tunnel lining it can also act as a load carrying medium, partially unloading the tunnel lining; deformation of the tunnel lining reduces the effective soil stresses in vertical direction and activates stabilising horizontal soil stresses.

Groundwater pressure
Groundwater pressure gives an omnidirectional load on tunnels that are completely or partially under the phreatic surface. As the hydrostatic water pressure increases with the depth, it is not regularly distributed over the tunnel perimeter. The variation of the phreatic surface during the intended life of the tunnel has to be taken into account.

Settlement
As result of stress changes in the past (e.g. as result of an embankment), creep and consolidation can cause deformations of the ground, specially in clay or peat. When a tunnel is bedded in such ground layers, the loads on the tunnel will change in course of time.

Self-weight
The self-weight includes the tunnel lining itself and all permanently present structural parts and objects inside the tunnel.

Variable actions
Variable actions due to normal use of the tunnel or the ground surface.

Accidental loads
Fire, explosion and collision forces.
Time dependant effects as shrinkage, temperature variation, delayed settlements of the soil and creep of the concrete have to be taken into account with respect to their special characteristics important for the calculations.

All rights reserved. Use of disclosure of this data is subject to the restriction stated on the first page of this document.

6.2.2 Execution phase

The construction time is equal to the time needed for the concrete to reach the nominal design strength. During construction of the tunnel lining the same loads are present as during normal use with a few modifications:

Effective soil stresses
The effective soil stresses on the lining have to be derived from the initial effective soil stresses caused by the concrete extrusion process. All notes on the effective soil stresses for normal use also count during the construction phase with exception of excavations and embankments that only have to be taken into account as far as they take place during construction of the tunnel.

Groundwater pressure
The variation of the phreatic surface during the intended construction time of the tunnel has to be taken into account.

Self-weight
The self-weight of the TBM, the formwork and all cables, pipes, etc. have to be added to the self-weight of the tunnel lining itself and all permanently present structural parts and objects inside the tunnel.

Concrete pressure
The pressure of the fluid concrete acting on the formwork and via the formwork on the lining have to be taken into account.

Concrete hardening loads
- Shrinkage by hardening:
  The temperature of the concrete rises during hardening because of hydration. Afterwards the temperature decreases and the stiff concrete shrinks. This shrinkage is counteracted by the surrounded soil wherein the tunnel is bedded. Consequently, tensile forces are introduced in the tunnel lining.
- Stresses by temperature gradient:
  Stresses are not only introduced by hardening, but also by the temperature gradient caused by the warm mortar which is pumped into the cold soil. Inside the hardening concrete, the temperature rises with about 10^0C to 20^0C, while on the soil-side the temperature hardly rises.
- Shrinkage by desiccation.

Variable actions
Variable actions due to construction equipment in the tunnel and normal use of the ground surface have to be taken into account. Special attention has to be given to the jack forces, needed for the movement of the TBM and working on the lining via the inner formwork.

The sequence in which the soil is loaded by the self-weight of the tunnel, the concrete pressure and the concrete hardening loads, is important for the reaction of the soil and consequently the resultant soil stresses.

All rights reserved. Use of disclosure of this data is subject to the restriction stated on the first page of this document.

The main loads during construction in longitudinal direction are summarised in figure 6.1

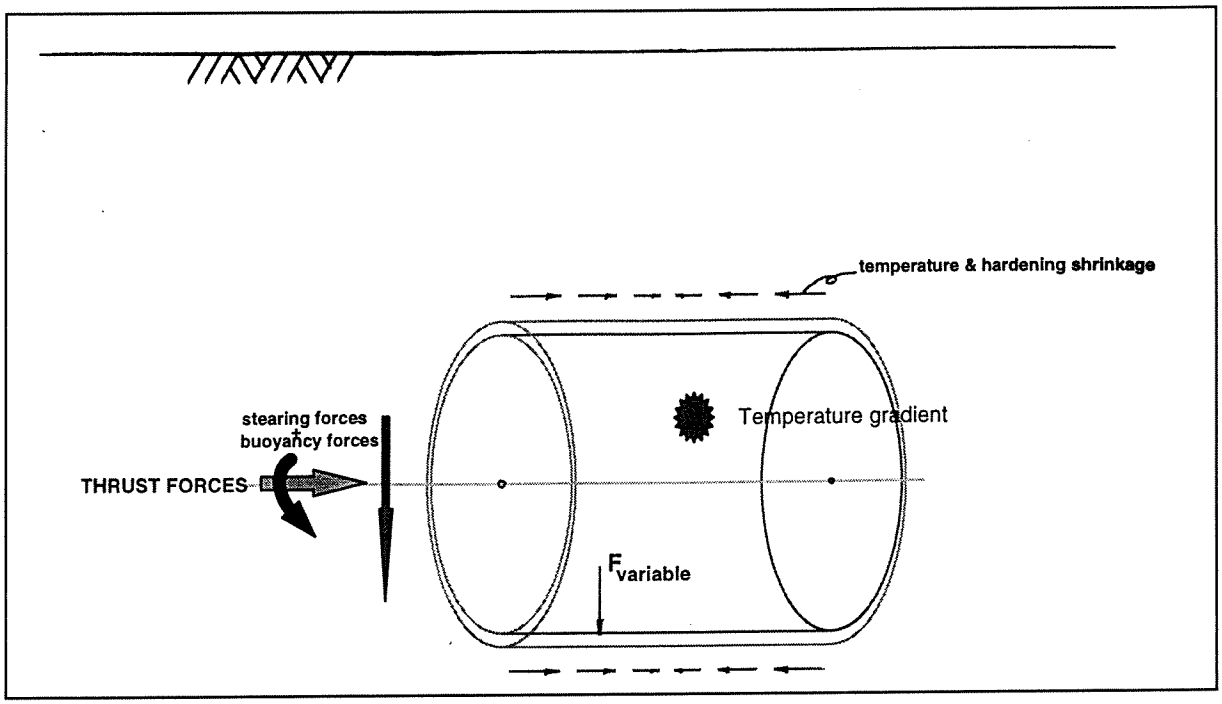

figure 6.1: loads on tunnel during construction in longitudinal direction
temperature gradient: gradient in the temperature of the concrete of the inner- and the outer side of the lining.

6.3 Calculation models

There are several models available to determine the forces and stresses in the tunnel lining [lit, 30, 31, 32, 33, 34]. A principal characteristic of these models is whether they do or don't take into account the interaction between the soil and the tunnel lining. This interaction is essential because the deformation of the lining due to the lining-ground relationship results in reaction stresses in the ground. Models which don't take into account the interaction between the soil and the tunnel lining only consider the initial situation (i.e. before any deformation has taken place).
The following situations can be distinguished:

- The interaction between the soil and the tunnel lining is not taken into account. The lining is considered to be infinitely stiff and the soil stresses are interpreted as periodic loads. This situation can be calculated analytically.
- The interaction between the tunnel lining and the soil is taken into account. In this case two mechanisms are distinguished:
  1. continuous spring-model (soil schematised as springs)
     This situation can be calculated analytically or by means of a frame-model (e.g. 2D-frame of SCIA-software)
  2. continuum -model (soil schematised as an elastic continuity)
     This situation can be calculated with a finite elements method.

All rights reserved. Use of disclosure of this data is subject to the restriction stated on the first page of this document.

Models which do not take into account the lining-ground interaction

Infinitely stiff ring model (Bouma-model) [lit, 32]
The lining deforms when it is loaded by the soil. This deformation, as result of the lining-ground interaction, is not taken into account in the Bouma-model. Only the initial soil-stresses and shear stresses are considered. Bouma has described the soil-stresses with Fourrier series (figure 6.2):

$$q(\theta) = \sum_{n=0}^{\infty} q_n \cos n\theta$$

with:

q	= load	[kN/m^2];
θ	= angle relative to the vertical axis through the hart of the tunnel (def.: θ = 0 at the upper side of the tunnel)	[^{0}].

The load terms for the values 0,1,2 and 3 of n are shown in figure 6.2.

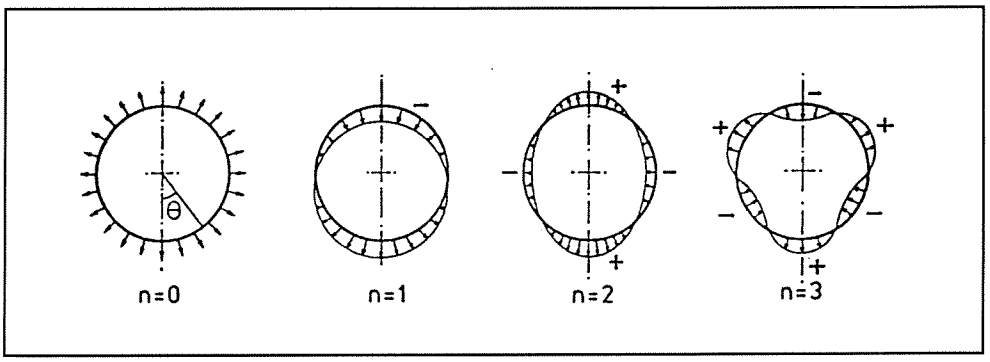

figure 6.2: harmonic loads $q(\theta) = q_n \cos(n\theta)$ for n= 0, 1, 2 and 3

Bouma has derived differential equations for hoop force and bending moment in circular rings (appendix 4). These differential equations are derived from equilibrium equations in tangential and radial direction of a ring-shaped segment.

Boundary conditions and starting-points [lit,32]

- Full elasticity of concrete and soil is assumed.
- The stiffness of the lining is taken as constant along the circumference.
- The soil stresses are symmetric.
- The vertical forces are in equilibrium.
- The cross-section is circular.

All rights reserved. Use of disclosure of this data is subject to the restriction stated on the first page of this document.

Models which do take into account the lining-ground interaction

Two types of models can be distinguished:

1. Continuous spring model

The tunnel lining is schematised as a ring-shaped element with bending stiffness EI and strain stiffness EA. The reacting ground is replaced by bedding springs; the tunnel lining can be analysed as a beam. The springs are distributed discontinuously over the tunnel tube and separated from each other at equal distance. The load on the system is formed by the initial soil-stresses. The continuous spring model is schematised in figure 6.4.

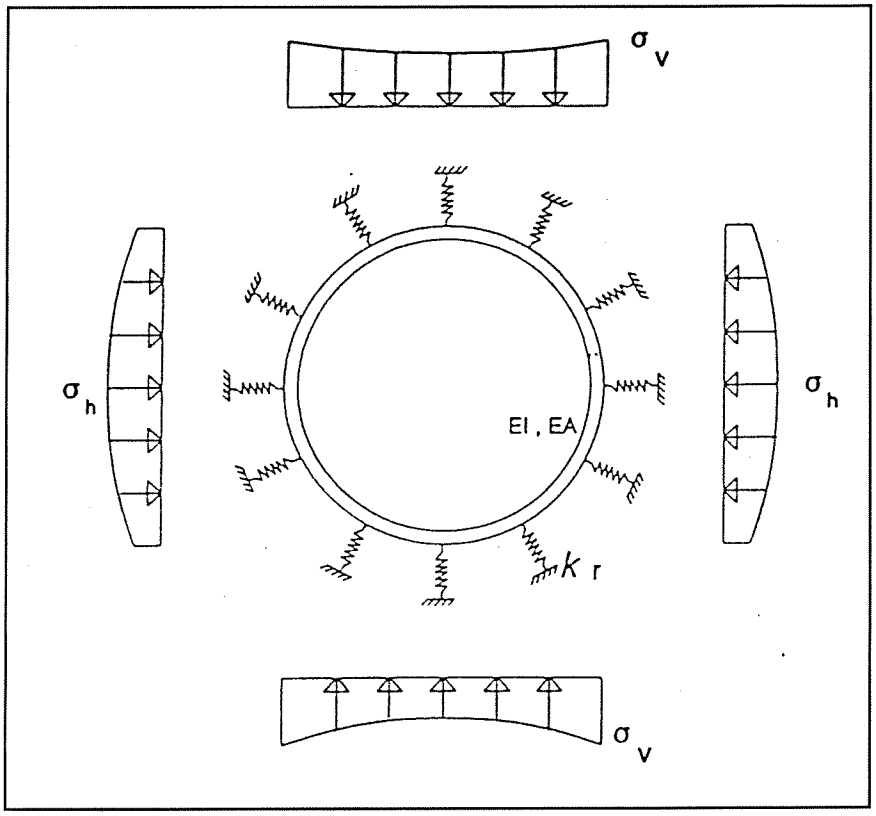

figure 6.4: continuous spring-model

All rights reserved. Use of disclosure of this data is subject to the restriction stated on the first page of this document.

2. Continuum model

A second category of models which take the lining-soil interaction into account is formed by the continuum models. One of these models is the one proposed by Duddeck (1984) [lit,17].
In these models the soil is schematised as an infinite medium. The stiffness of the soil is taken into account by the modulus of elasticity E_g and the Poisson's ratio υ. The tunnel tube is loaded and supported both in radial and in tangential direction by the soil.

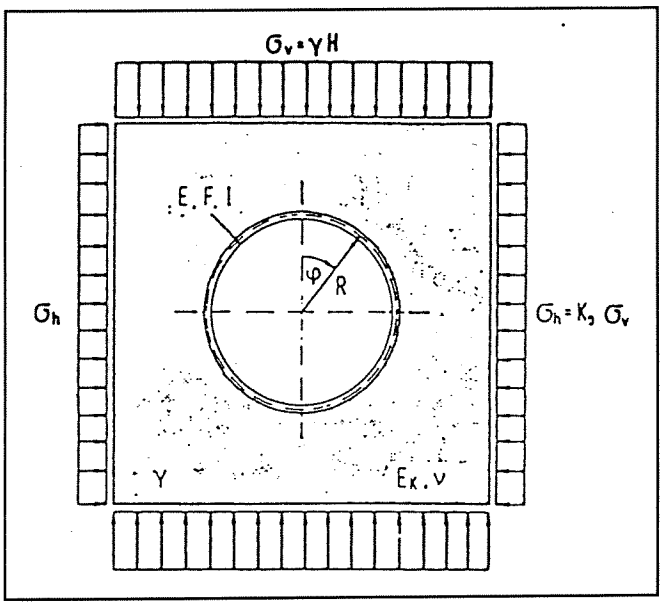

figure 6.5: continuum model

Boundary conditions and starting-points [lit,17]

- All the effects of the third dimension are ignored.
- The cross-section is circular.
- The stiffness of the lining is taken as constant along the circumference.
- Full elasticity of concrete and surrounding soil is assumed.
- There is an interaction between the lining and the soil with respect to the deformations and the transfer of forces in tangential and radial direction, or only in radial direction. In the latter case the tangential forces are ignored. With this starting-point, the model meets the equilibrium conditions and the compatibility at the boundary between the lining and the soil.
- Due to the lining-ground relationship, deformation of the lining results in reaction stresses in the ground.

All rights reserved. Use of disclosure of this data is subject to the restriction stated on the first page of this document.

Restrictions[15] (also with respect to the Bouma-model)
The soil is assumed to be linear elastic, which means that the plasticity of the soil is not taken into account. The validity of this assumption however is limited (see figure 6.6). Due to the deformation of the cross-section of the lining (ovalisation) the earth pressure descends at the top and the bottom of the section (figure 6.6a) and ascends on the sides (figure 6.6b)). At a certain displacement, dependent among others on the soil type, the soil becomes plastic. The loads do not change while the displacements increase.

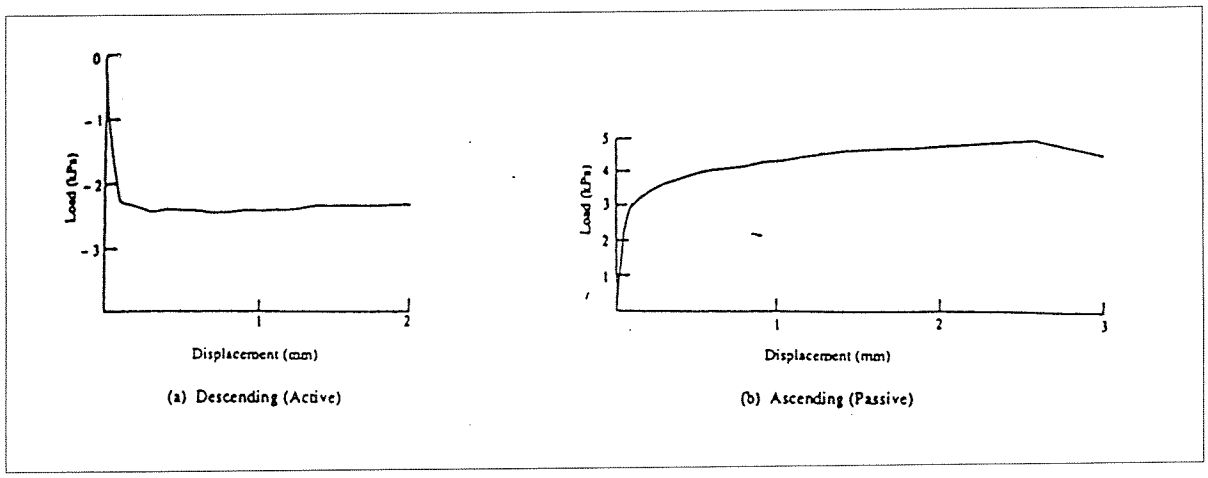

figure 6.6: load-displacement curve (Tanaka 1991) [lit,43]

Application of the models
In [lit, 5] above models have been compared with each other. The conclusion drawn in this report is that all the models give comparable results with exception of the Bouma-model because it does not take into account the lining-ground relationship. The lining-ground relationship is important because the ovalisation of the lining causes a considerable reduction of the bending moments in the lining. The continuum-model is the most user-friendly because it includes this lining-ground relationship automatically. For a continuous spring model, bedding springs with an appropriate bedding modulus have to be applied.

Remark
Above mentioned models may be consistent within the theoretical approach of a ring bedded in a continuum. However, no considerations are given to effects as those caused by assembling the lining ring, by the driving thrust, by driving an adjacent tunnel lining ,etc.

[15] Some continuum models, such as PLAXIS, do take into account the plasticity of the soil.

All rights reserved. Use of disclosure of this data is subject to the restriction stated on the first page of this document.

ITM design

The following models are used:

- **analytical model**
  Bouma-model with interaction coefficients; this model equals the model proposed by Duddeck [lit,17] (appendix 1) and is a continuum model.
- **frame model**
  (As frame-model is used the 2D-FRAME-program of SCIA-software)
  This frame-model is a continuous-spring model with radial and tangential springs and radial and tangential loads. Two cases are considered:
  1- a 2D-frame calculation, which is in the following referred to as Duddeck-Duddeck;
  2- a 2D-frame calculation at which the loads and spring values are calculated with PLAXIS and used as input in the 2D-frame calculation. This model is in the following referred to as Duddeck-continuum[16].
- **PLAXIS (PLAsticity AXISymmetric)**
  PLAXIS is a finite element code for the analysis of deformation and stability of geotechnical structures. PLAXIS is a continuum model.

The relation between these models has to be established, because they might deal in a different way with the safety aspect. Despite this possible different approach, the same strategy has to be applied at the execution of the reliability analysis.

6.3.1 Comparison of calculation models

Several pilot calculations have been made of N_{min} and M_{max} initiated by the initial soil stresses in order to establish the relation between the models. The results, for the different types of geotechnical profiles, are given in figure 6.7 and 6.8 .

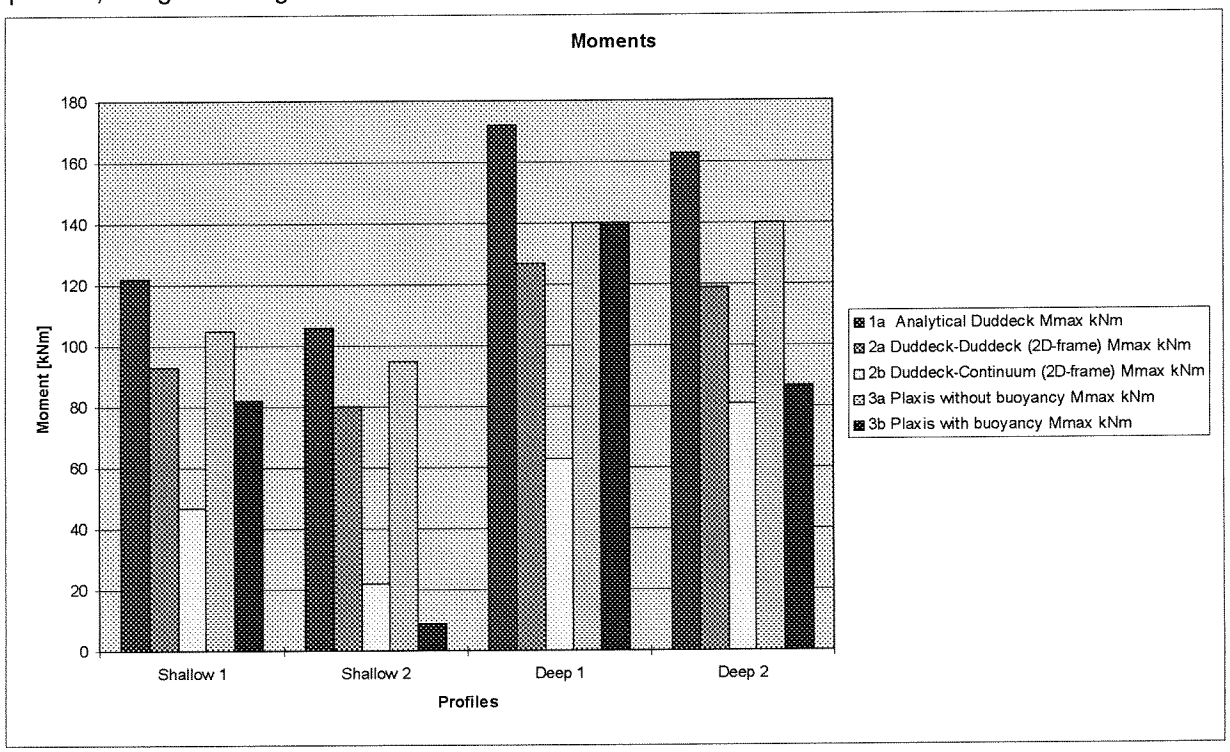

figure 6.7 : comparison of calculation models based on M_{max}

[16] With the 2D-frame program, cross-section forces can be computed taking into account the physical non-linearity of concrete. By using soil-loads and subgrade factors calculated with PLAXIS as input in the 2D-frame calculation, the results of the computation are dependent on the soil conditions.

All rights reserved. Use of disclosure of this data is subject to the restriction stated on the first page of this document.

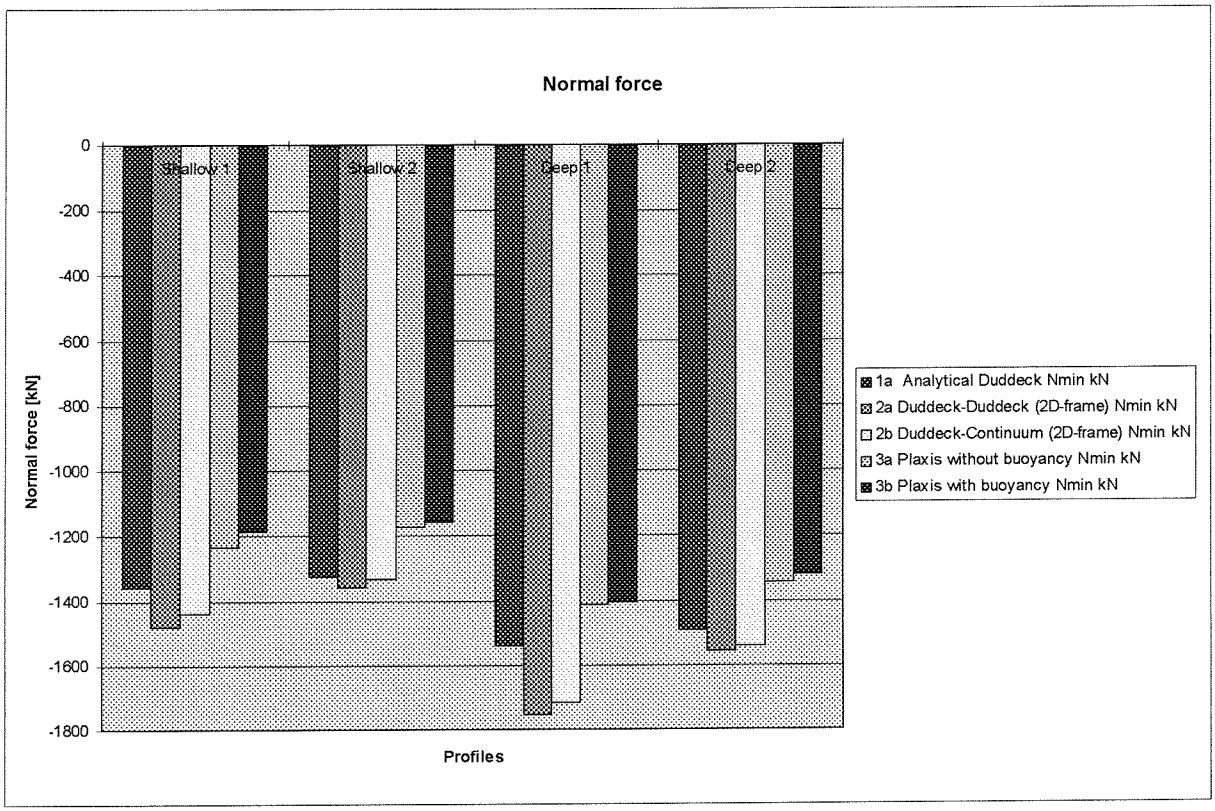

figure 6.8: comparison of calculation methods based on N_{min}

Conclusions (drawn from figure 6.7 and 6.8)

- The M_{max} calculated with the analytical model are larger than those calculated with the other models. The N_{min} calculated with 2D-frame are larger than the N_{min} calculated with the analytical model, but the differences are very small and approximately equal to 10%. The analytical model can be assumed to be the most conservative model.
- The 2D-frame model (Duddeck-Duddeck) should give the smallest differences with respect to the analytical model, because the interaction coefficients of the Duddeck-model are determined based on a continuous-spring model. This conclusion, however, does not correspond with figure 6.7. The reason for the differences is that in the 2D-frame calculation different values of the spring stiffness are used for the top, flank and bottom of the tunnel tube, while in the analytical Duddeck method the same value of the spring stiffness is applied along the whole ring.
- The difference between the 2D-frame spring model and PLAXIS can possibly be found in the used linear elastic springs and the disconnecting of the interaction between the lining and the soil in 2D-frame.
- PLAXIS is assumed to give the best approach of the reality and should therefore be used for the execution of the reliability analysis. As there is not an computerised version available of PLAXIS combined with a probabilistic analysis and as the manual probabilistic analysis with the results of PLAXIS (appendix 7) is very laborious, the analytical Duddeck method is chosen as model for the execution of the reliability analysis.

All rights reserved. Use of disclosure of this data is subject to the restriction stated on the first page of this document.

For the generality of the reliability analysis, it is important to know whether all the models use the same input parameters and if these parameters have the same impact on the calculation results. The latter shall be determined by means of a sensitivity analysis (see paragraph 6.3.2).
The input of the data of the lining is for all the models the same. There are some differences with respect to the input of the soil parameters:

- The analytical model uses a constant value of the spring stiffness around the tube. 2D-frame and PLAXIS use different values for the top, flank and bottom of the tube.
- PLAXIS has as 'extra' input, with respect to the other models, some soil parameters: the cohesion (c), the dilatation angle (ψ), the angle of internal friction (φ) and the Poisson's ratio (υ), so the calculation results depend on the soil conditions.

The choice with regard to the use of one or another model, depends on the available input-data, the desired accuracy and the purpose of the calculation.

6.3.2 Sensitivity analysis

A sensitivity analysis is executed in order to get insight in the impact of the input-parameters on the calculation results. In this way the important parameters are distinguished.
Strictly speaking, the sensitivity analysis should be performed for all the compared models (in 6.3.1) in order to determine if some parameters have a different impact on the calculation results when they are used in other models. Within the scope of this study, the analysis is limited to the analytical model.

The input-parameters of the analytical model depend on the following:

- R = $0.5(d_{lining} + D)$
  - d_{lining} : formwork (at the inside), soil (at the outside), shrinkage
  - D : d_{lining}, overcut ($\pm$ 5 cm), deformation of the cross section (ovalisation)
- E_{lining} = $22250 + 250\ f'_{ck}$ (short term, equation 5.1)
  - f'_{ck} : quality of the concrete
- E_g : soil type, soil deformations
- $\sigma_{vertical}$ = $\gamma_{dry} * h_{gw} + \gamma_{wet} (h_{tunnel} - h_{gw})$ (deep profile)
  - $\sigma_{vertical}$ = $h_{river} * \gamma_{water} + \gamma_{wet} * h_{tunnel}$ (shallow profile)
  - γ_{dry}, γ_{wet} : soil type
  - h_{gw} : season, location of the tunnel (e.g. nearby a river, then h_{gw} depends, among others, on the discharge of the river)
  - h_{tunnel} : accuracy of the TBM
  - h_{river} : season, discharge of the river
  - γ_{water} : this parameter is (rather) constant
- K_0 = $\sigma'_{horizontal}/\sigma'_{vertical}$ = ratio of effective stresses
  - K_0 :properties and conditions of the soil (K_0 can also be influenced by the driving process, because first the ground is loosened by the excavation and afterwards it is strained as result of the extrusion process.)

The results of the parameter study are presented in table 6.1 .

All rights reserved. Use of disclosure of this data is subject to the restriction stated on the first page of this document.

parameter	multiplication factor	increase (positive) / decrease (negative) in [%] of M_{max} and N_{min} as result of the parameter variation							
		M_{max}				N_{min}			
		d1	d2	s1	s2	d1	d2	s1	s2
d_{lining}	* 0.95	-9	-3	-9	-3	0	0	0	0
d_{lining}	* 1.05	8	3	8	3	0	0	0	0
D	* 0.95	-1	-7	-1	-7	-5	-5	-5	-5
D	* 1.05	0	7	0	7	5	5	5	5
h_{gw}	* 0.95	0	0			0	0		
h_{gw}	* 1.05	0	0			0	0		
h_{river}	* 0.95			-1	-1			-1	-1
h_{river}	* 1.05			1	1			1	1
γ_{dry}	* 0.95	0	0			0	0		
γ_{dry}	* 1.05	0	0			0	0		
γ_{wet}	* 0.95	-5	-5	-4	-4	-5	-5	-4	-4
γ_{wet}	* 1.05	5	5	4	4	5	5	4	4
K_0	* 0.95	4	12	4	12	-4	-5	-4	-5
K_0	* 1.05	-4	-12	-4	-12	4	5	4	5
E_g	* 0.95	3	1	3	1	0	0	0	0
E_g	* 1.05	-3	-1	-3	-1	0	0	0	0
E_{lining}	* 0.95	-3	-1	-3	-1	0	0	0	0
E_{lining}	* 1.05	3	1	3	1	0	0	0	0

table 6.1: results of the sensitivity analysis

remarks:

- γ_{water} and h_{tunnel} are not included in the parameter study; a sensitivity analysis of these parameters would not be realistic because these parameters do not vary in reality.
- The following geotechnical profiles have been considered: d1= deep1, d2 = deep2, s1= shallow1, s2 = shallow2

Conclusions (drawn from table 6.1)

- γ_{wet}, d_{lining} and K_0 have the largest impact on the cross-section forces.
- E_g is a parameter which in reality varies more than 5%. In that case the impact is larger than follows from the analysis. Besides, E_g is a rather uncertain parameter (variation coefficient V=25%), which means that E_g has also to be considered as a parameter with a large impact on the calculation results.
- The impact of the parameters E_g, E_{lining} and d_{lining} on the magnitude of M_{max} is larger in sand than in clay.
- The impact of the parameters K_0 and D on the magnitude of M_{max} is larger in clay than in sand.
- Variation of parameters hardly influences the magnitude of N_{min}; γ_{wet} , D and K_0 give the largest impact on N_{min}.

All rights reserved. Use of disclosure of this data is subject to the restriction stated on the first page of this document.

6.4 Definition of the resistance

At a certain combination of hoop force and bending moment the tunnel lining will collapse. As the load case 'combination of hoop force and bending moment' is a very common one, an interaction diagram (figure 6.10) is developed to simplify the calculation of this load case. This diagram is based on experiments which are executed as cube compressive tests, bending tests and eccentric compressive tests. From these experiments a stress-strain relation is derived which is presented in figure 6.9. Eventually the interaction diagram is composed by means of the eccentric compressive tests, where the eccentricity is taken equal to the ratio M/N.

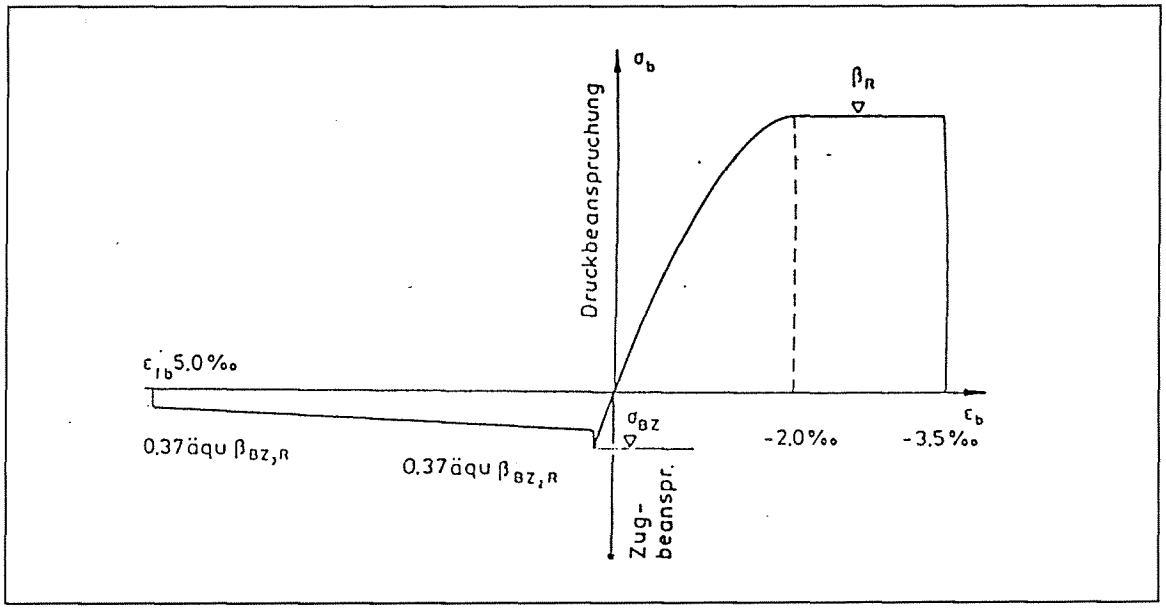

figure 6.9: strain-stress relation of steelfibre concrete [lit,2]

In figure 6.10 the interaction diagram (N&M diagram) for SFRC is presented. In the diagram three zones can be distinguished. In the first zone (I) the whole section is only loaded by compressive stresses and the addition of steelfibres does not influence the maximum compressive stress that can be borne. The following zone (II) is characterised by the enhancement of the bearing capacity as result of the addition of steelfibres. In the third zone (III) plain concrete does not have any bearing capacity, while steelfibre concrete still can bear loads.
Summarised:
zone I : only depends on compression capacity,
zone II : depends on compression and tensile capacity,
zone III : depends on tensile capacity.

All rights reserved. Use of disclosure of this data is subject to the restriction stated on the first page of this document.

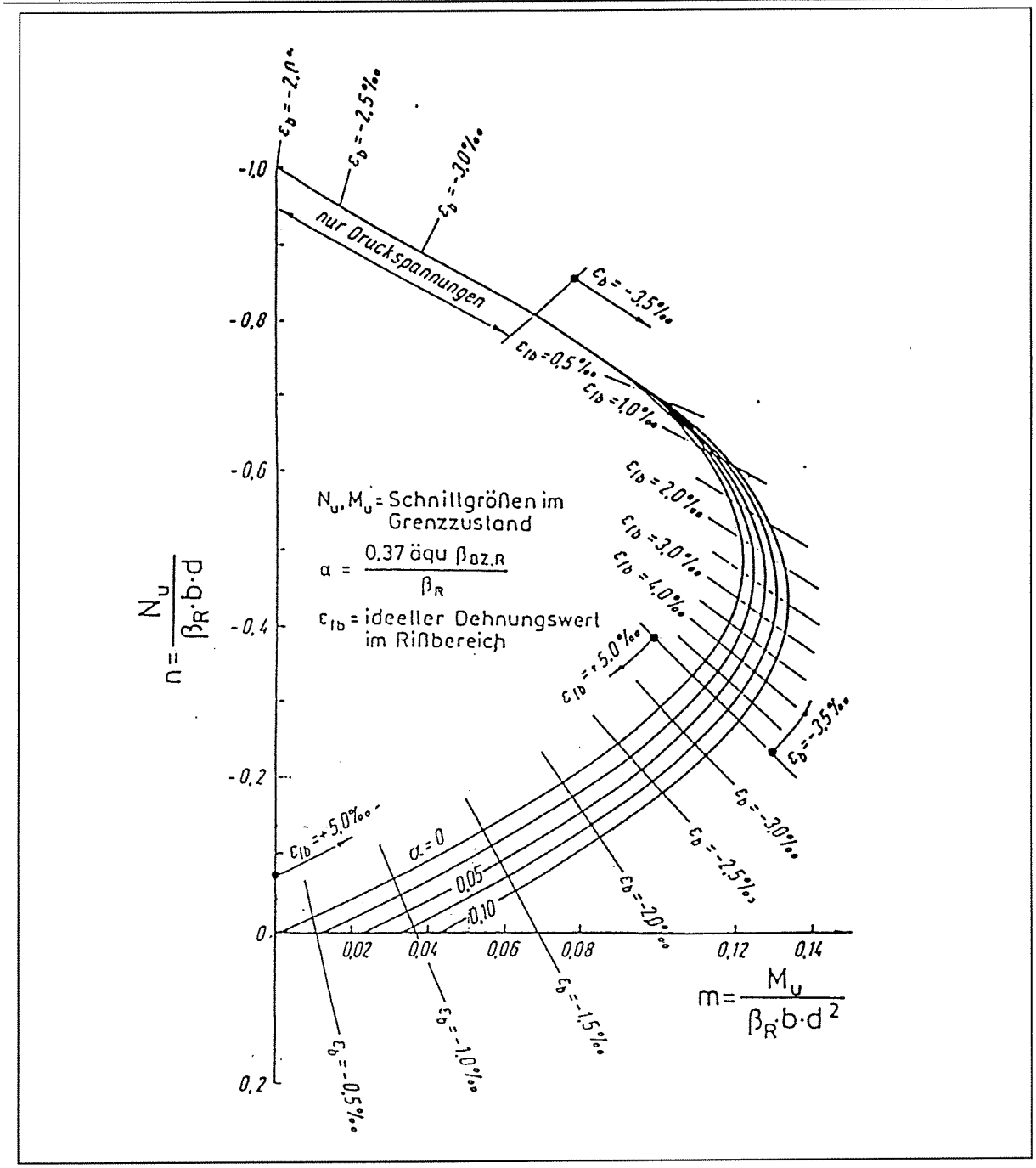

figure 6.10: interaction diagram (N&M diagram) [lit,2]

with:

n	= hoop force [-],
Nu	= ultimate hoop force [N],
β_R	= design value of the compressive concrete strength [N/mm^2],
b	= section width [mm],
d	= thickness of the tunnel lining [mm],
m	= bending moment [-],
Mu	= ultimate bending moment [Nm] ,
α	= ratio of (equivalent) flexural strength ($\ddot{a}qu\beta_{BZ,R}$) and compressive concrete strength (β_R), which depends on the amount of steelfibres per m^3 of concrete: $\alpha = 0{,}37\ddot{a}qu\beta_{BZ,R} / \beta_R$, (see figure 6.9). This factor is determined by means of tests.

All rights reserved. Use of disclosure of this data is subject to the restriction stated on the first page of this document.

The failure boundary for the load case 'combination of hoop force and bending moment', which is necessary for the probabilistic analysis, is determined with the curve of the N&M diagram (appendix 8).

6.5 Deformations (beaming, ovalisation)

Deformation of the cross-section (ovalisation)
The tunnel tube has little lateral support in soft soil. As the vertical earth-pressure is larger than the horizontal one, the tunnel deforms in ring direction and gets an elliptic shape. This deformation is called ovalisation (figure 6.11). As the width of the ring increases, additional horizontal soil stresses arise until a new equilibrium is reached. On the one hand, this ovalisation is determined by the stiffness of the soil and on the other hand by the stiffness of the lining. The stiffness of the lining is not only determined by the bending stiffness (EI), but also by the strain stiffness (EA).

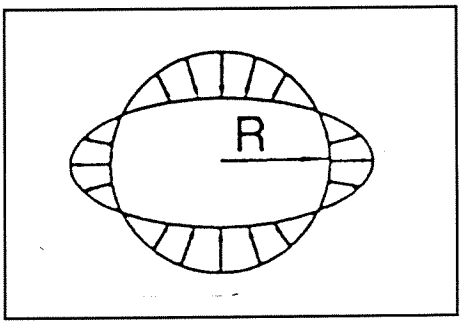

figure 6.11: ovalisation

Deformation of the longitudinal section (beaming).
The tunnel tube can be schematised in longitudinal direction as a beam. The support of the tunnel tube by the ground is equal to the resistance from the surrounding ground against deformation and is modelled as an elastic foundation (see figure 6.12).
The deformation of the tunnel in longitudinal direction is called beaming; it takes place when the characteristics of the ground, wherein the tunnel is bedded, change over a short range. At this transition of soil characteristics the settlement is irregular. As result the tunnel tube deforms and extra stresses are introduced. The tunnel lining has to transfer this stresses without losing its functionality [lit,20].

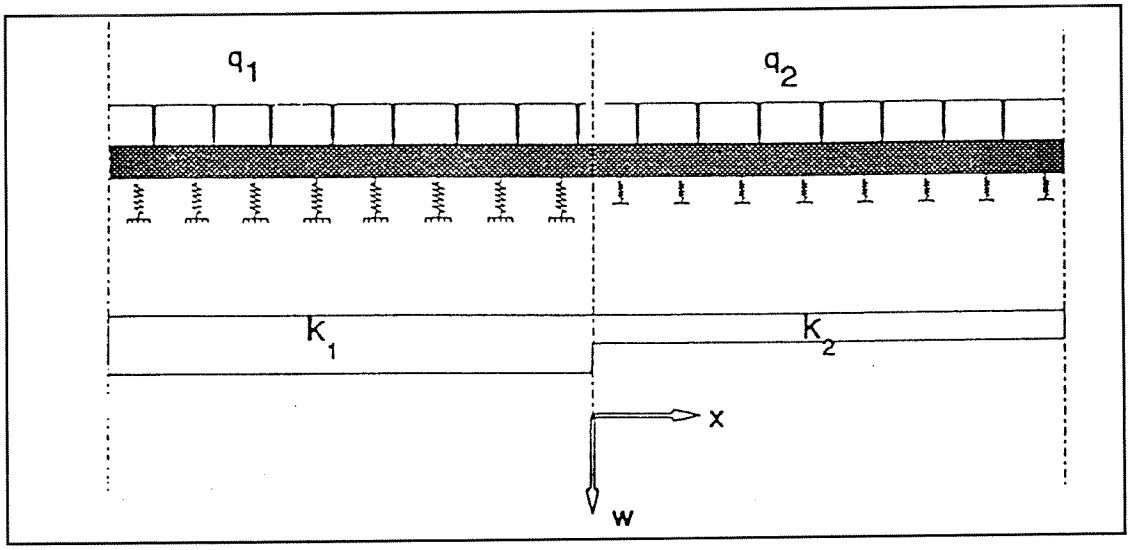

figure 6.12: beam supported by springs

with:
k = subgrade factor [kN/m^3];
q = load [kN/m^2]; = k . w ; w = settlement [m]

All rights reserved. Use of disclosure of this data is subject to the restriction stated on the first page of this document.

All rights reserved. Use of disclosure of this data is subject to the restriction stated on the first page of this document.

7. Reliability analysis (linear approach)

In this chapter a reliability analysis of the tunnel lining in the final phase is executed. The failure criterion of the lining is based on the load case 'combination of hoop force and bending moment' and is determined with the N&M diagram of steelfibre reinforced concrete. The reliability function of the analysis is determined in paragraph 7.1 based on this failure criterion. The reliability analysis is executed with a level II computation AFDA.. The input of AFDA is presented in paragraph 7.2. Next, in paragraph 7.3, the results of the reliability analysis are given. It can be concluded that the lining does not meet the requirements in all the considered cases. The most remarkable conclusion, however, is that the safety increases with increasing lining thickness. As this conclusion does not meet the expectations, the effect of non-linearity on the cross-section forces is examined in the following chapters.

7.1 Reliability function and acceptable failure probability

The reliability function[17] of the load case 'combination of hoop force and bending moment' is determined with the N&M diagram. The curve of the diagram is considered as failure boundary.

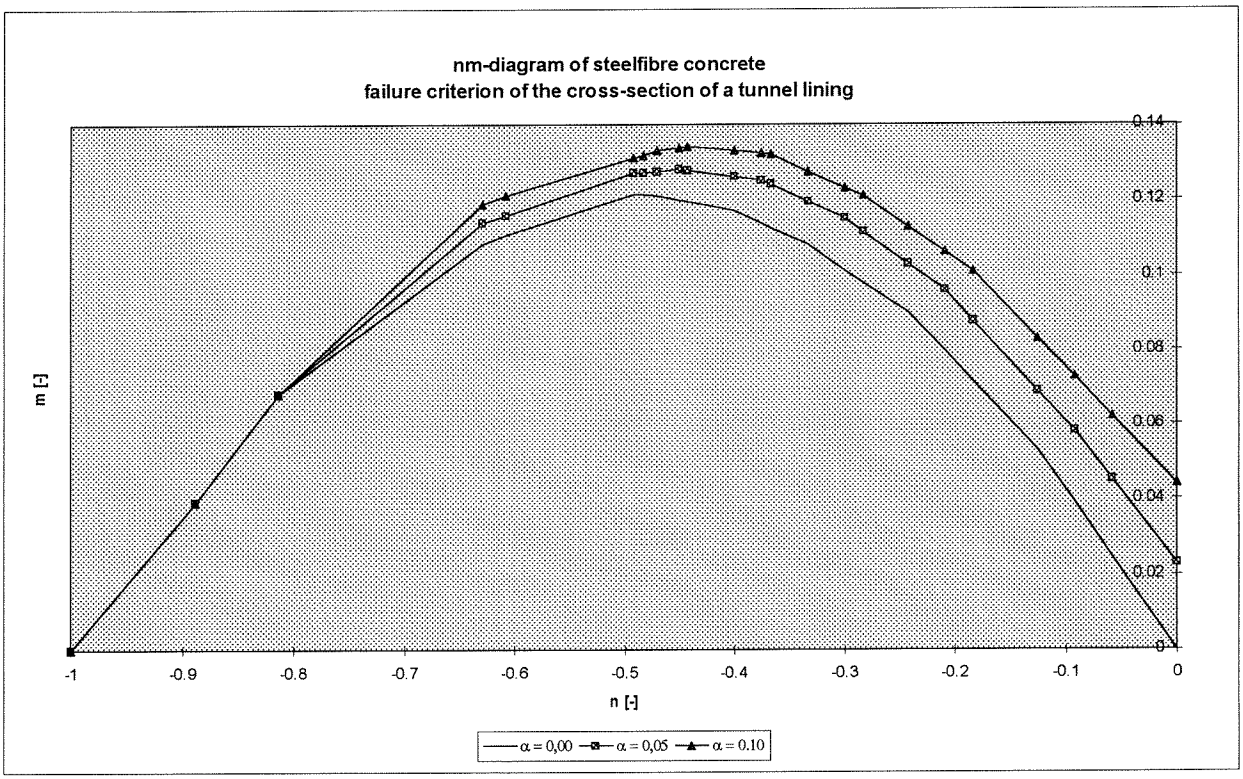

figure 7: failure criterion of the cross-section of a tunnel lining (the α of the legend refer to the steel fibre content ($\alpha = \alpha_{SFRC}$)

[17] The definition of reliability function is given in chapter 4, paragraph 4.4.1

All rights reserved. Use of disclosure of this data is subject to the restriction stated on the first page of this document.

Definition of the reliability function

- The failure boundaries are determined with the N&M diagram (see figure 6.10) for α_{SFRC} = 0,00 (i.e. concrete with no tensile strength, this is not equal to plain concrete), α_{SFRC} = 0,05 and α_{SFRC} = 0,10. The trendlines of these curves are defined as (see appendix 8):

α_{SFRC} = 0,10 : $m = -0{,}4505n^2 - 0{,}4016n + 0{,}043$ (7.1)

α_{SFRC} = 0,05 : $m = -0{,}4695n^2 - 0{,}44n + 0{,}0236$ (7.2)

α_{SFRC} = 0,00 : $m = -0{,}4876n^2 - 0{,}4812n + 0{,}0012$ (7.3)

with:

$$m = \frac{M}{\beta_R \cdot b \cdot d_{lining}^{\ 2}} = \frac{M_{max}}{Mu}$$

$$n = \frac{N}{\beta_R \cdot b \cdot d_{lining}} = \frac{N\,min}{Nu}$$

Mmax = maximum moment in the lining [kNm], (load)
Nmin = minimum hoop force in the lining [kN], (load)
Nu = ultimate hoop force determined with the N&M diagram [kN], (resistance)
Mu = moment (which is used in m to make it dimensionless) [kNm]. (resistance)

- Equations 7.1, 7.2 and 7.3 are combined and made function of α. This gives the following failure criterion (as function of α_{SFRC}):

$m = E\,n^2 + D\,n + C$ (7.4)

with:
E = $0{,}18\,\alpha_{SFRC}^{\ 2} + 0{,}353\,\alpha_{SFRC} - 0{,}4876$
D = $-0{,}56\,\alpha_{SFRC}^{\ 2} + 0{,}852\,\alpha_{SFRC} - 0{,}4812$
C = $-0{,}6\,\alpha_{SFRC}^{\ 2} + 0{,}478\,\alpha_{SFRC} + 0{,}0012$

- Equation 7.4 is rewritten into the following reliability function Z:

$$Z = M_u \cdot \left(C + D \cdot \left(\frac{N_{min}}{N_u} \right) + E \cdot \left(\frac{N_{min}}{N_u} \right)^2 \right) - M_{max} \quad (7.5)$$

This reliability function can be interpreted as follows:

Z = R_Z - S = Resistance - Load
= (ultimate bending moment) - (maximum bending moment in the lining)

with:
R_Z = $M_u(C - D(N_{min}/N_u) - E(N_{min}/N_u)^2)$,
S = $M_{max} = \dfrac{\sigma_v \cdot (1 - K_0) \cdot R^2}{4 + 0.342 \cdot \alpha_{Duddeck}}$

The definition of Z in AFDA is presented in appendix 9.

All rights reserved. Use of disclosure of this data is subject to the restriction stated on the first page of this document.

Acceptable failure probability
The calculated failure probability has to be compared with some target value, i.e. an acceptable failure probability. If the calculated failure probability is larger than the target value, the structure is considered to be unsafe.
Based on the present Dutch building codes ([lit, 14, 27], see table 4.2) the acceptable failure probability for the tunnel is equal to 10^{-4} and the reliability index β = 3,6 . These values are valid for a single mechanism and a reference period of 100 years (see paragraph 4.3).

7.2 Stochastic variables (input of AFDA)

The applied stochastic variables in AFDA with their mean value μ, variation coefficient V and standard deviation σ are given in table 7.1.
All the variables are supposed to have a normal distribution with the exception of:
- the resistance-parameters with a variation coefficient V > 0,15 ,
- the model factors,

which are supposed to be better represented by a lognormal distribution.

stochastic variable	distribution	description	μ	V[18]	σ
$K_{0,water}$	normal	coefficient of lateral pressure of the water [-]	1,0	0,01	0,01
K_0	normal	coefficient of lateral earth pressure [-] (sand / clay)	0,46 / 0,70	0,10	0,046 / 0,07
n_p	normal	porosity [-] (sand / clay)	0,36 / 0,55	0,03	0,011 / 0,017
g	deterministic	acceleration of gravity [m/s^2]	9,81	0,00	0,00
S_{dry}	normal	degree of saturation of the dry soil [-] (sand / clay)	0,4 / 0,8	0,01	0,004 / 0,008
S_{wet}	normal	degree of saturation of the wet soil [-] (sand / clay)	1,0	0,01	0,01
ρ_k	normal	density of the grains [kg/m^3]	2650	0,01	26,5
ρ_{water}	normal	density of the water [kg/m^3]	1000	0,01	10,00
γ_{water}	normal	volume weight of the water [kN/m^3]	10,0	0,01	0,10
R	normal	radius of the tunnel [m]	4,7	0,01	0,05
d_{lining}	normal	thickness of the tunnel lining [m]	0,4	0,05	0,02
h_{gw}	normal	phreatic surface [m - NAP]	1,0	0,00	0,50
h_{tunnel}	deterministic	depth of the tunnel-axis with respect to the groundlevel [m - NAP] (deep profile / shallow profile)	22,5 / 13,5	0,00	0,00
h_{river}	normal	waterlevel of the river [m + NAP]	9,0	0,00	0,50
f	lognormal	compressive concrete strength [N/mm^2]	43,2	0,15	6,48
E_g	lognormal	modulus of elasticity of the soil [Mpa] (sand / clay)	25 / 4	0,25	6,25 / 1,00
E_{lining}	normal	modulus of elasticity of the lining [N/mm^2]	33500	0,10	3350
α_{SFRC}	normal	ratio between the tensile- and the compressive concrete strength [-]	0,05 0,00 0,10	0,05	0,003 0,000 0,005
mb	lognormal	model factor for concrete [-]	1,00	0,10	0,10
mN	lognormal	model factor for the hoop force [-]	1,00	0,10	0,10
mM	lognormal	model factor for the bending moment [-]	1,00	0,20	0,20
φ_{creep}	lognormal	creep coefficient [-]	1,50	0,20	0,30
ν	normal	Poisson's ratio [-]	0,30	0,20	0,06

table 7.1: stochastic variables used in the reliability function Z

[18] The variation coefficient V is determined according to [lit,28, 18, 42]

All rights reserved. Use of disclosure of this data is subject to the restriction stated on the first page of this document.

Remarks

- The dry and the wet volume weight of the soil are correlated by means of the packing of the grains in the soil, i.e. the pore volume. These parameters should be expressed as function of the pore volume [lit, 53]:

$$\gamma_{wet} = S_{wet} \cdot n_p \cdot \rho_{water} \cdot g + (1 - n_p) \cdot \rho_k \cdot g$$

$$\gamma_{dry} = S_{dry} \cdot n_p \cdot \rho_{water} \cdot g + (1 - n_p) \cdot \rho_k \cdot g$$

with:

γ_{dry} = dry volume weight of the soil [kN/m^3];
γ_{wet} = wet volume weight of the soil [kN/m^3];
ρ_{water} = density of the water [kg/m^3];
ρ_k = density of the grains [kg/m^3];
S_{wet}, S_{dry} = degree of saturation [-] (S_{wet} = 1, complete saturation; S_{dry} = 0, dry soil; as in reality the soil is not completely dry, a value of S_{dry} unequal to zero is defined);
n_p = porosity [%].

The definition of the variation coefficients of S_{wet}, S_{dry}, n_p and ρ_k is based on the variation coefficients of γ_{wet} and γ_{dry} which are both equal to 0,05 according to [lit, 28].

- The formulae of the analytical Duddeck method, used in the reliability analysis, are based on *dry* soil. Consequently, the parameter K_0 is based on a dry soil situation. This means that K_0 can be interpreted as the ratio between the horizontal and the vertical *soil* stresses or as the ratio between the horizontal and the vertical *effective* stresses. For the reliability analysis, the latter (and real) definition of K_0 has to be used in order to model the overconsolidation of the soil correctly. As the Dutch soil is wet, the waterpressures have to be incorporated into the model separately by means of $K_{0,water}$ =1,0 . Summarising, the calculation of the cross-section forces is splitted up into two situations which have to be superposed to get the correct results (see appendix 2 for an example):
  1- only water with $K_{0,water}$ = 1,0
  2- only soil with: $K_{0,sand}$ = 0,46 ; $K_{0,clay}$ = 0,70 and $\gamma'_{wet} = \gamma_{wet} - \gamma_{water}$ (γ'_{wet} is used instead of γ_{wet} to discount the upward pressure of the water).
  This approach is applied in the reliability analysis.

- The modulus of elasticity of the lining E_{lining} is lower under load of long duration than under load of short duration due to creep. By introducing this reduced E_{lining} in the calculation the loads will decrease and the deformations will increase. The long term $E_{lining,\infty}$ is introduced in the reliability analysis as:

$$E_{lining,\infty} = \frac{E_{lining}}{1 + 0.75 \cdot \varphi} \qquad [\text{N/mm}^2]$$

with:

φ = creep coefficient = 1,5 [-] (see table 5.1)

- Duddeck uses in his formulae the modulus of elasticity of the soil according to the oedometertest, i.e. the modulus of elasticity of the soil in case of two-sided prevented deformation:

$$E_{oed} = \frac{(1 - \upsilon)}{(1 + \upsilon) \cdot (1 - 2\upsilon)} \cdot E_g$$

with: E_g = real value of the modulus of elasticity of the soil [Mpa];
υ = Poisson's ratio [-].

- Definition of the mean value of the compressive concrete strength μ_f :

$X_{kar} = \mu - 1{,}64\sigma$
$\mu = X_{kar} / (1\text{-}1{,}64\ V)$
with: B45 , f'_{ck} = 45 N/mm^2 , V=0,15
$X_{kar} = 0{,}72\ f'_{ck}$
μ_f = 43,2 N/mm^2

All rights reserved. Use of disclosure of this data is subject to the restriction stated on the first page of this document.

- Definition of the mean value of d_{lining}:
  The minimum value of d_{lining} that can be guaranteed is 0,40m. That is why the mean value of d_{lining} is assumed to be equal to 0,40m which is a conservative approach. Deviations of this value can be caused by the following 2 effects:
  1- Thickening of the lining due to:
  - inhomogeneous parts in soil,
  - inaccuracies in the regulation of the pressure of the injection system.
  2- Thinning of the lining due to:
  - hard obstacles in the soil (e.g. stones),
  - air locked in the concrete in the injection system (although this is very unlikely).
  Deviations of the lining thickness due to above mentioned effects are improbable, so that the mean value of d_{lining} is chosen equal to 0,40m.

- In behalf of the reliability analysis, the parameter α_{SFRC} should be splitted up in basic variables according to the formula:

$$\alpha_{SFRC} = \frac{0.37 \cdot \beta_{BZ,R}}{\beta_R}$$

with:
$\beta_{BZ,R}$ = tensile strength [N/mm^2];
β_R = compressive concrete strength [N/mm^2].

As a dataset is needed to determine the tensile strength, the exact value of α_{SFRC} can not be determined at this moment. It is recommended, however, to execute the reliability analysis as function of the basic variables $\beta_{BZ,R}$ and β_R whenever a dataset is available.

7.3 Results of the reliability analysis

The results of the reliability analysis are given in table 7.2, 7.3 and 7.4.

	deep 1	**deep 2**	**shallow 1**	**shallow2**
β	1.7	1.3	3.0	2.8
Pb	4.7E-2	9.0E-2	1.2E-3	2.6E-3

table 7.2: results of the reliability analysis with α_{SFRC} = 0.00

	deep 1	**deep 2**	**shallow 1**	**shallow2**
β	2.9	2.5	4.4	4.2
Pb	2.1E-3	5.8E-3	4.8E-6	1.3E-5

table 7.3: results of the reliability analysis with α_{SFRC} = 0.05

	deep 1	**deep 2**	**shallow 1**	**shallow2**
β	3.6	3.2	5.2	5.0
Pb	1.8E-4	5.8E-4	1.0E-7	3.1E-7

table 7.4: results of the reliability analysis with α_{SFRC} = 0.10

All rights reserved. Use of disclosure of this data is subject to the restriction stated on the first page of this document.

7.3.1 Impact of the input-parameters on the results of the reliability analysis

A special virtue of the AFDA reliability analysis is that it can serve quickly to indicate the sensitivity of the solution across the range of possible input parameters by means of the output parameter α_{AFDA}. In this way the parameters that principally cause the limit state are determined; these parameters should get priority in study or quality control.
The values of table 7.5 are valid for the case α_{SFRC} = 0,05.

stochastic parameter	α_{AFDA} [*10^{-2}] deep1	α_{AFDA} [*10^{-2}] deep2	α_{AFDA} [*10^{-2}] shallow1	α_{AFDA} [*10^{-2}] shallow2
K_{0water}	1.10	1.10	1.30	1.40
K_0	30.40	61.10	29.20	55.70
S_{wet}	-0.80	-1.80	-1.00	-2.20
S_{dry}	0.00	-0.10	0.00	0.00
n_p	4.40	9.50	5.10	11.50
ρ_k	-0.40	-0.40	-0.50	-0.50
ρ_{water}	-0.80	-1.80	-1.00	-2.20
h_{gw}	-6.90	-9.60	0.00	0.00
h_{river}	0.00	0.00	3.10	3.30
γ_{water}	3.40	4.40	4.30	5.70
R	1.70	-1.80	1.10	-2.20
d_{lining}	-8.00	8.50	-5.20	10.60
E_g	50.50	24.20	48.20	23.70
υ	24.50	13.90	21.00	12.50
E_{lining}	-19.40	-9.60	-18.10	-9.30
ϕ creep coefficient	23.40	10.70	23.30	10.70
f	21.30	21.60	22.90	23.30
m_b	14.30	14.50	15.30	15.60
m_N	17.20	17.40	17.90	18.30
m_M	-62.40	-63.20	-65.80	-67.30
α	4.50	4.50	5.00	5.10

table 7.5: impact of the input parameters on the solution of the reliability analysis

Conclusions

- m_M, K_0, E_g, ν, f and φ_{creep} have the largest impact on the failure of the tunnel; consequently, the definition of the magnitude of these parameters should get priority;
- the impact of K_0 on the failure of the tunnel is larger in clay than in sand;
- the impact of E_g, E_{lining}, φ_{creep} and ν on the failure of the tunnel is larger in sand than in clay.

All rights reserved. Use of disclosure of this data is subject to the restriction stated on the first page of this document.

7.4 Conclusions

- The safety requirements (Pb = 10^{-4} and β_{target} = 3,6) are only met in the case of
  - α_{SFRC} = 0,00: none of the geotechnical profiles;
  - α_{SFRC} = 0,05: only the shallow profiles;
  - α_{SFRC} = 0,10: all the geotechnical profiles with exception of deep 2.

  Hence it follows that concrete without tensile strength (α_{SFRC} = 0,00) does not meet the requirements and that the addition of steelfibres gives a considerable increase of the reliability of the construction. This result has to be handled with care however, because the reliability analysis is based on the analytical Duddeck model which is a very conservative model for the calculation of cross-section forces (see paragraph 6.3.1, figure 6.7 and 6.8). In fact, this analysis should be executed with a more realistic model, like e.g. PLAXIS. As there is not yet an computerised version available of PLAXIS combined with a probabilistic analysis, the reliability analysis has to be carried out manually. A possible working procedure is presented in appendix 7.
- The failure probability is the largest in case of a deep tunnel in clay. The fact that the failure probability is larger in case of deeper tunnels can be explained by the magnitude of the cross-section forces and specially by the magnitude of M_{max}. As M_{max} is larger in case of deeper tunnels and N_{min} remains approximately constant, the failure probability will also be larger.
  The failure probability is larger in case of a clay profile than in case of a sand profile. This can be explained by the stiffness of the soil, which is much larger in sand than in clay.
- As the bending moments decline with smaller bending stiffness of the lining (see figure in appendix 3) a thinner lining is favourable to prevent or to reduce tensile stresses and a thicker lining is favourable to prevent failure of the compression mode.
- According to figure 7.1, the safety requirements are on the whole better met for a more flexible and thinner lining. This is due to the considerable decrease of M_{max} with decreasing lining thickness.

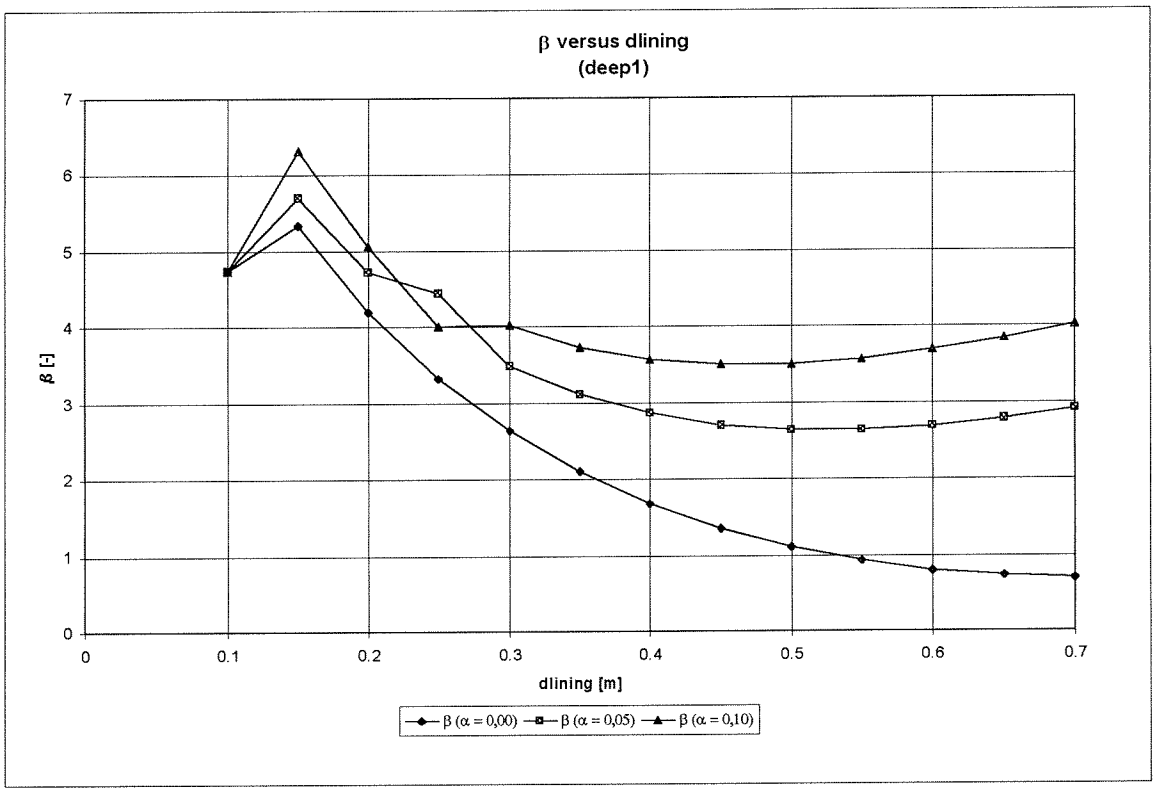

figure 7.1: d_{lining} versus reliability index β (long term) (The α in the legend of the graph refer to the steel fibre content ($\alpha = \alpha_{SFRC}$)
remark: figure 7.1 is only valid in case of linear elasticity

All rights reserved. Use of disclosure of this data is subject to the restriction stated on the first page of this document.

β decreases with increasing d_{lining} from d_{lining} = 0,15m. From d_{lining} = 0,60m (α_{SFRC} = 0,05) and d_{lining} = 0,50m (α_{SFRC} = 0,10) β starts increasing with increasing d_{lining} . In case of α_{SFRC} = 0,00 , β keeps decreasing with increasing d_{lining} until at least d_{lining} = 0,70m. A lining thickness larger than 0,70m is not examined because it is assumed to be not realistic.
This behaviour can be explained as follows:
The increase or decrease of β with increasing d_{lining} depends on the amount of increase of M_{max} (ΔM_{max}) with respect to the amount of increase of d_{lining} (Δd_{lining} =0,05m) (see figure 7.2):
- β decreases with an increase of d_{lining} when ΔM_{max} increases; in other words the load (M_{max} = S) increases more in proportion to the resistance (d_{lining} = R_Z);
- β increases with an increase of d_{lining} when ΔM_{max} decreases; in other words the load increases less in proportion to the resistance.
As the reliability index β_{AFDA} = $\mu(z)$ / $\sigma(z)$, the reliability increases with increasing value of Z (Z = R_Z - S) and decreases with decreasing value of Z.
- From d_{lining} < 0,10m the safety decreases rapidly. At d_{lining} < 0,10m the bending moment is very small, so this sudden decrease is due to failure of the compression mode caused by the hoop force N.

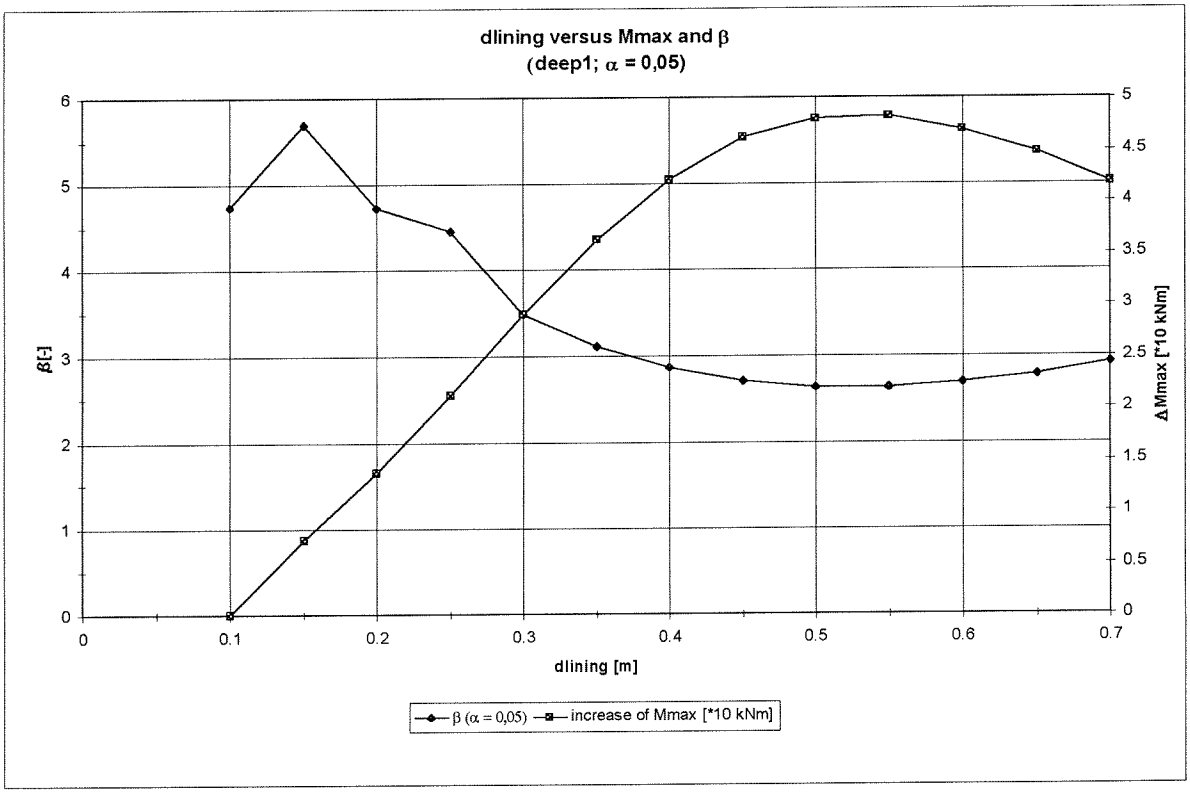

figure 7.2: d_{lining} versus ΔM_{max} and β (the α in the legend and the title of the graph refer to the steel fibre content (α = α_{SFRC}))
remark: figure 7.2 is only valid in case of linear elasticity

- In case of thin linings, i.e. d_{lining} = 0.10 m, serviceability requirements (watertightness, allowable displacements) have to be taken into account.
- The analytical Duddeck model has some limitations of application:
  - it assumes the material behaviour of soil and lining as being linear-elastic, while neither the soil nor, usually, the tunnel lining, behave in an elastic manner;
  - the geometrical and the physical non-linearity of the construction are not taken into account.
  These limitations should be expressed in terms of boundary conditions for the application of the linear model in a situation where non-linear effects play a part.
- In spite of the limitations, the method serves as a first, and very useful, indication of the principal factors, prior to a more refined analysis. These factors are m_M, K_0, E_g, ν, f and φ_{creep}.

All rights reserved. Use of disclosure of this data is subject to the restriction stated on the first page of this document.

Summarising, the following non-linear effects have not been taken into account in the reliability analysis:

- plastic material laws of soil and lining (see paragraph 8.1)
- non-linearity of the soil springs (see paragraph 8.2)
- second order effects: - geometric non-linearity (chapter 9)
  - physical non-linearity (chapter 10)

The reliability of the analysis will increase when these effects are taken into account. Nevertheless, the linear characteristic of an elastic or visco elastic analysis has great merit, particularly when, as frequently occurs, limitations of knowledge of the behaviour of the soil do no justify greater elaboration.

In short

There is a real merit in applying a simple method of analysis to a tunnel design problem then immediate recourse to computer methods, which may as a second stage far better serve in reproducing a more valid representation of the problem. The question is whether the assumption of linearity of the behaviour of soil and concrete is likely to be acceptable within the limitations of any two-dimensional tunnel analysis. In the following the non-linear effects and mainly the geometrical non-linear effect will be examined.

All rights reserved. Use of disclosure of this data is subject to the restriction stated on the first page of this document.

All rights reserved. Use of disclosure of this data is subject to the restriction stated on the first page of this document.

8. Non-linear elastic effects

In this chapter a general review is given of the non-linear properties of the soil and the concrete. Concrete does not behave linear elastic under strain of tension, due to crackformation[19], and under large pressure, i.e. when the concrete becomes plastic.
The plasticity of the soil and the concrete is described in paragraph 8.1. Next, in paragraph 8.2, a rough approach is given of the limit of the linearity of the soil springs. Finally, an introduction is given to the non-linear effects which will be examined in the following chapters, i.e. the geometrical and the physical non-linearity.

8.1 Plasticity of concrete and soil

The analytical Duddeck model assumes the material behaviour of soil and lining as being linear-elastic, while neither the soil nor, usually, the tunnel lining, behave in an elastic manner.
When the lining stiffness decreases, the lining, and therefore also the soil, will tend to deform: the more flexible the tunnel lining, the more the ground will loosen at the top and bottom of the tunnel due to ovalisation. This unloading, however, will not go on for ever, because the ground and the lining become plastic.

Plasticity of the soil
The earth pressure acting on the tunnel largely depends on the degree of displacement. The earth pressure acting on a tunnel from above can easily become loosening earth pressure with minute displacement of the ground above. Conversely, minute ascension generates earth pressure which is larger than the original earth cover load. At the sides of the tunnel, displacement at the tunnelling wall generates horizontal strain of the soil. In short, the magnitude of earth pressure acting on a tunnel is largely dependent on not only the tunnel depth and soil properties but also on displacement at the tunnelling wall in both the vertical and horizontal directions. Moreover, strain in the ground due to displacement may create a plastic zone.
In most cases the consideration of the plastic behaviour requires the application of numerical methods (e.g. FEM, like PLAXIS).

Plasticity of the concrete
In plastic or ultimate design the load capacity is exhausted when the structure fails by a collapse mode. For tunnel linings this may be replaced by the less restricting condition that plastic hinges have been developed. Within the non-linear analysis the ultimate 'load' may be reached by increasing the ground pressure as well as by decreasing the strength parameters, thus, working at least in first approximations with splitted safety factors.

[19] steelfibre concrete has a favourable behaviour after crackformation

All rights reserved. Use of disclosure of this data is subject to the restriction stated on the first page of this document.

8.2 Non-linearity of the soil springs

The assumption of linearity of the soil springs is closely connected with the deformation of the soil. The range wherein the soil springs can be assumed to be linear should be expressed in terms of a range of deformations of the tunnel lining and the soil wherein the assumption of linearity is valid. The limit of linearity of the soil springs given in this chapter is very rough and will only be used as an indication for the calculations made in this report.

As a general rule, the soil springs can be assumed to be linear when the displacements are small. The following rule of thumb can be given to determine the range wherein the assumption of linearity of the soil springs is valid [reference, FUGRO]:

$$\varepsilon = \frac{u}{R} < 0{,}5\ \%$$

with:

ε = strain = 0,5 % (remark: in reality there is a large difference between ε_{clay} and ε_{sand})
R = radius = 4700 mm;
u = displacement or deformation [mm].

$u = \varepsilon \cdot R = 0.005 \cdot 4700 = 23.5\ mm \approx 25\ mm$ (round off upwards)

This means that, as first approach, the soil springs can be assumed to be linear in case of displacements smaller than 25 mm. As the displacements of the lining of the considered situations (deep1, deep2, shallow1, shallow2) are smaller than 25mm, the assumption of linearity of the soil springs is justified.

As this is a very rough approach, further investigation on this topic is recommended.

8.3 Second order effects

Shell constructions, like tunnel linings, function optimal when they are only loaded by hoop forces. This means that bending moments have to be avoided as much as possible. Consequently the tunnel lining is sensitive for variations in the radial loads and the displacements. That is why second order effects have to be considered at the computation of the axial section of the lining.
The following non-linear effects have to be taken into account:
- geometrical non-linearity,
- physical non-linearity.

Geometrical non-linearity
In the linear mechanics, the calculations are based on the undeformed construction. Such calculations are called geometric linear or first order calculations.
When the stability of a construction is examined, the equilibrium of the deformed construction has to be checked. Such calculations are called geometric non-linear or second order calculations.
This non-linear effect will be examined thoroughly in chapter 9.
In figure 8.1 the geometrical linear behaviour versus the geometrical non-linear behaviour is presented.

All rights reserved. Use of disclosure of this data is subject to the restriction stated on the first page of this document.

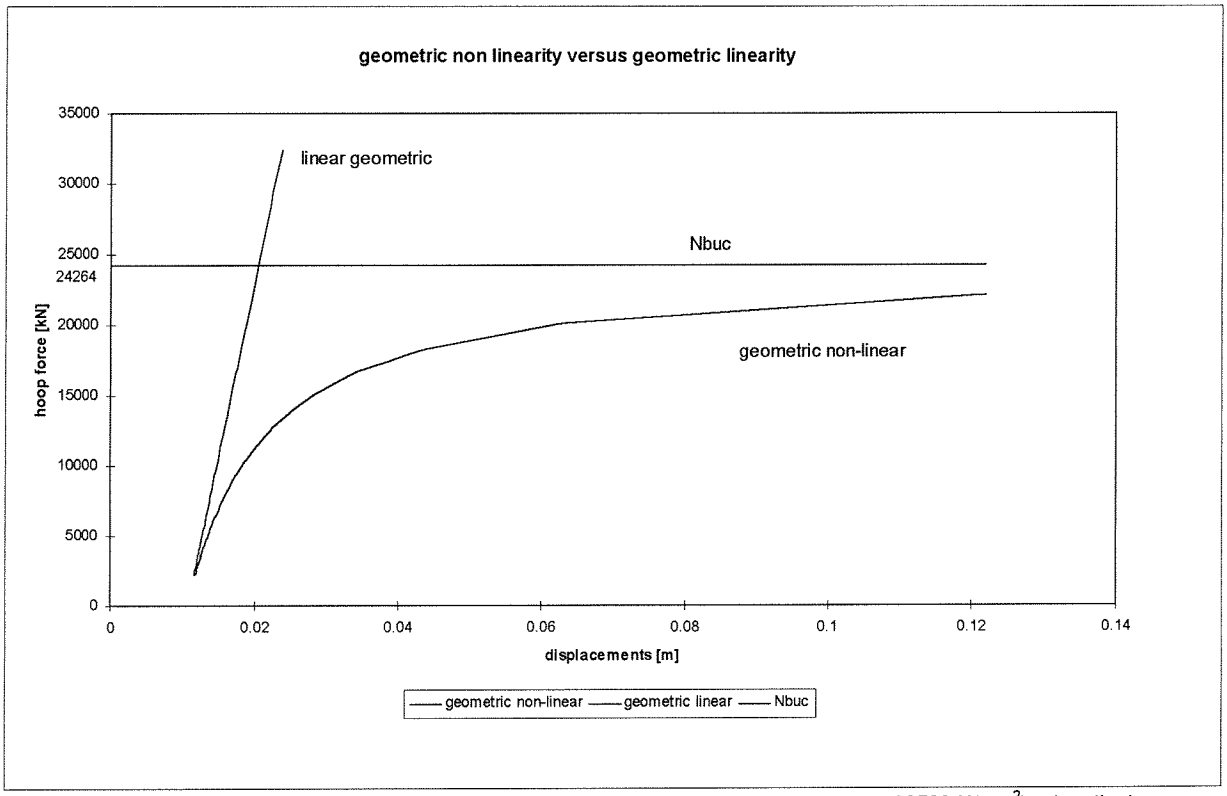

figure 8.1: behaviour according to a linear and a non-linear computation (in case of $E_{lining,\ short\ term}$ = 33500 N/mm^2); when the hoop force equals N_{buc} , the construction fails by buckling.

Physical non-linearity

When the lining cracks, EI decreases. Furthermore, EI also decreases with time as E_{lining} decreases under load of long duration due to creep. A decrease of EI unloads the tunnel lining and consequently the lining attracts smaller loads. The decrease of EI due to crackformation is called physical non-linearity.
This phenomenon also contributes to the geometrical non-linear effect, as a decrease of EI causes an increase of the displacements and consequently an increase of the geometrical non-linearity.
Important is to define the ratio between these contrary effects, i.e. the increase of the moments due to the geometrical non-linear effect and the decrease of the moments due to the physical non-linear effect. The latter is examined in chapter 10.

All rights reserved. Use of disclosure of this data is subject to the restriction stated on the first page of this document.

In short:
The impact of the geometrical and the physical non-linearity on the cross-section forces N_{min} and M_{max} given in literature is presented in figure 8.2. The geometrical non-linear effect increases M_{max} with respect to the first order linear theory, while the physical non-linear effect decreases M_{max}.

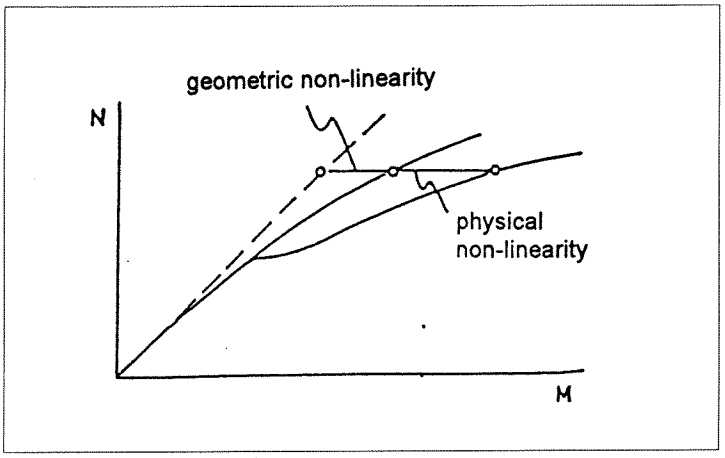

figure 8.2: impact of the 2nd order effects on the cross-section forces [lit,48]

All rights reserved. Use of disclosure of this data is subject to the restriction stated on the first page of this document.

9. The geometrical non-linear effect

In this chapter a study is carried out into the influence of the geometrical non-linear effects in tunnel tubes. This study is executed because insufficient knowledge is available on the effects due to deformations of the tunnel-construction. These effects can influence the instability, the deformations, rotation and the tension of the lining. First a study of existing literature about these effects and a calculation based on this literature are carried out. The results are compared with those of a calculation of the geometrical non-linear effect in case of the ITM-tunnel. The conclusion drawn of this analysis is that the calculated second order bending moments correspond with those defined according to the literature, i.e. an increase of the moments with respect to those calculated with the first order linear theory of approximately 10% in the short term and 15% in the long term.

9.1 Theory of elasticity of second order

The bedded lining is principally a slender compressed structure, so that the question may arise whether the ring can fail by buckling or the deformed ring has to be analysed.
The failure of the tunnel lining in the final phase can be caused by:

- exeedance of the strength (compression / tension mode (crackformation));
- instability (buckling).

When the stability of the construction is examined the 'buckling force' (F_{buc}) has to be taken into account, i.e. the force by which the equilibrium of the construction is at its limit. When the forces in the construction become larger than F_{buc}, the bearing capacity decreases and the construction deforms rapidly and finally buckles and collapses.

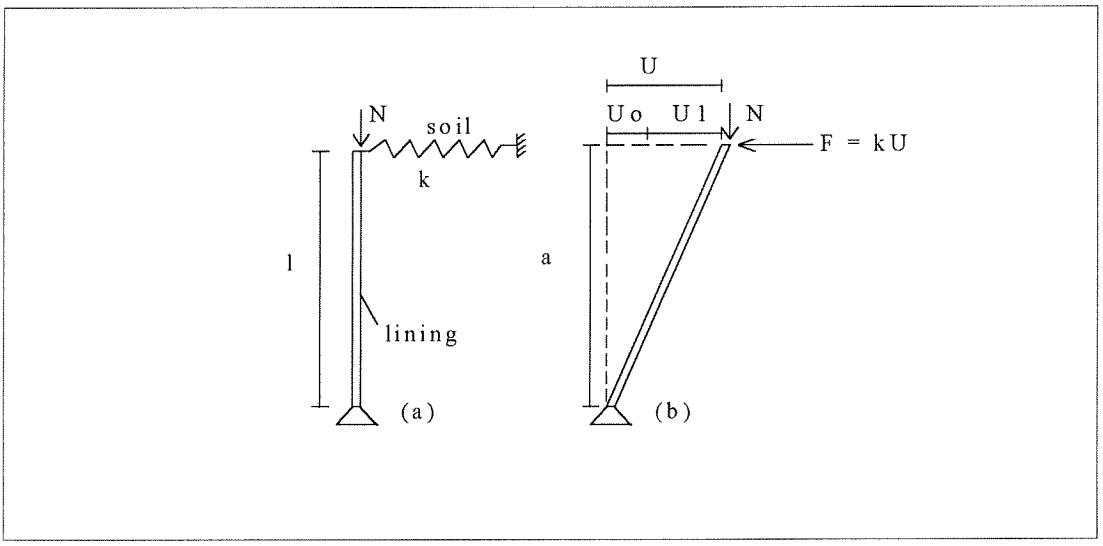

figure 9.1: buckling

with:

k	= spring stiffness (linear-elastic)	[kN/m];
u	= displacement	[m];
F	= force in the spring as result of the displacement u (fig. 9.1b)	[kN].

In spite of the linear elastic behaviour of the spring, there is a non-linear relation between F and u. This is caused by the impact of the changing geometry on the cross-section forces.

All rights reserved. Use of disclosure of this data is subject to the restriction stated on the first page of this document.

A displacement u_0, causes an increase of the bending moment M of N . u_0 (see figure 9.1). Due to the additional moment N.u_0 , the construction has to deform with u_1 in order to restore the equilibrium. But this deformation causes again an additional moment N.u_1 , with as result a deformation u_2, etc. so that eventually[20]:

$$u = u_0 + u_1 + u_2 + \ldots =$$

$$= u_0 \cdot \left(1 + \frac{1}{n_{buc}} + \frac{1}{n_{buc}^{\ 2}} + \frac{1}{n_{buc}^{\ 3}} + \ldots \right) = \frac{n_{buc}}{n_{buc} - 1} \cdot u_0$$

with:

u	= second order displacement	[m];
u_0	= first order displacement	[m];
$n_{buc}/(n_{buc}-1)$	= amplification factor[21]	[-];
N_{buc}	= critical or buckling force[22] under uniform external pressure [lit, 47] $= \frac{3 \cdot EI}{R^2}$	[kN];
E	= modulus of elasticity	[kN/m^2];
I	= moment of inertia = (1/12).b.d$^3_{lining}$	[m^4];
R	= radius	[m].

The eventual displacement u is equal to the summation of a geometrical series and is finite when $n_{buc} > 1$ or $N_{buc} > N$. When N becomes larger than N_{buc} or $n_{buc} < 1$, the displacements grow rapidly and finally the construction buckles and collapses.

The resulting moment, including geometrical non-linearity equals[23]:

$$M = M_0 + \frac{n_{buc}}{n_{buc} - 1} \cdot u_0 \cdot N \qquad (9.1)$$

with:

M	= second order bending moment	[kNm];
M_0	= first order bending moment	[kNm];
N	= hoop force	[kN];
u_0	= initial displacement (or eccentricity)	[m];
n_{buc}	= N_{buc} / N	[-].

---

[20] equilibrium (figure 9.1): N . u_0 = F_0 . l = k . u_0 . l => $F_0 = N \cdot \frac{u_0}{l}$ and N_{buc} = k . l

displacement u_1: $u_1 = \frac{F_0}{k} = \frac{N \cdot u_0}{k \cdot l} = \frac{N}{N_{buc}} \cdot u_0 = \frac{1}{n_{buc}} \cdot u_0$ and $F_1 = N \cdot \frac{u_1}{l}$

displacement u_2: $u_2 = \frac{F_1}{k} = \frac{N \cdot u_1}{k \cdot l} = \frac{N}{N_{buc}} \cdot u_1 = \frac{1}{n_{buc}} \cdot u_1 = \frac{1}{n_{buc}^{\ 2}} \cdot u_0$ etc.

[21] The expression $n_{buc}/(n_{buc}-1)$ is in fact only valid for constructions with one degree of freedom. When there are more degrees of freedom a more complex expression should be derived. However, when the displacements are small, like those of a tunnel lining, it is allowed to use $n_{buc}/(n_{buc}-1)$. Another requirement for the use of this expression is: $N_{buc} >> N$ or $n_{buc} >> 1$ [lit,49].

[22] The definition of N_{buc} given here, is conservative as this expression gives the buckling force of an unsupported ring without hinges loaded by an uniform radial load while the loads which cause the instability are positively influenced by the presence of a bedding. The reason for this approach is that the displacements increase slowly, through which the support at the sides of the ring is less due to relaxation and creep of the soil (appendix 13). It should be investigated whether the coefficient 3 in the formula is correct when it is applied in the calculation of a tunnel lining.

[23] Remark: M_0 is in reality also a hoop force multiplied by a displacement, which also inclines due to the geometrical non-linear effect. This effect is not taken into account in equation 9.1 .

All rights reserved. Use of disclosure of this data is subject to the restriction stated on the first page of this document.

The magnitude of the geometrical non-linear effect depends on the ratio n_{buc} between the buckling force and the hoop force.
The hoop forces N do not change significantly with bending deformations. Therefore, a second order 'bending' theory can be applied introducing N as a constant value which acts on the deformed geometry of the bedded ring.
As long as the deformation mode does include the buckling mode, the second order theory covers also the instability problem.

9.2 Definition of the geometrical non-linearity according to literature

In this paragraph the geometrical non-linear effect is defined with models found in literature. The following models are used:
- Duddeck,
- Ahrens.

Another model found in literature is that of Windels [lit, 52]. Windels determines the cross-section forces and displacements including the geometrical non-linear effect, and not a second order factor like Ahrens does. This model is not used in this report.

Starting points of above mentioned models:
- both the models of Ahrens and Windels use the model of Duddeck as starting point, i.e. a bedded ring with radial springs;
- the above mentioned models are based on rather stiff and dry ground (e.g. sand), through by the ratio between the horizontal and vertical earth pressure is equal to approximately 0.5 ($K_0 \cong 0{,}5$). In the case of wet ground, waterpressures have to be taken into account in order to obtain the correct hoop force in the ring, which is necessary for the consideration of the second order effect.

9.2.1 Duddeck

In figure 9.2 the cross-section forces M and N versus the angle φ are presented for the cases linear-, geometrical non-linear- and physical non-linear behaviour.

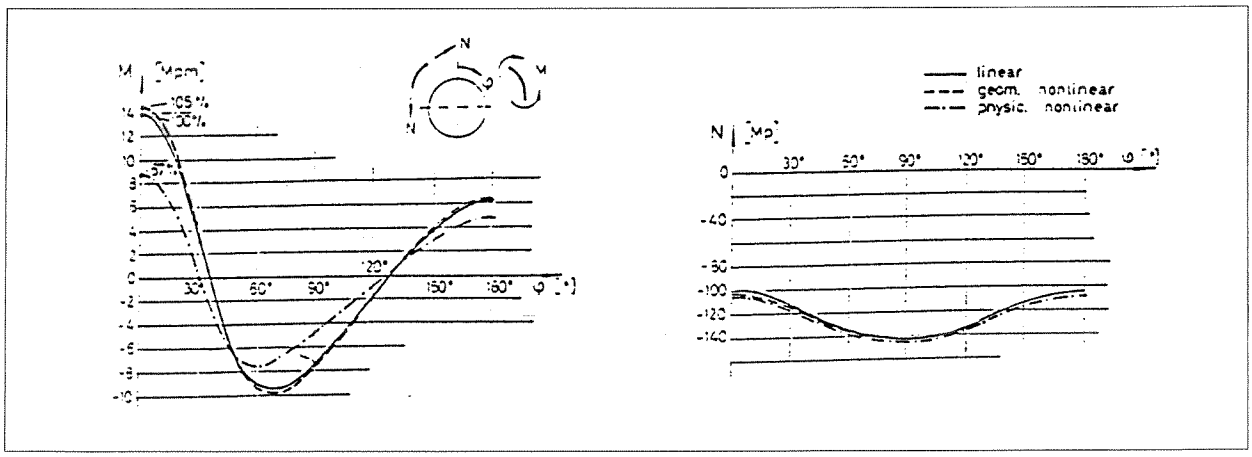

figure 9.2: M and N for a concrete lining with d_{lining} = 0.20 m R = 2.65 m including plastic material behaviour [lit, 50]
(φ = angle with respect to the top of the tunnel: $\varphi_{top} = 0^0$)

Conclusion
- According to Duddeck (figure 9.2) the effect of geometrical non-linearity on the cross-section forces is of minor importance.
- Physical non-linearity gives a considerable deviation of the bending moments; according to figure 9.2, the physical non-linearity is the largest in case of $\varphi = 0^0$.
- The above mentioned conclusions have to be handled with care because the used Duddeck model is based on *dry* ground.

All rights reserved. Use of disclosure of this data is subject to the restriction stated on the first page of this document.

9.2.2 Ahrens

The Ahrens [lit,45] model is valid under the condition that N in the lining is not or minimally influenced by the second order effects.

Ahrens computes the second order effect factor $n_{AHRENS} = M_{II}/M_I$ with design-graphs. In these graphs (appendix 12) the ratio n_{AHRENS} is plotted out over a factor β_{AHRENS} on a logarithmic scale:

M_{II} = second order bending moment [kNm];
M_I = first order bending moment [kNm];

β_{AHRENS} = ground/lining stiffness ratio = $\frac{k_r \cdot R^4}{EI} = \frac{E_s \cdot R^3}{EI}$; $k_r = \frac{E_s}{R}$

(notice that: $\beta_{AHRENS} = \alpha_{DUDDECK}$)

with:

k_r = bedding modulus [MN/m^3];
E_s = modulus of elasticity according to the oedometertest
$= \frac{(1-\upsilon)}{(1+\upsilon)\cdot(1-2\upsilon)} \cdot E_g$
E_g = modulus of elasticity of the ground [MPa];
I = moment of inertia = (1/12).b.d_{lining} [m^4].

The graphs are valid for a given radius R, the earth pressure p_v at the top of the tunnel and the bending stiffness of the tube EI':

$$EI' = EI + N \cdot (1+\kappa) \cdot \frac{R^2}{3}$$

with:

EI' = reduced bending stiffness of the lining [MNm^2];
EI = bending stiffness of the lining [MNm^2];
N = N_0 = constant part of the hoop force of the lining [kN];
(according to Duddeck (see appendix 1))
κ = W_o/W_1 [-];
with: W_0 = dimensional variation = R/200 [m];
W_1 = first order radial displacement [m].
The ITM tunnel does not have dimensional variations, so the parameter κ = 0.

All rights reserved. Use of disclosure of this data is subject to the restriction stated on the first page of this document.

As the graphs are based on homogenous ground without groundwater and K_0 = 0,5 , the factor n_{AHRENS} of the graphs has to be multiplied with an amplification factor in order to adjust to the water pressures[24]. Otherwise the hoop forces and consequently the geometrical non-linear effects are underrated. The amplification factor is defined as follows:

$n_{AHRENS,\ without\ water}$ * amplification factor = $n_{AHRENS,\ with\ water}$

with :

$n_{AHRENS} = M_{II} / M_I$

M_{II} = second order bending moment = $\dfrac{M_I + \dfrac{n_{buc}}{n_{buc} - 1} \cdot N \cdot u_1}{M_I}$

M_I = first order bending moment

n_{buc} = $\dfrac{N_{buc}}{N_{max}}$

N_{buc} = buckling force

The amplification factor can be derived as follows (subindex 1: situation without water; subindex 2: situation with water):

$n_{AHRENS,\ 1}$ * amplification factor = $n_{AHRENS,\ 2}$

$$\frac{M_I + \dfrac{n_{buc,1}}{n_{buc,1} - 1} \cdot N_1 \cdot u_1}{M_I} \cdot amplification - factor = \frac{M_I + \dfrac{n_{buc,2}}{n_{buc,2} - 1} \cdot N_2 \cdot u_2}{M_1}$$

$$\frac{M_I + \dfrac{n_{buc,1}}{n_{buc,1} - 1} \cdot N_1 \cdot u_1}{M_I} \cdot \frac{M_I + \dfrac{n_{buc,2}}{n_{buc,2} - 1} \cdot N_2 \cdot u_2}{M_I + \dfrac{n_{buc,1}}{n_{buc,1} - 1} \cdot N_1 \cdot u_1} = \frac{M_I + \dfrac{n_{buc,2}}{n_{buc,2} - 1} \cdot N_2 \cdot u_2}{M_1}$$

The amplification factor with which the readings ($n_{AHRENS,\ without\ water}$) of the graphs of Ahrens have to be multiplied:

$$amplification - factor = \frac{M_I + \dfrac{n_{buc,2}}{n_{buc,2} - 1} \cdot N_2 \cdot u_2}{M_I + \dfrac{n_{buc,1}}{n_{buc,1} - 1} \cdot N_1 \cdot u_1} \qquad (9.2)$$

[24] The geometrical non-linear effect is larger in case of groundwater because:
- With time the soil passes on from loading medium to load-carrying medium; water does not have this positive load reducing property.
- The hoop force N is larger in case of wet ground than in case of dry ground.

All rights reserved. Use of disclosure of this data is subject to the restriction stated on the first page of this document.

In table 9.1 general dependencies with respect to the second order effect factor n_{AHRENS} are presented. These are derived from the graphs of Ahrens (appendix 12).

(diminished) parameter	**n_{AHRENS} = M_{II} / M_I**
ratio of stiffness β_{AHRENS}	increase
bedding modulus kr	increase
lining stiffness: EI (of curve) EI (in factor β)	 increase decrease
load p_v	decrease
radius R	decrease

table 9.1: general dependencies derived from Ahrens

Remarks:

- As the geometrical non-linear effect decreases with decreasing p_v, the shallower the tunnel, the smaller the geometrical non-linear effect.
- There are some contrary effects with respect to the following parameters, which appear both in the factor β_{AHRENS} and as coefficient of the graphs:
  - radius R:
  R in factor β_{AHRENS} : a smaller R leads to a larger geometrical non-linear effect;
  R as coefficient of the graph: a smaller R corresponds with a curve which lays lower in the graph with as result a smaller geometrical non-linear effect.
  - bending stiffness EI:
  EI in factor β_{AHRENS}: a smaller EI leads to a smaller geometrical non-linear effect;
  EI as coefficient of the curve in the graph: a smaller EI leads to a larger geometrical non-linear effect.

  These contrary effects are probably due to the contrary effects of two other phenomenons, i.e. physical- and geometrical non-linear non-linearity.

The geometry (R), the bending stiffness (EI) and the load (p_v) of the ITM tunnel lining do not correspond to the coefficients of the graphs, so that an interpolation and extrapolation have to be executed to determine the geometrical non-linear effect.

Results of the analysis according to Ahrens (appendix 12)
(remark: only uncracked concrete is taken into consideration)

The calculation of the geometrical non-linear effect is executed for two situations:
1. uncracked concrete in the short term with E_{lining} = 33500 N/mm^2 ;
2. uncracked concrete in the long term with EI_{00}[25] calculated as follows [lit, 48]:

$$E_{\infty} = \frac{E_{lining}}{1 + \frac{3}{4} \cdot \varphi}$$

with:
φ = creep coefficient = 1.5 (see table 5.1: relative humidity: 85% ...100% (very humid))

[25]This is only an approach of the real long term EI_{00}, because the physical effect is not included, only the effect of creep is taken into account. Actually, E_{00} should be defined by means of a NMκ-diagram.

All rights reserved. Use of disclosure of this data is subject to the restriction stated on the first page of this document.

Geometrical non-linear effect in the short term: E_{lining} = 33500 N/mm^2

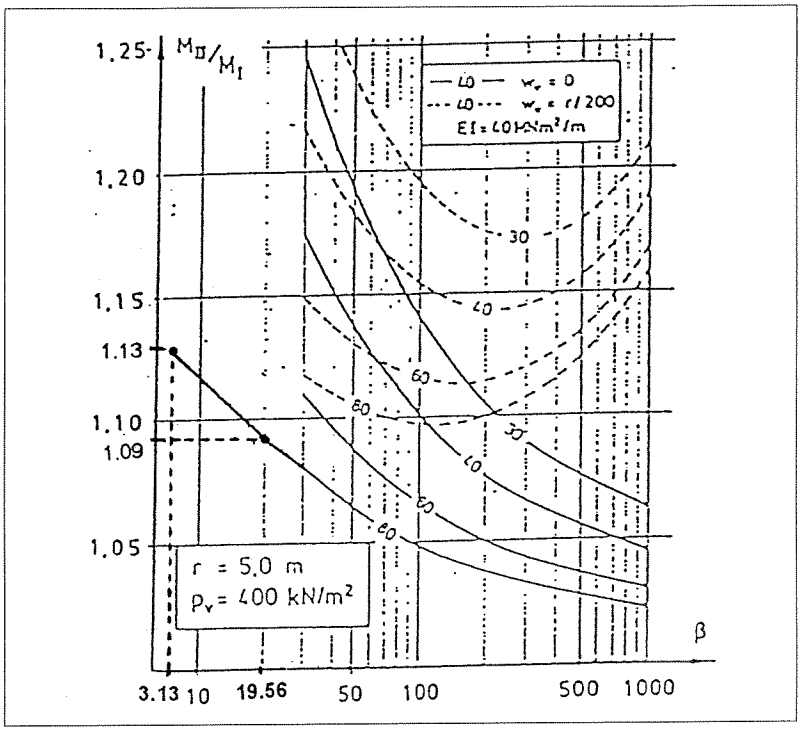

figure 9.3: readings short term calculation with:
r = R = 4.7m; EI = 80 MNm^2/m; $\beta_{AHRENS,\ sand\ profile}$ = 19,6 ; $\beta_{AHRENS,\ clay\ profile}$ = 3,1

geotechnical profile	p_v [kN/m^2]	n_{AHRENS} (without groundwater) = reading	n_{AHRENS} after linear inter- / extrapolation (no groundwater)	amplification factor	n_{AHRENS} (including ground-water)
deep 1	196	1,09	1,044	1,036	1,08
deep 2	123	1,13	1,040	1,036	1,08
shallow 1	88	1,09	1,020	1,036	1,06
shallow 2	53	1,13	1,017	1,035	1,05

table 9.2: geometrical non-linear effect according to Ahrens: $n_{AHRENS} = M_{II} / M_I$ (short term)
$n_{AHRENS\ (including\ groundwater)}$ = amplification factor * $n_{AHRENS\ (without\ groundwater)}$

All rights reserved. Use of disclosure of this data is subject to the restriction stated on the first page of this document.

Geometrical non-linear effect in the long term: E_{00} (according to equation 5.2) (only creep is included, not the physical non-linearity): E_{00} = 15764.7 N/mm^2

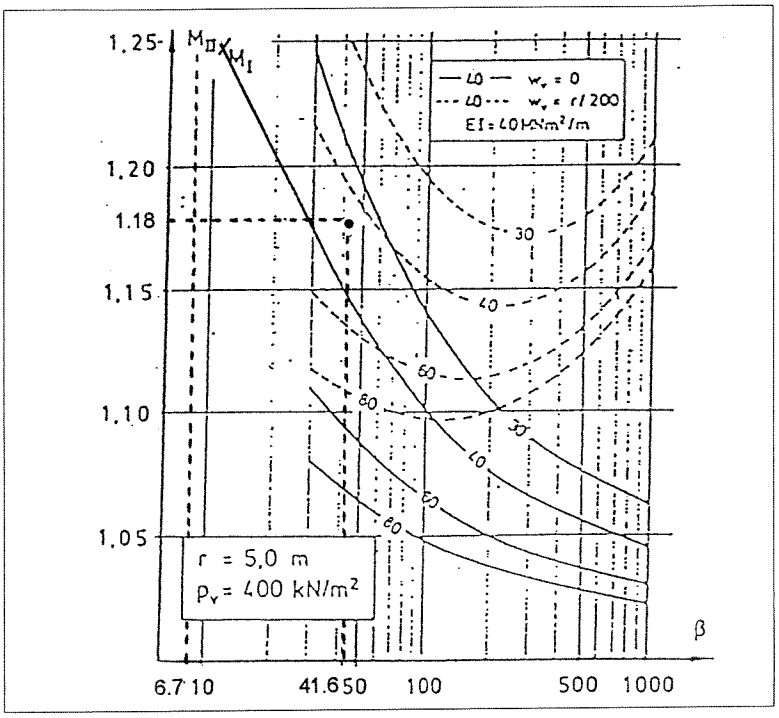

figure 9.4: readings long term calculation with:
r = R = 4,7m; EI = 35 MNm^2/m; $\beta_{AHRENS,\ sand\ profile}$ = 41,6 ; $\beta_{AHRENS,\ clay\ profile}$ = 6,7

geotechnical profile	p_v [kN/m^2]	n_{AHRENS} (without groundwater) = reading	n_{AHRENS} after linear inter- / extrapolation (no groundwater)	amplification factor	n_{AHRENS} (including ground-water)
deep 1	196	1,18	1,088	1,079	1,17
deep 2	123	1,25	1,077	1,080	1,16
shallow 1	88	1,18	1,040	1,092	1,12
shallow 2	53	1,25	1,033	1,079	1,11

table 9.3: geometrical non-linear effect according to Ahrens: $n_{AHRENS} = M_{II} / M_I$ (long term)
$n_{AHRENS\ (including\ groundwater)}$ = amplification factor * $n_{AHRENS\ (without\ groundwater)}$

Conclusions

- In the Ahrens model, the ratio between the horizontal and vertical load is based on dry ground with K_0 = 0,5 . This ratio is very important for the computation of the correct load p_v and geometrical non-linear effect factor n_{AHRENS}. In the considered profiles, this ratio is essentially different (K_0 . 0,46 ... 0,7) through by the results will rather differ.
- The hoop force N increases in wet ground with regard to dry ground; consequently the geometrical non-linear effect will be larger in wet ground than in dry ground. This effect is adjusted in the computation by means of an amplification factor (equation 9.2).
- The geometrical non-linear effect is larger in the deep profiles and smaller in the shallow profiles; this sequence is equal to the sequence of the magnitude of the load p_v.
- The smaller $\beta_{AHRENS} = E_s.R^3 / EI$, i.e. smaller R and E_s and larger E_{lining} and d_{lining}, the larger the geometrical non-linear effect.
- The deeper the tunnel, the larger the effect of the water on the geometrical non-linearity.
- The geometrical non-linear effect is larger in clay (due to a smaller E_s) than in sand.
- As the values of the input-parameters p_v and R for the ITM-tunnel do not appear in the graphs, the definition of n_{AHRENS} is based on inter- and extrapolations. This means that the results have to

All rights reserved. Use of disclosure of this data is subject to the restriction stated on the first page of this document.

be interpreted with care. As the values of p_v in the graphs are rather high, the graphs are probably meant for deeper tunnels than the ITM tunnel.

- For the considered sections, the geometrical non-linear effect is proven to be of considerable importance, with values of about 1,05 to 1,08 in the short term and 1,11 to 1,17 in the long term.

9.3 Calculation of the geometrical non-linear effect in case of the ITM-tunnel

The calculation is carried out for the geotechnical profile deep1, because in this case the geometrical non-linear effect is expected to be the largest according to Ahrens (see paragraph 9.2).
The purpose of the calculation[26] is to determine:

- d_{lining} at which the geometrical non-linear effect starts playing a part;
- d_{lining} at which the construction fails due to the geometrical non-linear effect.

9.3.1 Working procedure

- Calculation of the second order moments M_{II} due to geometrical non-linearity with equation 9.1:

$$M_{II} = M_I + \frac{n_{buc}}{n_{buc} - 1} \cdot u_0 \cdot N_{\min}$$

The amplification factor $n_{buc}/(n_{buc} -1)$ is determined with: $n_{buc} = N_{buc}/N_{max}$ and $N_{buc} = 3EI/R^2$
This is a conservative approach, because:
- the maximum value of N is used instead of the varying N along the circumference;
- N_{buc} is determined for an unsupported ring; the reason for this approach is that the displacements increase slowly, through which the support at the sides of the ring is less due to relaxation and creep of the soil (see appendix 13).

- The calculated M_{II} are checked on:
-failure by buckling:
criterion: $n_{buc} <1$
-failure of the compression mode:
criterion: M_{II} is checked with the failure curves of the N&M-diagram (figure 6.10); these are described in equations (7.1 to 7.3).

A parameter study is executed to determine the impact of the decline of the following variables on the geometrical non-linear effect:

- d_{lining}:
a lower d_{lining} can be the result of the choice of a lower design-value or due to crackformation (physical non-linearity, see chapter 10);
- E_{lining}:
a decline of E_{lining} under load of long duration due to creep;
- EI
i.e. a decline of E_{lining} combined with a decline of d_{lining}.

[26] the calculation in this paragraph is conservative because the plasticity of the concrete and the ground and the physical-non linearity are not taken into account.

All rights reserved. Use of disclosure of this data is subject to the restriction stated on the first page of this document.

9.3.2 Calculation results

In appendix 14, the results of the geometrical non-linear computation of the geotechnical profile deep1 are given.

Summarising:

- Failure by buckling:

  - due to a decrease of $d_{lining,0}$,
  d_{lining} = 0,17m

  - due to a decrease of $E_{lining,0}$
  no buckling

  - due to a combined decrease of d_{lining} and E_{lining} :
  buckling starts playing a part from d_{lining} < 0,20 m combined with a reduction of E_{lining} of 40%.

- Failure of the compression mode:

  - due to a decrease of $d_{lining,0}$,
  d_{lining} = 0,19m : in case of the failure curve as function of α_{SFRC} = 0,00
  d_{lining} = 0,18m : in case of the failure curve as function of α_{SFRC} = 0,05
  (failure also takes place in case of d_{lining} = 0,40m , α_{SFRC} = 0,00; but this is due to the conservatism of the Duddeck model).

  - due to a decrease of $E_{lining,0}$,
  failure takes place at a reduction of E_{lining} of 10%; this is due to the conservatism of the analytical Duddeck method

  - due to a combined decrease of d_{lining} and E_{lining} :

d_{lining} [m]	reduction of $E_{lining,0}$ [%]	α_{SFRC} [-]	M_{II}/M_{I}
0,20	30	0,05	6,6
0,20	20	0,00	3,6

table 9.4: failure of the compression mode due to a decline of EI

remark
In case of α_{SFRC} = 0,00 and a reduction of $E_{lining,0}$ of 10%, the lining just not collapses (limit of failure).

All rights reserved. Use of disclosure of this data is subject to the restriction stated on the first page of this document.

9.3.3 Conclusions

- A decrease of d_{lining} causes:
  - an increase of the deformations u;
  - a decrease of N_{min};
  - a decrease of M_I,

  but an increase of the geometrical non-linear effect and consequently an increase of M_{II} . This means that the increase of u dominates the decrease of N_{min}.
- Buckling starts playing a significant part from $d_{lining} \leq 0{,}17$ m; if the long term effect (i.e. a decrease of E_{lining}) is also taken into account the lining fails by buckling from $d_{lining} = 0{,}20$ m combined with a decrease of E_{lining} of 40%.
- Failure of the tunnel lining due to compression takes place from:
  $d_{lining} = 0{,}20$ m combined with a decrease of E_{lining} of 20% in case of $\alpha_{SFRC} = 0{,}00$
  $d_{lining} = 0{,}20$ m combined with a decrease of E_{lining} of 30% in case of $\alpha_{SFRC} = 0{,}05$
- As failure due to compression occurs before buckling, failure of the compression mode is the decisive failure mechanism.
- The geometrical non-linear effect increases with decreasing lining thickness according to table 9.5.

d_{lining} [m]	$n_{buc} = N_{buc} / N_{max}$ (short term)	M_{II} / M_I (short term)	$n_{buc} = N_{buc} / N_{max}$ (long term)	M_{II} / M_I (long term)
0,50	22,3	1,03	10,6	1,08
0,45	16,6	1,05	7,9	1,11
0,40	11,9	**1,07**	5,7	**1,16**
0,35	8,1	1,11	3,9	1,27
0,30	5,2	1,18	2,5	1,51
0,25	3,1	1,37	1,5	2,62
0,22	2,1	1,70	1,0	**buckling**
0,20	1,6	2,26		
0,17	1,0	**buckling**		

table 9.5: geometrical non-linear effect in the short term ($E_{lining} = 33500$ N/mm^2) versus long term ($E_{00} = 15764{,}7$ N/mm^2, according to equation 5.2)

Boundary condition: an increase of M with 20% ($M_{II} / M_I < 1{,}20$) due to the geometrical non-linear effect is acceptable on the condition that no failure of the compression mode takes place. Consequently, the geometrical non-linear effect starts playing a part from $d_{lining} < 0{,}30$m in the short term and from $d_{lining} < 0.40$m in the long term.

- For the considered section, the geometrical non-linear effect is proven to have to be taken into account. The bending moments increase with 10% in the short term and with 15% in the long term. However, in case of more slender constructions, i.e. $d_{lining} < 0{,}40$m the geometrical non-linear effect starts playing a part and can not be neglected, specially when the long term effect is considered.

In short

- d_{lining} at which the geometrical non-linear effect starts playing a part:
  short term: $d_{lining} < 0.30$ m
  long term: $d_{lining} < 0.40$ m
- d_{lining} at which the construction fails due to the geometrical non-linear effect:
  $d_{lining} < 0.20$ m

All rights reserved. Use of disclosure of this data is subject to the restriction stated on the first page of this document.

9.4 Conclusions

The following conclusions can be drawn from the examination of the geometrical non linear effect:

- The geometrical non-linear effect is larger in case of:
  - deeper tunnels,
  - smaller R, E_{lining}, E_g and d_{lining}.
- The geometrical non-linear effect is larger in case of wet ground, i.e. tunnels under the phreatic surface. The deeper the tunnel, the larger the effect of the water on the geometrical non-linearity.
- The results of the computation with Ahrens and the analytical computation are presented in table 9.6.

geotechnical profile	M_{II} / M_I (short term) literature (Ahrens)	M_{II} / M_I (short term) computation	M_{II} / M_I (long term) literature (Ahrens)	M_{II} / M_I (long term) computation
deep1	1,08	1,07	1,17	1,16
deep2	1,08	1,07	1,16	1,15
shallow1	1,06	1,06	1,12	1,14
shallow2	1,05	1,06	1,11	1,13

table 9.6: comparison of the geometrical non-linear effect according to literature versus the computation.

The following conclusions can be drawn from table 9.6:
- The close resemblance of the results of both methods supports the accuracy of the used models;
- The contribution of the geometrical non-linear effect on the cross sectional forces is proven to have to be taken into account, specially when EI is reduced (due to physical non-linearity or creep (long term effect)).

- d_{lining} at which the geometrical non-linear effect starts playing a part:
  short term: $d_{lining} < 0,30$ m
  long term: $d_{lining} < 0,40$ m
- d_{lining} at which the construction fails due to the geometrical non-linear effect:
  $d_{lining} < 0,20$ m
- For the considered sections, the geometrical non-linear effect is proven to have to be taken into account. The bending moments increase with 10% in the short term and with 15% in the long term. However, in case of more slender constructions, i.e. $d_{lining} < 0,40$m the geometrical non-linear effect starts playing a significant part and can not be neglected, specially when the long term effect is considered.
- Failure of the tunnel lining due to compression takes place from:
  $d_{lining} = 0,20$ m combined with a decrease of E_{lining} of 20% in case of $\alpha_{SFRC} = 0,00$
  $d_{lining} = 0,20$ m combined with a decrease of E_{lining} of 30% in case of $\alpha_{SFRC} = 0,05$
- The magnitude of the geometrical non-linear effect depends on the ratio between the buckling force and the hoop force. When the buckling force becomes larger than the hoop force the construction fails by buckling.
- Buckling starts playing a part from d_{lining} 0,17m; if creep of the concrete due to long duration load is taken into account, the lining fails by buckling from $d_{lining} = 0,22$m. In figure 9.5, the first order linear M_{max} versus the geometrical non-linear M_{max} are presented in the short term and the long term.

All rights reserved. Use of disclosure of this data is subject to the restriction stated on the first page of this document.

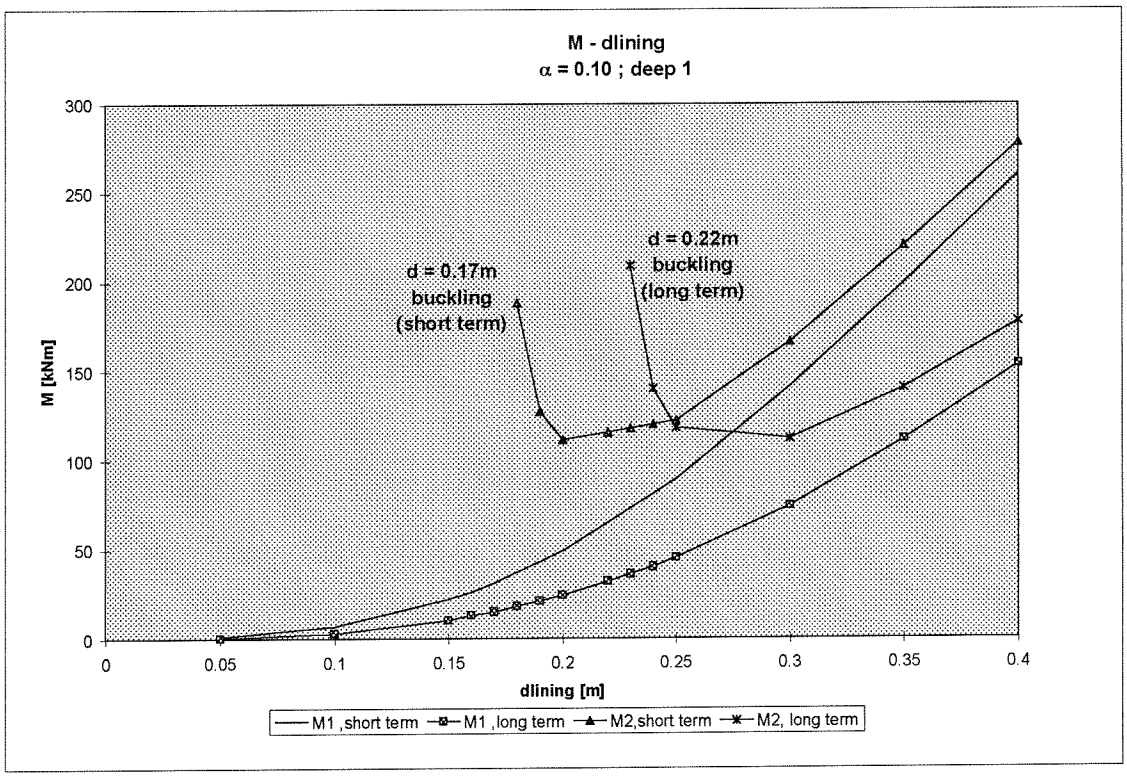

figure 9.5: first order linear bending moment (M1) versus geometrical non-linear bending moment (M2) (The α in the title of the graph refers to the steel fibre content ($\alpha = \alpha_{SFRC}$)

In contrast with the first order linear theory, M_{max} increases with decreasing d_{lining} due to the geometrical non-linear effect. As the physical non-linearity causes a contrary effect, i.e. a decrease of M_{max} with decreasing d_{lining}, both the effect should be taken into account to make a realistic analysis. Hence the physical-non linearity is examined in the following chapter.

All rights reserved. Use of disclosure of this data is subject to the restriction stated on the first page of this document.

All rights reserved. Use of disclosure of this data is subject to the restriction stated on the first page of this document.

10. The physical non-linear effect

In this chapter a study is carried out into the influence of the physical non-linear effect in tunnel tubes. In the first paragraph, the physical non-linearity is described and the aspects which have to be taken into account at the calculation of the physical non-linear effect are given. In paragraph 10.2, the physical non-linear effect is calculated for the ITM-tunnel (geotechnical profile 'deep1'). Then in paragraph 10.3, M is calculated including both the geometrical and the physical non-linear effect. From the results, it can be concluded that the physical non-linear effect causes a larger deviation of M than the geometrical non-linear effect. However, in case of slender constructions and including the long term effect (creep of the concrete) the impact of the geometrical non-linear effect increases with regard to that of the physical non-linear effect. It must be noticed that the combined effect of the non-linear effects is only examined for one situation in order to determine which of the non-linear effects governs over the other. A more thorough analysis is recommended in order to draw more general conclusions.

10.1 General

When the lining cracks, EI decreases. Furthermore, EI also decreases with time as the concrete becomes plastic and as E_{lining} decreases under load of long duration due to creep. A decrease of EI unloads the tunnel lining and consequently the lining attracts smaller loads. The decrease of EI due to crack formation is called physical non-linearity
In this report the physical non-linearity is not examined thoroughly. Only one situation (profile deep1) is examined in order to give an indication of the physical non linear behaviour with respect to the geometrical non-linear behaviour. The profile deep1 is chosen for the calculation as the geometrical non-linearity resulted to be the largest in this case (see paragraph 9.4).

The following points have to be examined at a physical non-linear calculation:

- definition of the diminished EI due to crack formation by means of a NMκ-diagram and computation of the second order bending moments;
- definition of plastic hinges as the reduction of the lining stiffness is local;
- examination of the amount of redistribution of forces due to the decrease of EI as consequence of crack formation; the simultaneous decrease of the resistance against deformation has to be taken into account.

Within the scope of this study, only the first aspect is examined.

All rights reserved. Use of disclosure of this data is subject to the restriction stated on the first page of this document.

10.2 Calculation of the physical non-linearity

In behalf of the calculation of the physical non-linearity, some NMK-diagrams have been determined (see appendix 15; for the definition of these diagrams is referred to [lit, 54]). These diagrams apply for the geotechnical profile deep1. Two of the curves have been drawn in figure 10.1, one with respect to the short term with E_{lining} = 33500 N/mm^2 and one with respect to the long term with E_{lining} = 15765 N/mm^2.

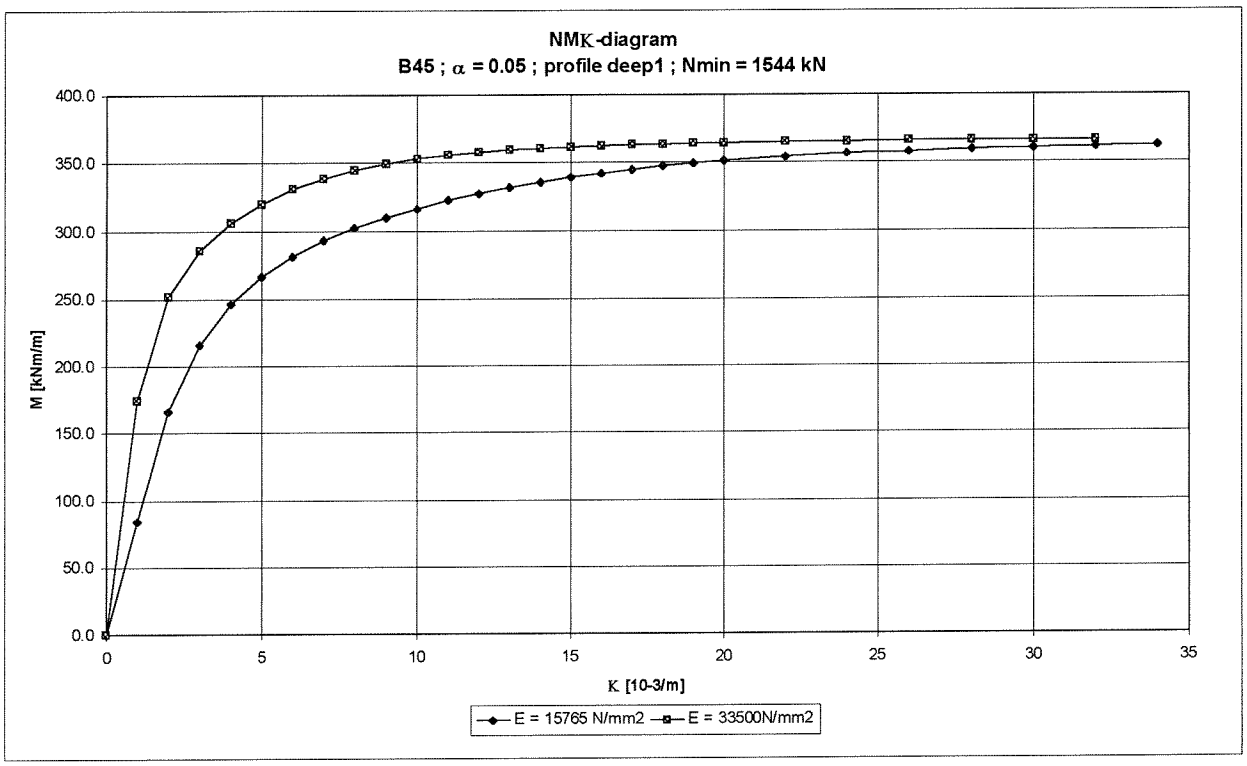

figure 10.1: NMK-diagrams [lit,54] (remark: these diagrams count only for the concrete strength class B45, d_{lining} =0,40m, N = 1544 kN and α_{SFRC} = 0,05)

Remark

- The NMK-diagrams of 10.1 are defined based on concrete without tensile strength that is already cracked. When these diagrams would be based on uncracked concrete with tensile strength, the elastic part of the curve would be larger.
- In appendix 15, a graph with NMK-diagrams for several N and d_{lining} is presented. The larger N (larger d_{lining}), the sooner the cross-section will fail by compression. The smaller N (smaller d_{lining}), the larger the ability to deform, but the smaller the ultimate M.

The calculation of M taking into account the physical non-linear behaviour of the concrete (M_{fnl}) is explained in figure 10.2.

All rights reserved. Use of disclosure of this data is subject to the restriction stated on the first page of this document.

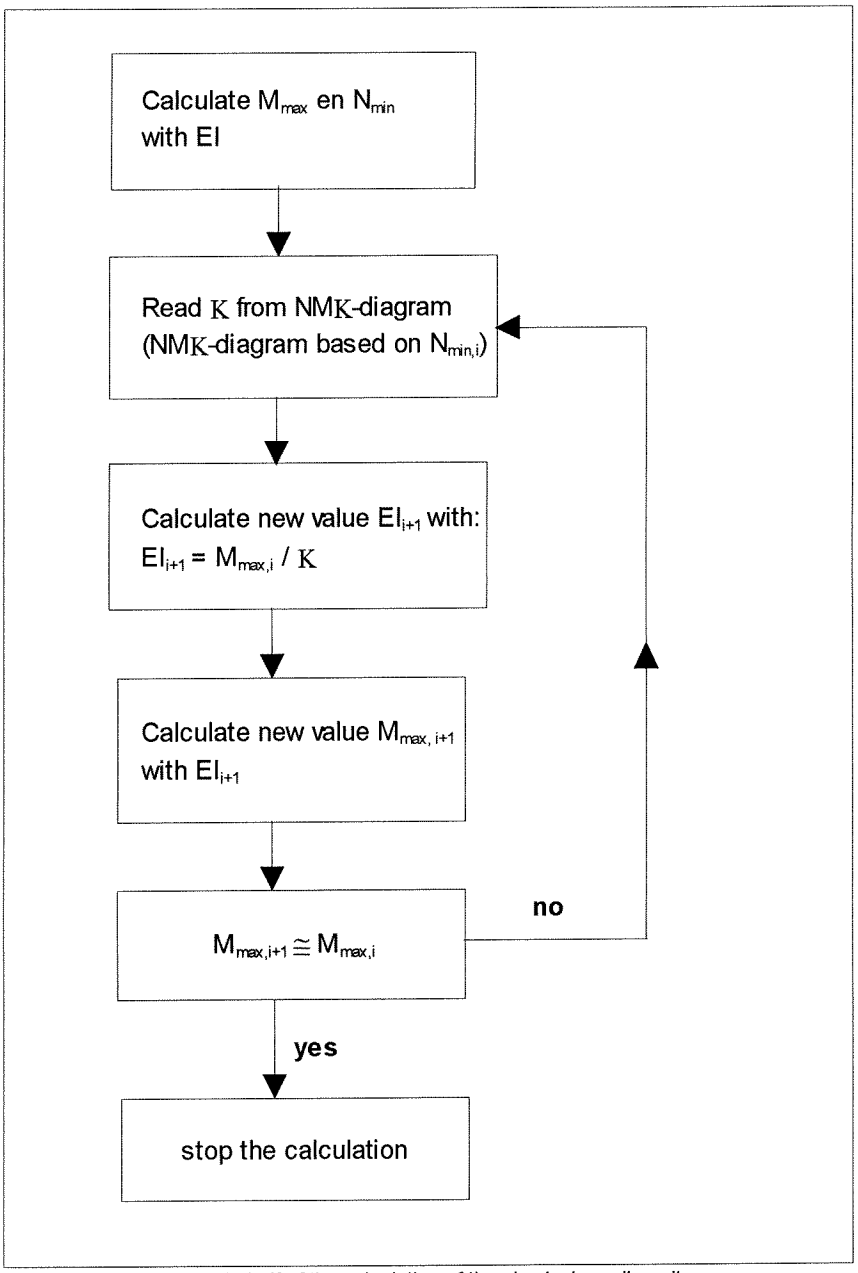

figure 10.2: scheme in behalf of the calculation of the physical non-linearity

The calculation of the cross-section forces, including the physical non-linear effect, executed in this chapter is based on some assumptions (according to figure 10.2):

- The calculation is executed with only one NMK-diagram per lining thickness. This is done instead of calculating a new NMK-diagram with N_{min} as function of $EI_{reduced}$ for each loop of the calculation.
- The analytical Duddeck method, used for the calculation of M_{max} and N_{min}, considers the cross-section as homogenous, while the reduction of the stiffness of the section is local due to local crack formation. This means that the reduction of the loads is also local and not along the whole ring like in the Duddeck model. The reduction of the stiffness will be the largest where the displacements are the largest and consequently in case of the maximum bending moment. In the rest of the section, the reduction of the stiffness will probably be none or minimum.
  As the reduction of the stiffness is considered along the whole ring in this study, the calculation results will be conservative. This neglect could be approached by using a lower EI as input of the calculation.

All rights reserved. Use of disclosure of this data is subject to the restriction stated on the first page of this document.

Results of the calculation of the physical non-linearity of a tunnel in geotechnical profile deep1 (d_{lining} = 0,40m, α_{SFRC} = 0,05):

short term (E_{lining} = 33500 MPa)
M_{max} according to Duddeck: M_{max} = 260.2 kNm with EI = 178.7 MNm^2
M_{max} calculated according to figure 10.2: M_{fnl} = 219.9 kNm with EI = 138.2 MNm^2

long term (E_{lining} = 15765 MPa)
M_{max} according to Duddeck: M_{max} = 152,7 kNm with EI = 84,08 MNm^2
M_{max} calculated according to figure 10.2: M_{fnl} = 151,3 kNm with EI = 83,06 MNm^2

Conclusion (with regard to d_{lining} = 0,40m)
- M_{max} reduces with 15% and EI with 23% in case of the short term evaluation.
- M_{max} and EI reduce only a little (1%) in case of the long term evaluation.

Influence of the load σ_v on the physical non-linear effect
As in the latter situations M_{max} reduces only a little due the physical non-linear effect, another calculation is executed with a larger load. This larger load may be reached by decreasing the strength parameters as well as by increasing the ground pressure. In order to use the NMK-diagram of figure 10.1, the strength parameters may not be changed, hence the load is increased.
The calculation of the second order bending moments M_{fnl} according to figure 10.2 resulted to be very laborious, as the iteration process did not converge easily. Hence another calculation method has been applied. This method is the reverse of the one given in figure 10.2 and consists of the following:

M_{max} according to Duddeck:

$$M_{\max} = \frac{\sigma_v \cdot (1 - K_0) \cdot R^2}{4 + 0.342 \cdot \alpha_{Duddeck}} \qquad (10.1)$$

with $$\alpha_{Duddeck} = \frac{E_g \cdot R^3}{E_{lining} \cdot I}$$

This means that M_{max} is a function of σ_v and EI (considering E_g and R as constants).
Equation 10.1 can be rewritten into the following expression, with which the load σ_v is calculated as function of M_{max} and EI:

$$\sigma_v = \frac{M_{\max} \cdot (4 \cdot EI + 0.342 \cdot E_g \cdot R^3)}{(1 - K_0) \cdot EI \cdot R^2} \qquad (10.2)$$

Substitution of a combination of M and EI determined from the NMK-diagram (figure 10.1) in equation 10.2 gives the load σ_v that causes the substituted M due to physical non-linearity (M_{fnl}). In this way the M_{fnl} due to a larger load are determined (figure 10.3).

All rights reserved. Use of disclosure of this data is subject to the restriction stated on the first page of this document.

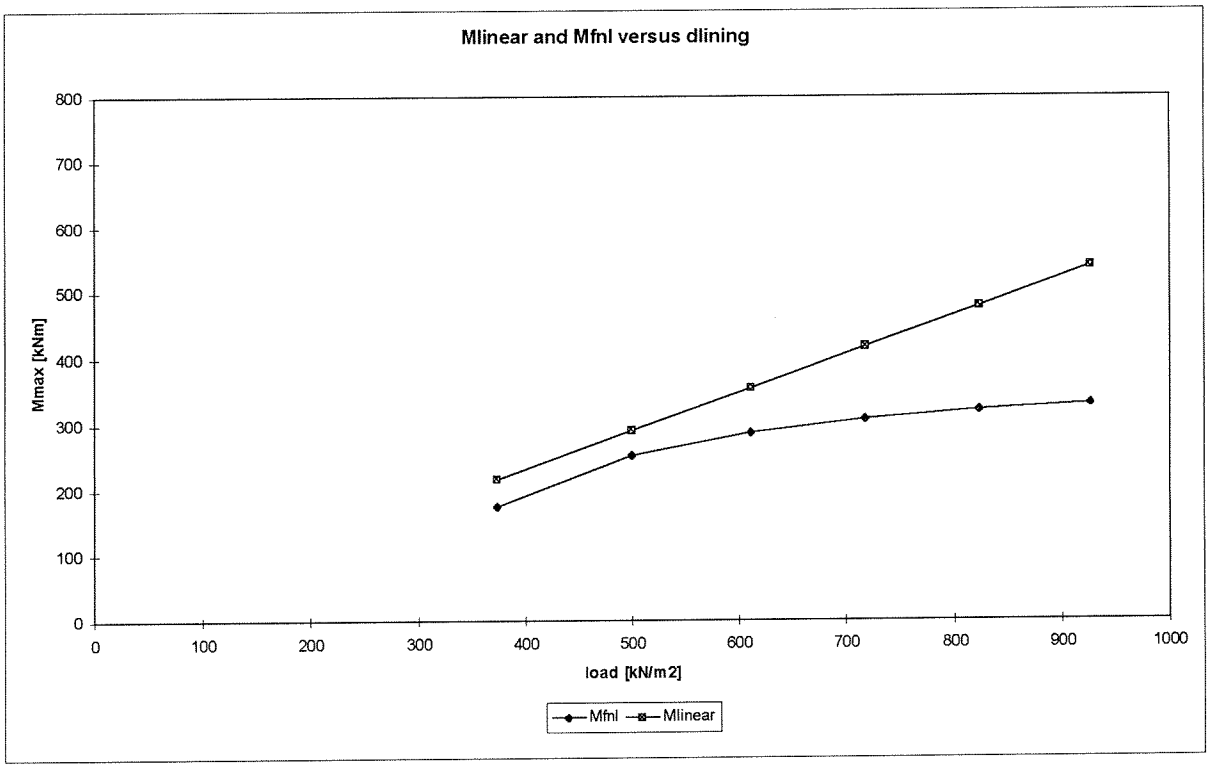

figure 10.3: M_{linear} versus M_{fnl}
(**remark:** α_{SFRC} = 0,05)

Conclusion

The bending moments decrease considerably due to the physical non-linearity in case of larger loads.

All rights reserved. Use of disclosure of this data is subject to the restriction stated on the first page of this document.

Influence of d_{lining} on the physical non-linear effect

The physical non-linear effect is calculated for several lining thicknesses according to the NMK-diagrams presented in appendix 15. The results of the calculation are given in table 10.1 .

d_{lining} [m]	M_{linear} [kNm]	M_{fnl} [kNm]	reduction of M_{linear} due to the physical non-linear effect [%]
0,70	551,3	414,9	25
0,60	474,7	319,7	33
0,50	377,0	231,4	39
0,40	260,2	219,9	15
0,35	199,0	174,2	12
0,30	140,7	131,4	7
0,25	89,5	88,3	1
0,20	49,2	49,1	0
0,15	21,8	21,8	0

table 10.1: comparison of M_{fnl} and M_{linear}
(**remark:** M_{fnl} count for a steel fibre content which corresponds with α_{SFRC} = 0,05)

In figure 10.4, the first order linear bending moment (M_{linear}) versus the physical non-linear bending moment (M_{fnl}) are presented.

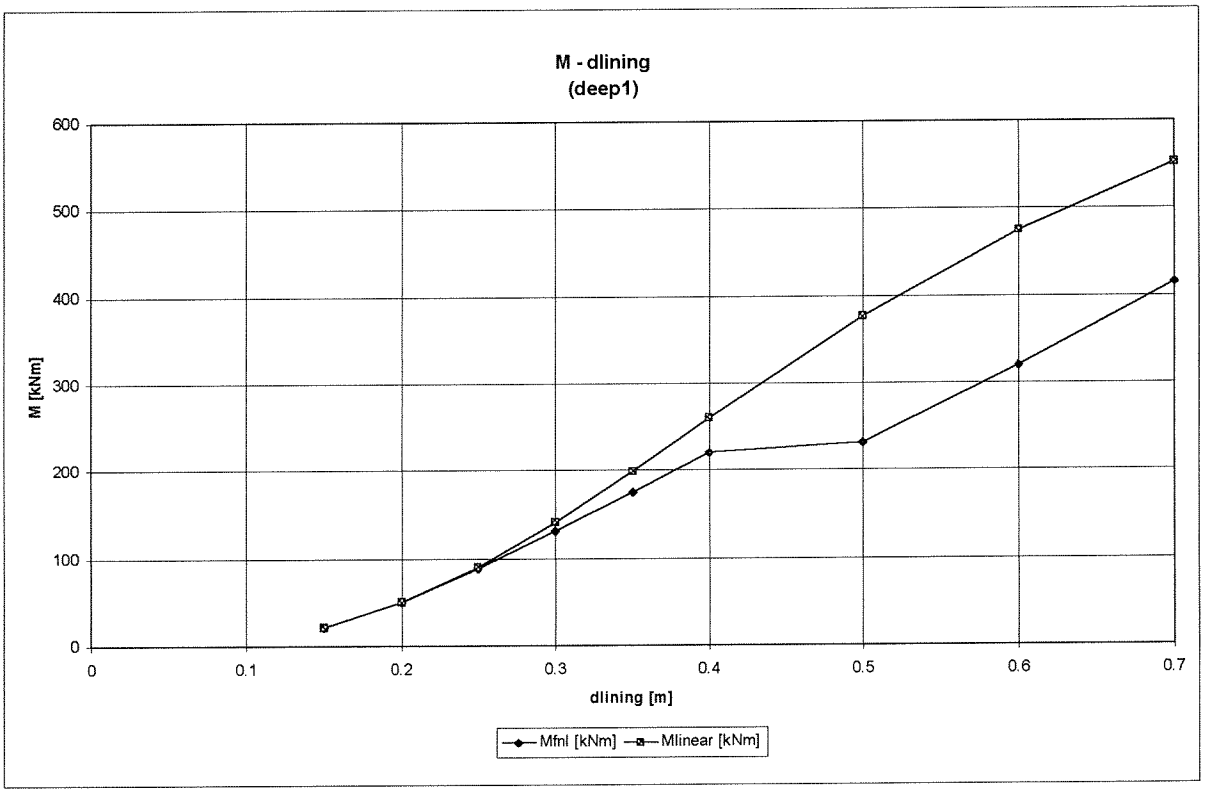

figure 10.4: M_{fnl} and M_{linear} versus d_{lining} (α_{SFRC} = 0,05)

Conclusion

From table 10.1 and figure 10.4 it can be concluded that the physical non-linear effect is smaller in case of slender constructions, because slender constructions are more flexible than thicker ones. In case of a load of σ_v = 448 kN/m^2 (e.g. deep1), the physical non-linear effect is the largest for d_{lining} = 0,50 m. From d_{lining} > 0,50m, the physical non-linear effect starts decreasing due to the increase of the stiffness of the lining.

All rights reserved. Use of disclosure of this data is subject to the restriction stated on the first page of this document.

10.3 Calculation of M_{max} including the physical and the geometrical non-linear effect

(**Remark:** as the geometrical non-linear effect depends on the tunnel radius R, it must be noticed that the calculations made in this chapter are based on R = 4,7 m)

The physical and the geometrical non-linear effect influence each other mutually. Due to the physical non-linear effect, EI decreases and consequently the displacements u increase. The result is an increase of the geometrical non-linear effect which causes a further increase of u and consequently a decrease of EI. This brings the process back again at the beginning.
If only the physical non-linear effect is taken into account, the tunnel lining is designed too flexible as the strength is overrated (upper limit approach). This is due to the overestimation of the positive, load reducing effect of the physical non-linearity.
If only the geometrical non-linearity is taken into account, the tunnel lining is designed too rigid as the strength is underestimated (lower limit approach).
Consequently, it can be concluded that the best approach is to consider both the non-linear effects.

A scheme of the calculation of M_{max} including both the geometrical and the physical non-linear effect is presented in figure 10.5 .

All rights reserved. Use of disclosure of this data is subject to the restriction stated on the first page of this document.

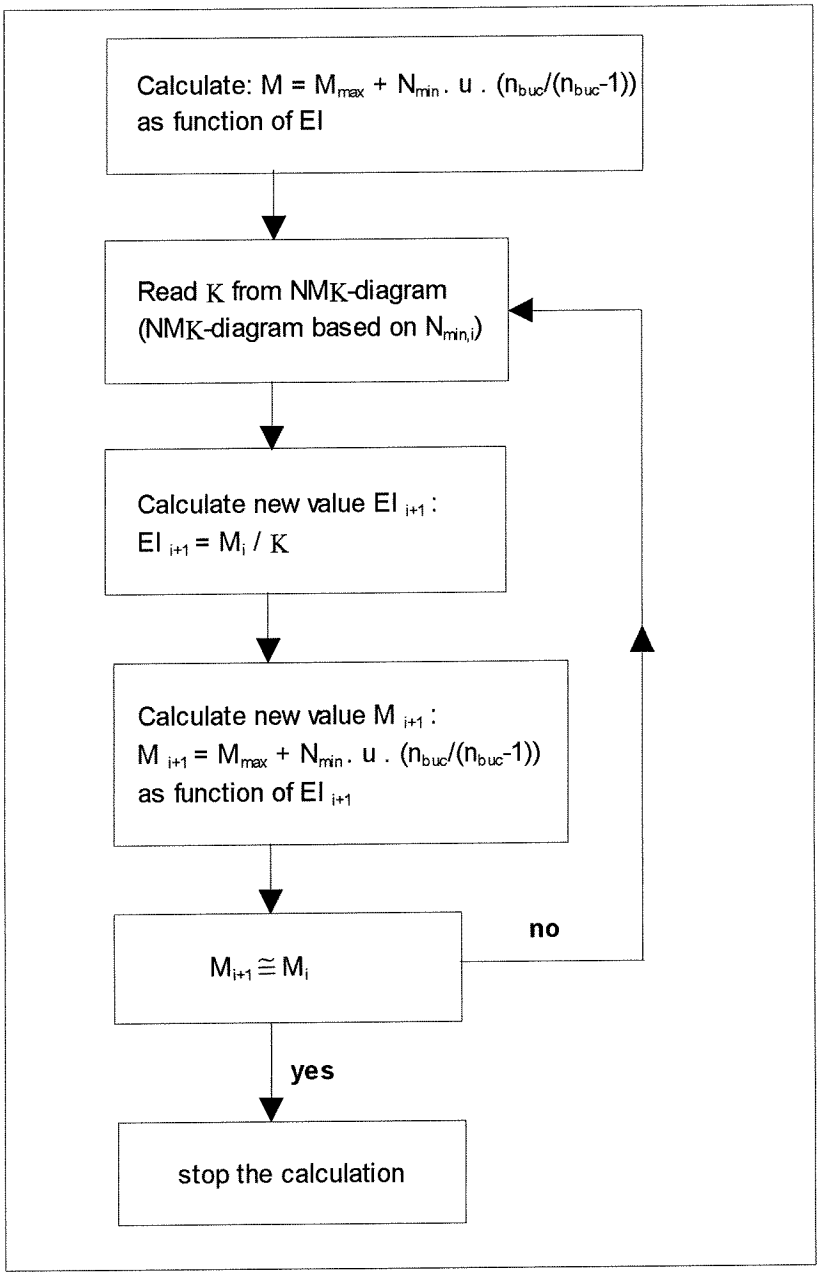

figure 10.5: scheme of the calculation method in behalf of the calculation of the cross-section forces taking into account both the physical and the geometrical non linear effect.

with:
$M = M_{max} + N_{min} . u . (n_{buc} /(n_{buc} -1))$ = geometrical non linear bending moment

M_{max} ,N_{min}, and u are calculated with the analytical Duddeck method (see appendix 1 for the equations). By calculating M_{max}, N_{min}, u and n_{buc} as function of $EI_{reduced}$ the physical non linear effect is introduced into the calculation.

All rights reserved. Use of disclosure of this data is subject to the restriction stated on the first page of this document.

Remarks
As the calculation executed according to figure 10.5 is only meant to give an indication of the mutual effect of both the non-linear effects, the calculation is based on some assumptions:

- The calculation is executed with only one NMK-diagram per lining thickness. This is done instead of calculating a new NMK-diagram with N_{min} as function of $EI_{reduced}$ for each loop of the calculation.
- The analytical Duddeck method, used for the calculation of M_{max} and N_{min}, considers the cross-section as homogenous, while the reduction of the stiffness of the section is local due to local crack formation. This means that the reduction of the loads is also local and not along the whole ring like in the Duddeck model. The reduction of the stiffness will be the largest where the displacements are the largest and consequently in case of the maximum bending moment. In the rest of the section, the reduction of the stiffness will probably be none or minimum.
  As the reduction of the stiffness is considered along the whole ring in this study, the calculation results will be conservative. This neglect could be approached by using a lower EI as input of the calculation.
- At the calculation of M caused by the geometrical non-linear effect, N_{min} has to be calculated as function of a reduced EI. As N_{min} is function of $\beta_{Duddeck} = (E_g \cdot R) / (E_{lining} \cdot A)$, the magnitude of E_{lining} has to be determined with $EI_{reduced}$. When the moment of inertia I is based on the uncracked section, a fictitious value $E_{fictitious}$ which includes the reduction of the stiffness of the cross-section can be determined. This $E_{fictitious}$ is used at the calculation of N_{min} and is determined as:

$$E_{fictitious} = \frac{EI_{reduced}}{I_{uncracked-section}}$$

Due to the mentioned assumptions, the calculation results have to be interpreted with care; the results have to be considered as a qualitative approach of the reality. It is recommended to execute this calculation more thoroughly.

10.3.1 Calculation results

In this paragraph, calculations are executed of M taking into account both the geometrical as well as the physical non-linear effect. These calculations count for the geotechnical profile 'deep1' and R = 4,7m.

Calculation of the bending moments as function of a variable d_{lining}
The calculation of $M_{fnl-gnl}$ has been executed according to the scheme presented in figure 10.5. The results are compared with M_{linear}, M_{fnl} and M_{gnl} in table 10.2.

d_{lining} [m]	M_{linear} [kNm]	M_{gnl} [kNm]		M_{fnl} [kNm]		$M_{fnl-gnl}$ [kNm]		N_{linear} [kN]	u [mm] (fnl-gnl)
		M_{gnl}	factor	M_{fnl}	factor	$M_{fnl-gnl}$	factor		
0,70	551,3	558,5	1,01	414,9	0,75	434,7	0,79	-1572	8,4
0,60	474,7	484,3	1,02	319,7	0,67	340,9	0,72	-1561	10,3
0,50	377,0	389,9	1,03	231,4	0,61	253,9	0,67	-1552	12,0
0,40	260,2	278,1	1,07	219,9	0,85	233,7	0,90	-1544	11,9
0,35	199,0	220,1	1,11	174,2	0,88	191,0	0,96	-1540	12,6
0,30	140,7	166,0	1,18	131,4	0,93	149,0	1,06	-1535	13,5
0,25	89,5	122,3	1,37	88,3	0,99	115,6	1,29	-1528	14,2
0,20	49,2	110,9	2,26	49,1	1,00	buckling	-	-1518	-
0,15	21,8	buckling	-	21,8	1,00	-	-	-1503	-

table 10.2: comparison of the second order bending moments with respect to the first order bending moments (short term).
factor = multiplication factor with respect to M_{linear}
remark: the values of table 10.2 apply for the geotechnical profile 'deep1', α_{SFRC} = 0,05 and R = 4,7m.

with:
M_{linear} = bending moment according to the first order linear theory (calculated with the analytical Duddeck method),
M_{gnl} = geometrical non-linear bending moment,
M_{fnl} = physical non-linear bending moment,
$M_{fnl-gnl}$ = bending moment including the geometrical and the physical non linear effect.

All rights reserved. Use of disclosure of this data is subject to the restriction stated on the first page of this document.

The bending moments of table 10.2 are presented in figure 10.6 versus d_{lining}.

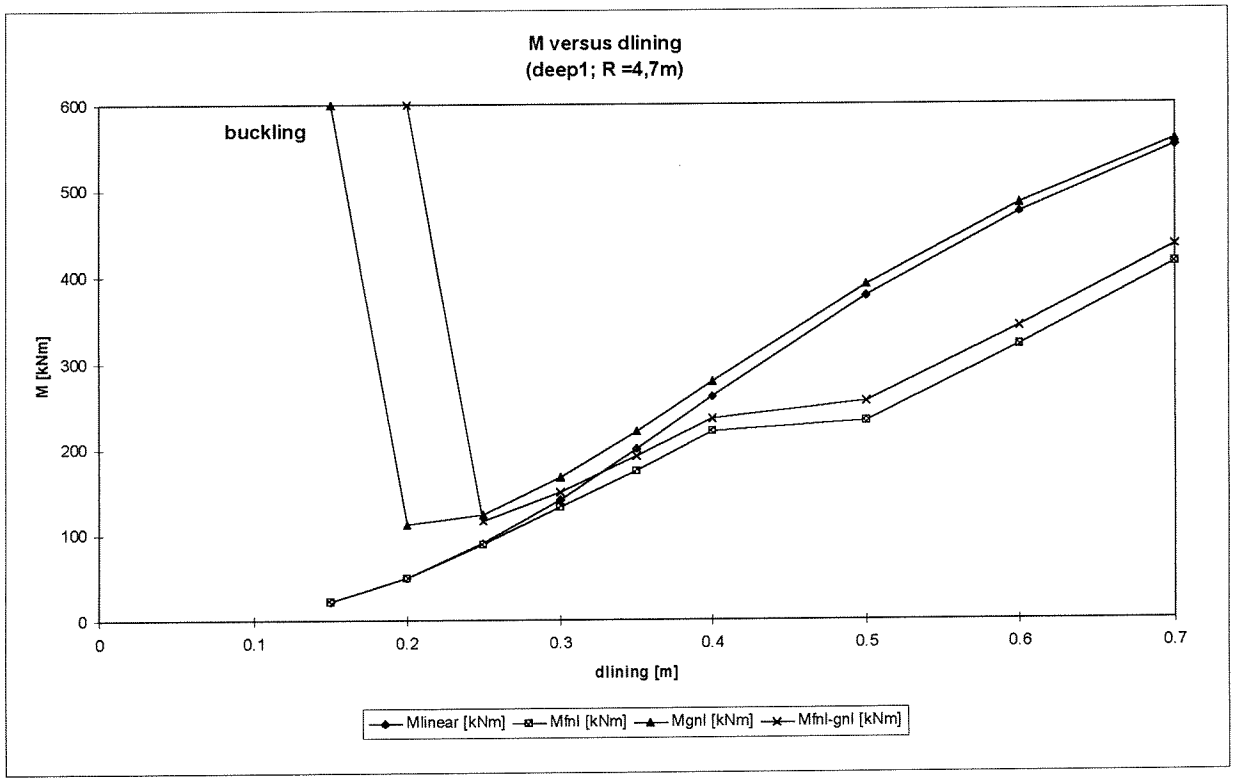

figure 10.6: bending moment versus d_{lining}

Conclusions (according to table 10.2)

(remark: these conclusions are only valid for the situation deep1, α_{SFRC} = 0,05 and R = 4,7m in the short term; the analysis should be executed more thoroughly in order to draw more general conclusions (e.g. with FEM (Diana))

- The physical non-linear effect governs over the geometrical non-linear effect in case of d_{lining} > 0,30m. In case of slender constructions, i.e. d_{lining} < 0,30m the geometrical non-linear effect governs over the physical non-linear effect. (**remark:** as the geometrical non-linear effect depends on the tunnel radius, the qualitative values of this conclusion are valid for R = 4,7m).
- The magnitude of the hoop forces is hardly influenced by the non-linear effects.
- The calculation results, given in table 10.2, are only valid if the soil springs are linear. The soil springs can be assumed to be linear in case of displacements smaller than 25 mm (see paragraph 8.2). As the displacements are 10 to 14 mm, the assumption of linearity of the soil springs is justified.
- In case of the calculation of both the non-linear effects, the construction buckles at a larger d_{lining} than in the case of the calculation of only the geometrical non-linear effect. This is the result of the physical non-linear effect which causes a decrease of the bending stiffness and consequently of the buckling force (see paragraph 9.1 for the definition of the buckling force).
- From table 10.2, it can be concluded that M_{linear} for d_{lining} < 0,30m is smaller than $M_{fnl-gnl}$. This means that the calculation of M with the analytical Duddeck model underrates the real value. Consequently, the safe use of the analytical Duddeck method for the calculation of the cross-section forces is limited to d_{lining}> 0.30m.

All rights reserved. Use of disclosure of this data is subject to the restriction stated on the first page of this document.

Approach of the influence of the load σ_v on the combined geometrical and physical non-linear effect

The latter calculations of $M_{fnl\text{-}gnl}$ are all based on a load σ_v = 448 kN/m^2 (i.e. the situation 'deep1'). In case of larger loads, the influence of the physical non-linear effect increases (see figure 10.3).
As in this report only NMK-diagrams are used based on the deep1 situation (figure appendix 15) for the calculation of M_{fnl} and $M_{fnl\text{-}gnl}$, the increase of the load might not be too large because otherwise the N_{min} increases too much and consequently the NMK-diagrams may not be used anymore. That is why σ_v (and N_{min}) is increased with less than 10%. The intention of this parameter study is to give a qualitative approach of the impact of the combined non-linear effects with increasing load. This means that the values of table 10.3, in case of σ_v =488 kN/m^2 might not be interpreted qualitatively.

	σ_v = 448 kN/m^2 ; N_{min} = -1544 kN		**σ_v = 488 kN/m^2 ; N_{min} =-1685 kN**	
	M_i [kNm]	decrease (-) or increase (+) of M_i with respect to M_{linear} [%]	M_i [kNm]	decrease (-) or increase (+) of M_i with respect to M_{linear} [%]
M_{linear}	260,2		282,0	
M_{gnl}	278,1	+7	304,0	+ 8
M_{fnl}	219,9	-18	232,0	- 22
$M_{fnl\text{-}gnl}$	233,7	-11	249,5	- 13

table 10.3: increase of the combined effect of the geometrical and the physical non-linearity caused by an increasing load σ_v (**remark:** the values given in this table count for a tunnel with R = 4,7m and d_{lining} =0,40m)

conclusion

According to table 10.3 it can be concluded that an increase of the load results in an increase of the combined geometrical and physical non-linear effect.

All rights reserved. Use of disclosure of this data is subject to the restriction stated on the first page of this document.

10.4 Conclusions

The following conclusions can be drawn from the analysis executed in this chapter.

With respect to the physical non-linear effect

- From table 10.1 and figure 10.4 it can be concluded that the physical non-linear effect is smaller in case of slender constructions, because slender constructions are more flexible than thicker ones. In case of a load of σ_v = 448 kN/m^2 (e.g. deep1), the physical non-linear effect is the largest for d_{lining} = 0,50 m. From d_{lining} > 0,50m, the physical non-linear effect starts decreasing due to the increase of the stiffness of the lining.
- The bending moments decrease considerably due to the physical non-linear effect in case of larger loads (see figure 10.3).

With respect to the combined geometrical and physical non-linear effect

(remark: these conclusions are only valid for the situation deep1 and R = 4,7m in the short term; the analysis should be executed more thoroughly in order to draw more general conclusions (e.g. with FEM (Diana))

- The physical non-linear effect governs over the geometrical non-linear effect in case of d_{lining} > 0,30m. In case of slender constructions, i.e. d_{lining} < 0,30m the geometrical non-linear effect governs over the physical non-linear effect. (**remark:** as the geometrical non-linear effect depends on the tunnel radius, the qualitative values of this conclusion are valid for R = 4,7m).
- The magnitude of the hoop forces is hardly influenced by the non-linear effects.
- The calculation results, given in table 10.2, are only valid if the soil springs are linear. The soil springs can be assumed to be linear in case of displacements smaller than 25 mm (see paragraph 8.2). As the displacements are 10 to 14 mm, the assumption of linearity of the soil springs is justified.
- In case of the calculation of both the non-linear effects, the construction buckles at a larger d_{lining} than in the case of the calculation of only the geometrical non-linear effect. This is the result of the physical non-linear effect which causes a decrease of the bending stiffness and consequently of the buckling force (see paragraph 9.1 for the definition of the buckling force).
- From table 10.2, it can be concluded that M_{linear} for d_{lining} < 0,30m is smaller than $M_{fnl\text{-}gnl}$. This means that the calculation of M with the analytical Duddeck model underrates the real value. Consequently, the safe use of the analytical Duddeck method for the calculation of the cross-section forces is limited to d_{lining}> 0.30m.
- According to table 10.3 it can be concluded that an increase of the load results in an increase of the combined geometrical and physical non-linear effect.

All rights reserved. Use of disclosure of this data is subject to the restriction stated on the first page of this document.

11. Reliability analysis (non-linear approach)

In this chapter a reliability analysis is executed of the tunnel lining in the final phase taking into account both the geometrical and the physical non-linear effect. The failure criterion is the same as at the linear analysis of chapter 7. Consequently, the same reliability function is used. Only a qualitative interpretation is given with respect to the impact of the non-linear effects on the safety of the tunnel lining, as only one reference case, deep1, is considered. By taking into account the non-linear effects the safety of the tunnel lining increases. The 'safe' application of the analytical Duddeck method is limited to tunnel linings with d_{lining} > 0,30m. Though these (quantitative) conclusions are only valid for a load σ_v = 448 kN/m^2 (e.g. the reference case ,'deep1') and a tunnel lining with R = 4,7m and σ_{SFRC} = 0,05.

11.1 Introduction

One of the conclusions of the linear reliability analysis (chapter 7) was that the safety increases with decreasing lining thickness. As this conclusion did not meet the expectations, the impact of the non-linear effects on the cross-section forces is examined in chapter 9 and 10.
The geometrical non-linear effect (chapter 9) causes a considerable increase of M with decreasing lining thickness (see figure 9.5) and consequently a decrease of the safety. On the other hand the physical non-linear effect (chapter 10) results in a contrary effect as it causes a decrease of the moments with decreasing lining thickness.
In this chapter a reliability analysis is executed of the tunnel lining in the final phase taking into account both the geometrical and the physical non-linear effect. Within the scope of this study, the non-linear reliability analysis is only executed for the geotechnical profile 'deep1'.

11.2 Reliability function and acceptable failure probability

Reliability function
The reliability function (eq. 7.5) used in the linear reliability analysis, is also used in the non-linear approach because both situations are based on the same failure boundary. This function is repeated here:

$$Z = M_u \cdot \left(C + D \cdot \left(\frac{N_{\min}}{N_u} \right) + E \cdot \left(\frac{N_{\min}}{N_u} \right)^2 \right) - M_{\max} \qquad \text{(equation 7.5)}$$

with:

$E = 0.18\ \alpha_{SFRC}^2 + 0.353\ \alpha_{SFRC} - 0.4876$

$D = -0.56\ \alpha_{SFRC}^2 + 0.852\ \alpha_{SFRC} - 0.4812$

$C = -0.6\ \alpha_{SFRC}^2 + 0.478\ \alpha_{SFRC} + 0.0012$

$M_u = \beta_R \cdot b \cdot d^2_{lining}$

$N_u = \beta_R \cdot b \cdot d_{lining}$

$M_{max} = M_{fnl} + N_{min} \cdot u \cdot (n_{buc} / (n_{buc} - 1))$ (equation 9.1)

$$M_{fnl} = \frac{\sigma_v \cdot (1 - K_0) \cdot R^2}{4 + 0.342 \cdot \alpha_{Duddeck}}$$

The parameters $\alpha_{Duddeck}$, N_{min}, u and n_{buc} are calculated as function of $EI_{reduced}$. Furthermore, as N_{min} is function of $\beta_{Duddeck} = (E_g \cdot R) / (E_{lining} \cdot A)$, the magnitude of E_{lining} has to be determined with $EI_{reduced}$. When the moment of inertia I is based on the uncracked section, a fictitious value $E_{fictitious}$ which includes the reduction of the stiffness of the cross-section can be determined. This $E_{fictitious}$ is used at the calculation of N_{min}.

All rights reserved. Use of disclosure of this data is subject to the restriction stated on the first page of this document.

By defining M_{max} as above (eq. 9.1) the geometrical and physical non-linear behaviour of the construction is introduced into the reliability analysis.

The definition of Z in AFDA is given in appendix 9.

Acceptable failure probability
The same acceptable failure probability is used as for the linear reliability analysis (see paragraph 7.1).

11.3 Stochastic variables (input of AFDA)

The input of AFDA is the same as in the case of the linear calculation (see paragraph 7.2, table 7.1) with exception of:

- E_{lining}, this value is substituted by $E_{fictitious}$; the variation coefficient of $E_{fictitiuos}$ is V = 0,10 .
- creep coefficient φ, as the creep of the concrete is included in $E_{fictitious}$.

$E_{fictitious}$ is determined according to: $E_{fictitious} = \dfrac{EI_{reduced}}{I_{uncracked-section}}$ [N/mm^2]

$EI_{reduced}$ is determined according to the calculation in paragraph 10.3. The calculation results are given in table 11.1

d_{lining} [m]	$M_{gnl\text{-}fnl}$ [kNm]	$EI_{reduced}$ [MNm^2]	$E_{fictitious}$ [MPa]
0,70	434,7	393,8	13776
0,60	340,9	240,9	13382
0,50	253,9	146,1	14022
0,40	233,7	132,0	24750
0,35	192,7	96,2	26925
0,30	149,0	62,8	27908
0,25	115,6	38,3	29372
0,23	buckling	14	15777

table 11.1: results of the calculation of M including the non-linear effects ($M_{gnl\text{-}fnl}$)
(profile deep1, R = 4,7m, α_{SFRC} = 0,05)

11.4 Results of the reliability analysis

The results of the reliability analysis are given in table 11.3. These results count for a tunnel in deep1, with R = 4,7m and α_{SFRC} = 0,05 .

d_{lining} [m]	β	P_b
0,70	3,05	1,2E-3
0,60	2,87	2,1E-3
0,50	2,72	3,2E-3
0,40	1,78	3,8E-2
0,35	1,75	4,0E-2
0,30	1,73	4,2E-2
0,25	1,71	4,4E-2
0,23	-0,45	6,7E-1

table 11.3: results of the non-linear reliability analysis
(**remark**: in this AFDA calculation the reduction of E_{lining} due to creep is not taken into account, because otherwise the reduction of EI would be already that large due to the long term effect that the physical non-linearity would not have a representative impact)

All rights reserved. Use of disclosure of this data is subject to the restriction stated on the first page of this document.

Conclusion

- The safety requirements β_{target} = 3,6 and $P_b = 10^{-4}$ are still not met, in spite of the increase of the safety with regard to the linear analysis.
- The safety of the lining decreases with decreasing d_{lining}, this in contrast to the conclusion drawn at the linear reliability analysis that the safety of the lining increases considerably with decreasing d_{lining} (see paragraph 7.4).

11.4.1 Impact of the input-parameters on the results of the reliability analysis

A special virtue of the AFDA reliability analysis is that it can serve quickly to indicate the sensitivity of the solution across the range of possible input parameters by means of the output parameter α_{AFDA}. In this way the parameters that principally cause the limit state are determined. These parameters should be given special attention at the determination of their magnitude.
The values of table 11.4 are valid for 'deep1' with α_{SFRC} = 0,05

stochastic parameter (deep1)	α_{AFDA} [*10^{-2}] (short term)	α_{AFDA} [*10^{-2}] (long term)	α_{AFDA} [*10^{-2}] (linear model) (long term)
K_{0water}	1.0	0.9	1.1
K_0	32.9	31.6	30.4
S_{wet}	-0.9	-0.9	-0.8
S_{dry}	0.0	0.0	0
n_p	4.9	5.0	4.4
ρ_k	-0.5	-0.5	-0.4
ρ_{water}	-0.9	-0.9	-0.8
h_{gw}	-7.2	-7.1	-6.9
γ_{water}	3.7	3.6	3.4
R	0.6	0.8	1.7
d_{lining}	-2.8	-3.9	-8
E_g	51.6	56.4	50.5
υ	27.7	27.0	24.5
$E_{fictitous}$	-17.8	-18.0	-19.4
f	23.2	22.9	21.3
m_b	15.5	15.3	14.3
m_N	16.1	14.5	17.2
m_M	-63.3	-60.5	-62.4
α	4.9	4.7	4.5

table 11.4: impact of the input parameters on the failure probability

Conclusion

The α_{AFDA} of the non-linear analysis show a large resemblance with those of the linear analysis. Consequently, the same conclusions can be drawn as at the linear analysis (see paragraph 7.3.1).

All rights reserved. Use of disclosure of this data is subject to the restriction stated on the first page of this document.

11.5 Comparison of the results of the linear and the non-linear reliability analysis

In table 11.5 the results of the non-linear reliability analysis are shown versus the results of the linear reliability analysis.

d_{lining} [m]	β linear	β non-linear
0,70	2,16	3,05
0,60	1,72	2,87
0,50	1,42	2,72
0,40	1,41	1,78
0,35	1,57	1,75
0,30	1,87	1,73
0,25	2,34	1,71
0,23	2,85	-0,45

table 11.5: the results of the linear reliability analysis versus the results of the non-linear reliability analysis valid for the situation deep1 and α_{SFRC} = 0,05

Conclusions

- The safety of the tunnel lining increases by taking into account the non-linear effects in case of d_{lining} > 0,30m. This can be explained by the fact that the physical non-linearity governs the geometrical non-linearity in case of a 'large' lining thickness. This results in a decrease of the cross-section forces with respect to those calculated with the first order linear theory and consequently in an increase of the safety. In case of d_{lining} < 0,30m, the geometrical non-linear effect starts governing the physical non-linear effect. This results in an increase of the cross-section forces with respect to those calculated with the first order linear theory and consequently in a decrease of the safety. Finally, the lining fails by buckling at d_{lining} = 0,23.
- From the preceding it can be concluded that the safe use of the analytical Duddeck method is limited to d_{lining} > 0,30m. Consequently, the analytical Duddeck method can not be used for the optimisation of d_{lining}.

All rights reserved. Use of disclosure of this data is subject to the restriction stated on the first page of this document.

11.6 Conclusions

In figure 11.1, the reliability index β calculated with the linear and the non-linear models is plotted over d_{lining}.

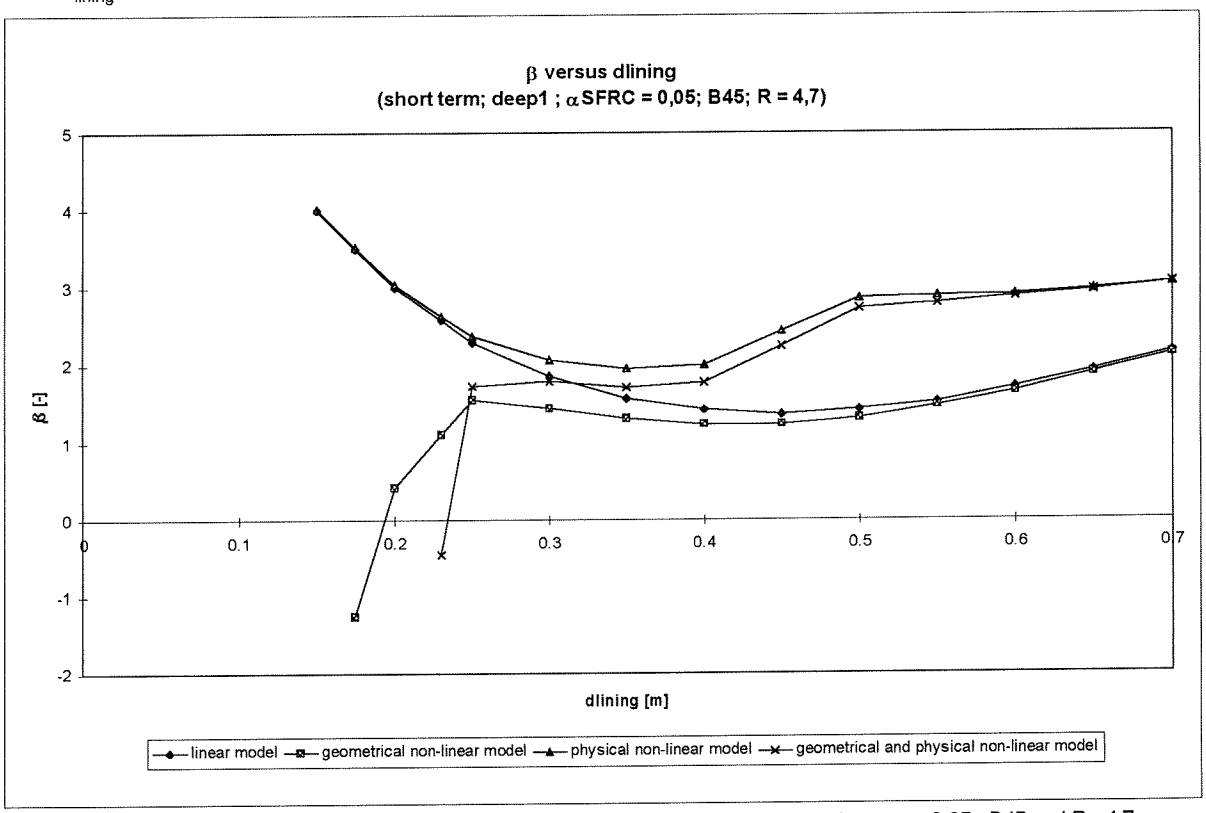

figure 11.1: reliability index β versus d_{lining} (short term), this graph counts for the profile deep1, α_{SFRC} = 0,05 , B45 and R =4,7

Conclusions (drawn from figure 11.1)
(remark: figure 11.1 counts for the short term; the safety in the long term is larger)

- The safety requirements β_{target} = 3,6 and $P_b = 10^{-4}$ are still not met, in spite of the increase of the safety due to the non-linear effects.
- The safety of the lining decreases with decreasing d_{lining}, this in contrast to the conclusion drawn at the linear reliability analysis that the safety of the lining increases considerably with decreasing d_{lining} (see paragraph 7.4).
- It is safe to use the analytical Duddeck method in case of d_{lining} > 0,32 m as from this lining thickness the linear model is conservative with respect to the model that includes both the geometrical and the physical non-linear effect. In case of d_{lining} < 0,32m , the analytical Duddeck method underrates the cross-section forces. Consequently, it is not safe to use the analytical Duddeck method for the optimisation of the lining thickness.

All rights reserved. Use of disclosure of this data is subject to the restriction stated on the first page of this document.

12. Calculation of the safety factors for the calculation of the ITM tunnel lining

At the computation of the ITM tunnel, (partial) safety factors have to be used to cover uncertainties in the design of the tunnel lining. However, at the moment no legislation specifying safety factors for the design of a tunnel lining is available. In this chapter, (partial) safety factors for the ITM-tunnel are calculated. In paragraph 13.1, the strategy applied at the calculation of the partial safety factors is described. Next in paragraph 13.2, the calculated partial safety factors for the ITM-tunnel are presented. In paragraph 13.3, the (partial) safety factors calculated for the ITM tunnel lining are compared with the (partial) safety factors given in the present building codes and used in present Dutch tunnel design; the calculated safety factors show a large resemblance with the prescribed safety factors and have a value of 1,8 .

12.1 Calculation of the (partial) safety factors

The (partial) safety factors are determined according to the theory presented in paragraph 4.5 (equations 4.1 and 4.2).

The linear reliability analysis (chapter 7) is used as basis for the computation of the safety factors as:
- all the reference cases have been examined with the linear reliability analysis, while with the non-linear analysis only the case 'deep1' is examined.
- it is safe to use the linear model for the calculation of the safety factors of the nominal case of the ITM-tunnel which has a lining thickness of 0,40m (see the conclusions of paragraph 11.6).

First of all, the parameters of the calculation have to be divided into load- and resistance parameters. The latter, however, is not unambiguous in case of soil retaining constructions, like tunnels. Dependent on the situation, certain parameters can have a contradictory contribution; e.g. an increase of d_{lining} causes an increase of the cross-section forces and thus an increase of the loads (load parameter). On the other hand an increase of d_{lining} causes an increase of the ultimate bending moment M_u and thus an increase of the strength (resistance parameter; $M_u = \beta_R \cdot b \cdot d_{lining}$). Consequently, it is not unambiguous to determine one load factor γ_S and one resistance factor γ_R , or an overall safety factor γ that represents the safety of the whole construction.
An objective approach of the latter is to determine the partial safety factors per input parameter of the calculation. The division into load- and resistance parameters, can be realised by checking whether the concerning parameter contributes to an increase or a decrease of Z(X*), or in words, to a decrease or an increase of the difference between the loads and the resistance. The parameters which give an increase of Z(X*) are considered to be resistance parameters and those which give a decrease of Z(X*) are considered to be load parameters. The latter is based on the definition of Z = R - S; an increase of Z means an increase of R (resistance) with respect to S (loads). It has to be noticed that the division into load- and resistance parameters as executed in this report is only valid for the situation of a lining in the ultimate limit state.
The safety factors are defined for the four considered geotechnical profiles in this report. The results are generalised by calculating the average factor of the four considered profiles. Summarising, the following strategy has been applied.

All rights reserved. Use of disclosure of this data is subject to the restriction stated on the first page of this document.

Strategy applied at the calculation of the safety factors (see also chapter 4, paragraph 4.5)

1. Calculate the reliability index β and the design point values X^*_i by means of an AFDA calculation (see paragraph 4.4.2).
2. Define which parameters contribute to the loads and which to the resistance of the construction in the considered limit state by means of the following criterion:
   - if an increase of X^*_i causes an increase of $Z(X^*)$, then X_i is a resistance parameter
   - if an increase of X^*_i causes an decrease of $Z(X^*)$, then X_i is a load parameter
3. Calculate the characteristic value of the parameters:
   - load parameter: $S_{k,i} = \mu + 1{,}64\sigma$
   - resistance parameter: $R_{k,i} = \mu - 1{,}64\sigma$
4. Calculate the partial safety factors $\gamma_{S,i}$ and $\gamma_{R,i}$ per parameter (according to equations 4.1 and 4.2)
   $\gamma_{R,i} = R_{k,i} / R^*_i$
   $\gamma_S = S^*_i / S_{k,i}$
   Compute $\gamma_{S,i}$ and $\gamma_{R,i}$ for all the parameters and all the reference cases.
5. Calculate the eventual $\gamma_{S,i}$ and $\gamma_{R,i}$ by computing the average value of the partial safety factors of the reference cases.

The above strategy can be applied as such in case of the shallow profiles, because these profiles meet the safety requirements. The deep profiles, however, do not meet the safety requirement β=3,6 (see paragraph 7.3). In order to achieve the required safety, the following strategy has to be applied:

1. Determine the new design point values of the input parameters by imposing β = 3,6 and by using the α_{AFDA} of the previous calculation with AFDA :
   $X_i^* = \mu - \alpha_{AFDA}\beta\sigma$ normal distribution
   $X_i^* = \mu \exp(-\alpha_{AFDA}\beta V)$ lognormal distribution
2. Use these values as input of the new AFDA calculation.
3. Calculate the new reliability index β and the design point values X^*_i by means of an AFDA calculation:
   - if $\beta \geq 3{,}6$: the strategy above (points 1 to 5) can be applied to determine the safety factors.
   - if $\beta < 3{,}6$: points 1 and 2 have to be repeated until $\beta > 3{,}6$

In fact, the above is based on the determination of the partial safety factors so that:
$\Sigma\, p_i \,.\, \{\beta_i(\gamma) - \beta^t\}$ is minimum (see also paragraph 4.5 : procedure in behalf of the computation of the safety factors [lit,15])

with:
p_i = weighing factor,
$\beta_i(\gamma)$ = reliability index that belongs to reference case i,
β^t = target value of the reliability index = 3,6 .

Consequently, the smaller the difference between β_i and β^t, the better the value of the partial safety factors. This optimisation of the partial safety factors is not executed in this report. It is recommended, however, to optimise the partial safety factors of the deep profiles by adjusting them to the required reliability index β = 3,6 .

All rights reserved. Use of disclosure of this data is subject to the restriction stated on the first page of this document.

12.2 Calculation results

The results of the calculation of the safety factors are presented in appendix 16.

It must be noticed that most of the partial safety factors are smaller than 1. This result is known from the calculation of partial safety factors in case of other soil retaining constructions [lit, 55].
The partial safety factors smaller than 0,95 have been rectified to values larger than 0,95 in order to obtain values which can be round off upwards to a value of 1,0. This is done by calculating the partial safety factor as function of the mean value of the concerning parameter instead of the characteristic value:
$\gamma_R = R_{mean\ value} / R^*$
$\gamma_S = S^* / S_{mean\ value}$
The average values of the calculated partial safety factors are presented in table 13.1.

resistance factor γ_R	
parameter	**average γ_R**
K_{0water}	1.0
K_0	1.0
n_p	1.0
h_{river}	1.0
γ_{water}	1.0
R	1.0
d_{lining}	1.0
E_g	1.3
υ	1.1
ϕ_{creep}	1.1
f	1.1
m_b	1.1
m_N	1.1
α	1.0

resistance factor γ_R	
parameter	**average γ_S**
S_{wet}	1.0
S_{dry}	1.0
γ_{wet}	1.0
γ_{dry}	1.0
ρ_k	1.0
ρ_{water}	1.0
h_{gw}	1.1
E_{lining}	1.0
m_M	1.3

table 13.1: load- and resistance factors for the calculation of the lining of the ITM-tunnel

The design point values of the cross-section forces are presented in table 13.2.

β = 3,6	deep1	deep2	shallow1	shallow2
N^*_{min} [kN]	-1430	-1419	-1221	-1201
M^*_{max} [kNm]	372	361	328	310

table 13.2: design point values of the cross-section forces

Remark
In case of cross-section forces with a value that rather differs from the design point values given in table 13.2, the (partial) safety factors calculated in this chapter might not be applicable.

All rights reserved. Use of disclosure of this data is subject to the restriction stated on the first page of this document.

Figure 13.1 shows the position of the design point values of the cross-section forces with respect to the failure curve.

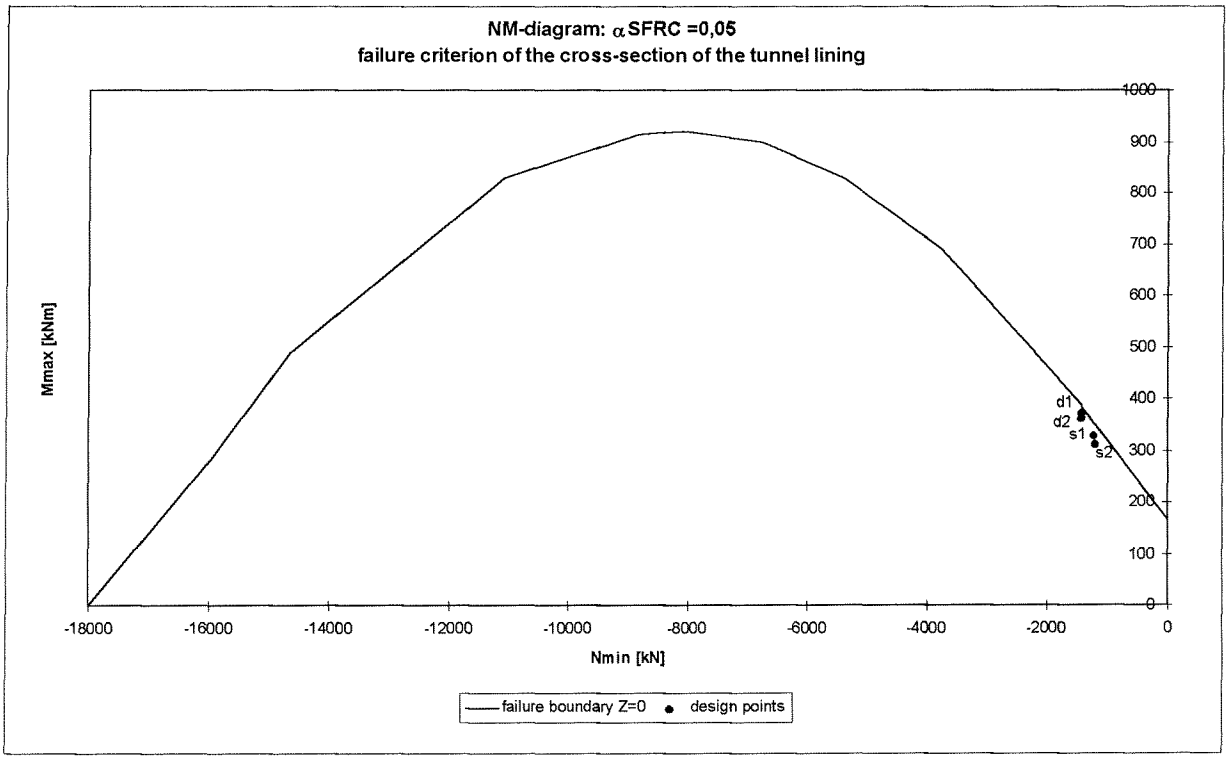

figure 13.1: position of the design point values of the cross-section forces with respect to the failure curve

12.3 Comparison of the calculated safety factors with the safety factors given in the present building codes

In paragraph 4.5.3 of this report an abstract is given of the safety factors based on the present building codes. In this paragraph these values are compared with the calculated ones for the ITM tunnel lining.
Although an overall safety factor is not unambiguous in case of soil retaining constructions (see paragraph 13.1), an overall safety factor is calculated for the ITM-tunnel in order to be able to make a comparison with the values given in the present building codes.

The calculation of the overall safety factor has been executed according to the strategy presented in paragraph 4.5 . In short, the overall safety factor is calculated by multiplying the resistance factor γ_R by the load factor γ_S : $\gamma = \gamma_R \cdot \gamma_S$

The overall factor γ, the resistance factor γ_R and the load factor γ_S calculated for the ITM tunnel lining are presented in table 13.3 .

safety factors calculated in this report				
profile	γ_R	γ_S	γ	β
deep1	1,1	1,7	1,8	2,9
deep2	1,1	1,4	1,5	2,5
shallow1	1,0	1,8	1,8	4,4
shallow2	1,0	1,8	1,8	4,2

table13.3: safety factors which can be applied for the ITM tunnel lining (see appendix 16)

All rights reserved. Use of disclosure of this data is subject to the restriction stated on the first page of this document.

In case of the geotechnical profile 'deep2', the load factor γ_S and the overall factor γ rather differ from the other (partial) safety factors. It is recommended, specially in this case, to optimise the values of the (partial) safety factors by adjusting them to the required $\beta = 3,6$.

In table 13.4, the safety factors calculated for the ITM tunnel lining are compared with those given in the present building codes and used in present Dutch tunnel design. These safety factors count for the ductile failure mode.

source	γ
Dutch regulations [lit,40]	1,7
DBV Merkblatt [lit, 2]	1,8
present Dutch tunnel design [lit, 37]	1,75
ITM design (derived from preliminary study)	1,75
calculation in this report:	
deep1	1,8
deep2	1,5
shallow1	1,8
shallow2	1,8

table 13.4: comparison of the calculated safety factors with the values given in the present building codes and used in present Dutch tunnel design (these safety factors count for the ductile failure mode)

Conclusion

The overall safety factors γ, calculated in this report, for the ITM tunnel lining show a large resemblance with those given in the present building codes and used in present Dutch tunnel design. Consequently, $\gamma = 1,8$ can be prescribed for the calculation of the ITM tunnel lining.

All rights reserved. Use of disclosure of this data is subject to the restriction stated on the first page of this document.

All rights reserved. Use of disclosure of this data is subject to the restriction stated on the first page of this document.

13. Conclusions and recommendations

In this chapter the results of the reliability analysis are summarised and recommendations for future investigation are given.

13.1 Conclusions

The purpose of the ITM project is the development of both a tunnel building method and a tunnel boring machine that are considered to be competitive with the conventional ones. An important characteristic of this new tunnel building method is the lining that is built with extruded steel fibre reinforced concrete in a continuous process.
At the computation of the ITM-tunnel, safety factors are needed to cover the uncertainties in the design of the concrete lining. At the moment there is no legislation specifying safety factors for tunnels.
The scope of the study, executed in this report, is a reliability analysis of the ITM tunnel lining, the calculation of the failure probability of the tunnel lining in the final phase and the definition of (partial) safety factors.

It must be noticed explicitly that the conclusions given in this chapter (mainly) apply for the nominal design case of the ITM (see chapter 1.4 for the boundary conditions).

Summarising, the following conclusions may be drawn:

With respect to the application of a probabilistic analysis for tunnel design

- A probabilistic analysis allows a more realistic design to be used in the prevailing design methods, than the conventional deterministic methods. It avoids a too pessimistic load determination.
- The application of a semi-probabilistic design method provides a quantitative insight into the influence of the stochastic uncertainty of the basic parameters. It thus forms an important tool in assigning priorities in study or quality control of specific parameters of theoretical models. It contributes moreover to an overall risk analysis of the system by providing the probability of failure of each element of the system.

With respect to the tunnel lining

- Calculation of the cross-section forces with the analytical Duddeck method gives conservative results. This conclusion applies for a *linear* calculation of a tunnel lining in the *final* phase.
- The application of the analytical Duddeck method has some limitations:
  - it assumes the material behaviour of the soil and the lining as being linear elastic, while neither the soil nor, usually, the tunnel lining, behave in an elastic manner;
  - the geometrical and the physical non-linearity of the construction are not taken into account.
  There is, however, a real merit in applying a simple method of analysis to a tunnel design problem. It may give far more insight into the relative importance of the relevant factors than immediate recourse to computer methods (i.e. naturally, starting from the fact that the impact of the parameters on the calculation results is the same at the simple method as at the computer method). Though in a second stage, the computer methods will far better serve in reproducing a more valid representation of the problem.
- A sensitivity analysis, executed with the analytical Duddeck method, of parameters which are used at the calculation of the lining in the final phase, gives the following results:
  - γ_{Wet}, d_{lining} and K_0 have the largest impact on the cross-section forces; an increase of γ_{wet} or d_{lining} causes an increase of M; an increase of K_0 causes a decrease of M.
  - the impact of K_0 is larger in clay than in sand.
  - the impact of E_g, E_{lining} and d_{lining} is larger in sand than in clay; an increase of E_g causes a decrease of M and an increase of E_{lining} causes an increase of M.

All rights reserved. Use of disclosure of this data is subject to the restriction stated on the first page of this document.

With respect to the linear reliability analysis

- The safety requirements, $P_b = 10^{-4}$ and $\beta_{target} = 3,6$, are only met in some of the considered cases. In case of a lining of concrete without tensile strength ($\alpha_{SFRC} = 0,00$), the safety requirements are not met. Addition of steel fibres gives a considerable increase of the safety.
- The failure probability is larger in case of deep tunnels than in case of shallow tunnels. This is due to the fact that the loads are larger in deep tunnels than in shallow tunnels.
- The failure probability is a little larger in case of a clay profile than in case of a sand profile. This can be mainly explained by the stiffness of the soil, which is much larger in sand than in clay.
- The safety requirements are on the whole better met in case of a more flexible and thinner lining. This is due to the considerable decrease of the bending moments with decreasing lining thickness in case of a calculation with the first order *linear* theory (**remark:** this conclusion is refuted with the non-linear reliability analysis)
- As the bending moments decline with smaller bending stiffness of the lining, a thinner lining is favourable to prevent or to reduce tensile stresses due to bending and a thicker lining is favourable to prevent failure of the compression mode.
- The model factor of the bending moments, the coefficient of lateral effective pressure, the stiffness of the soil and the compressive concrete strength should be given priority in study and quality control as their stochastic uncertainty is the largest with respect to the failure of the tunnel. Of all these factors, the model factor of the bending moments has by far the largest impact on the cross-section forces.

With respect to the geometrical non-linear effect

- The geometrical non-linear effect increases with:
  - increasing depth of the tunnel, increasing R,
  - decreasing E_{lining}, E_g and d_{lining}.
- The geometrical non-linear effect is larger in case of tunnels under the phreatic surface, because:
  - with time, the soil passes on from loading medium to load carrying medium, while water does not have this positive load reducing effect;
  - due to the hydrostatic water pressure, the hoop force increases, although this increase is of minor importance with respect to the above mentioned effect.

  The deeper the tunnel, the larger the effect of the water on the geometrical non-linearity.

(**remark:** as the geometrical non-linear effect depends on the tunnel radius R, it most be noted explicitly that the following conclusions are based on the ITM tunnel design case with R = 4,7m)

- The contribution of the geometrical non-linear effect is proven to have to be taken into account. The bending moments increase with 10% in the short term and with 15% in the long term. However, in case of more slender constructions, i.e. $d_{lining} < 0,40$m, the geometrical non-linear effect increases considerably, specially when the long term effect is taken into account.
- Buckling starts playing a significant part from $d_{lining} < 0,17$m; if creep of the concrete due to long duration load is taken into account, the lining fails by buckling from $d_{lining} \leq 0,22$ m.

With respect to the physical non-linear effect

- The physical non-linear effect is smaller in case of slender constructions, because slender constructions are more flexible than thicker ones.
- The bending moments decrease considerably due to the physical non-linear effect in case of larger loads.

With respect to the combined effect of the physical and the geometrical non-linearity

(**remark:** these conclusions count for a load of approximately $\sigma_v = 448$ kN/m^2 (e.g. deep1) and R = 4,7m in the short term)

- The physical non-linear effect governs over the geometrical non-linear effect in case of $d_{lining} >$ 0,30m. In case of slender constructions, i.e. $d_{lining} < 0,30$m, the geometrical non-linear effect governs over the geometrical non-linear effect.
- The magnitude of the hoop force is hardly influenced by the non-linear effects.
- The thicker the lining, the stiffer and consequently, the smaller the non-linear effects.
- The bending moments calculated, including both the non-linear effects, in case of $d_{lining} < 0,30$m are smaller than the bending moments calculated with the (linear) analytical Duddeck method.

All rights reserved. Use of disclosure of this data is subject to the restriction stated on the first page of this document.

Consequently, the calculation of the cross-section forces with the analytical Duddeck method is only conservative in case of $d_{lining} > 0,30m$.

With respect to the non-linear reliability analysis (only qualitative conclusions)

- The safety requirements, $P_b = 10^{-4}$ and $\beta = 3,6$ are not met, in spite of the increase of the safety with respect to the linear analysis.
- The safety of the tunnel lining decreases with decreasing d_{lining}, this in contrast to the conclusion drawn at the linear reliability analysis that the safety of the lining increases considerably with decreasing d_{lining}.
- It is safe to use the analytical Duddeck method for the calculation of the cross-section forces in case of $d_{lining} > 0,30m$ as from this lining thickness the (linear) model is conservative with respect to the model which includes the non-linear effects. In case of $d_{lining} < 0,30m$, the analytical Duddeck method underrates the cross-section forces. Consequently, it can be concluded that it is not safe to use the (linear) analytical Duddeck method for the optimisation of d_{lining}.

With respect to the calculation of the safety factors

- As a tunnel is a soil retaining construction, it is not unambiguous to express its reliability by means of an overall safety factor. An objective approach is to determine a partial safety factor for each parameter of the calculation. The calculated partial safety factors of the parameters of the calculation are small with values between 1,0 and 1,3 .
- Calculation of an overall safety factor for the ITM tunnel results in a value of $\gamma = 1,8$ which corresponds with the value given in the present building codes.
  (**remark:** although the definition of an overall safety factor is not unambiguous, an overall safety factor is calculated in order to be able to make a comparison with the safety factors given in the building codes)

All rights reserved. Use of disclosure of this data is subject to the restriction stated on the first page of this document.

13.2 Recommendations

The following recommendations are given for further study:

With respect to the reliability analysis

- Certain situations, like a change of the groundwaterlevel, a tunnel within the sphere of influence of a second tunnel, an embankment or an excavation can cause an increase of the loads. These situations should also be analysed with a reliability analysis.
- No consideration is given to the impact on the cross-section forces of, among others, effects caused by the assembling of the lining, dynamic loads, settlement of the soil, etc. These effects should also be analysed.
- As the model factors, specially the model factor of the bending moment, have a large impact on the failure of the tunnel more attention should be paid to the definition of their magnitude, e.g. by means of a linear regression analysis.
- The exact value of α_{SFRC}, i.e. the ratio between the tensile strength ($\beta_{BZ,R}$) and the compressive concrete strength (β_R) of steelfibre concrete, depends on the amount of steel fibres and should be determined by means of tests. It is recommended to execute the reliability analysis with α_{SFRC} as function of the basic variables $\beta_{BZ,R}$ and β_R when the magnitude of the tensile strength $\beta_{BZ,R}$ is known.
- The length-effect of the tunnel should be determined in order to give a better indication of the failure probability of the tunnel as a whole.

With respect to the geometrical non-linear effect

- In this study the buckling force is defined as $N_{buc} = 3EI / R^2$. It should be checked whether the use of the coefficient 3 is correct in the application of N_{buc} in a tunnel lining calculation.

With respect to the physical non-linear effect

- It is recommended to examine the physical non-linearity more thoroughly by considering also the following aspects:
  - definition of plastic hinges as the reduction of the lining stiffness is local;
  - examination of the amount of redistribution of forces due to the decrease of EI as consequence of crack formation; the simultaneous decrease of the resistance against deformation has to be taken into account.

With respect to the definition of the safety factors

- As the division into resistance and load parameters is an important part of the definition of the partial safety factors more attention should be paid to the interpretation of the parameters.
- In this study, the results have been generalised by means of a pragmatic approach, i.e. by calculating the average safety factor of the four reference profiles. More attention should be paid to the generalisation of the results.
- As the (partial) safety factors of the deep profiles have been determined with $\beta < \beta_{target} = 3{,}6$, these (partial) safety factors should be optimised by adjusting them to the required reliability index $\beta = 3{,}6$.

All rights reserved. Use of disclosure of this data is subject to the restriction stated on the first page of this document.

References

[1] CUR, nieuwe betonsoorten: *Staalvezelbeton; oriënterende rapportage over eigenschappen en toepassingsmogelijkheden*, rapport 89. september 1977
[2] Deutscher Beton-Verein, *Merkblatt Bemessungsgrundlagen für Stahlfaserbeton im Tunnelbau*, Fassung September 1992
[3] Deutscher Beton-Verein, *Technologie des Stahlfaserbetons und Stahlfaserspritzbetons*, Fassung August 1992
[4] Hilbrandie, R.K., *Optimalisatie van de geëxtrudeerde boortunnel: de binnenbekisting*, afstudeerverslag, TU Delft, januari 1997
[5] ITM-FUG-R-004, *Snedekrachten tunnel lining*, may 1995
[6] NEN 6720, *Regulations for concrete, Structural requirements and calculation methods (Voorschriften Beton TGB 1990. Constructieve eisen en rekenmethoden, VBC 1995)*
[7] NS Railinfrabeheer, *Kunstwerk Sophia*, lijn 152 km 325.450 - 7.302 Document 2DS: Prestatiebestek Double Stack Boortunnel, Utrecht, mei 1996
[8] NS Railinfrabeheer, *Botlekspoortunnel*, km 950/413.000 - 414.575, Document 2: Prestatiebestek, Utrecht, november 1995
[9] Maidl,-Bernard R., *Steelfibre Reinforced Concrete*, Berlin 1995
[10] Oosteren van, K., *Toepassing van geëxtrudeerd staalvezelbeton in Nederlandse tunnel bouw*, afstudeerverslag, TU Delft, januari 1996
[11] Ruitenberg, J., *Krachtswerking in de wand van een geboorde tunnel*, afstudeerverslag, TU Delft, januari 1997
[12] Schnütgen, B. & Dams, S., *Stahlfaserbeton im Tunnelbau*, Beton-Informationen, Heft 5, 1994
[13] TU Delft, rapportnummer 25.5-96-10, *Staalvezelbeton in de lining van boortunnels, een state-of-the-art*, december 1996
[14] NEN 6700, *Regulations for concrete, Technical principles for building structures (Voorschriften Beton TGB 1990, Technische grondslagen voor bouwconstructies)*
[15] Prof. drs. ir. J.K.. Vrijling & Prof. ir. A. C. W. M. Vrouwenvelder, *Probabilistisch ontwerpen,* dictaat b3, TU Delft, 1984
[16] Kosa,-K, A. Naaman, *Corrosion of Steelfibre Reinforced Concrete*. ACI Materials Journal, januari/februari 1990, pag. 27-37
[17] Duddeck, H. and J. Erdmann, *Structural design models for tunnels,* Tunnel lining '81, the Institution of Mining and Metallurgy, pag. 83-91, 1981
[18] Prof. drs. ir. Vrijling,J.K., *Probabilistisch ontwerpen in de waterbouwkunde*, dictaat f30, TU Delft, november 1996
[19] ITM-rapport,*Concrete hardening; description of loads and hardening process*
[20] Blom, K., *Liggerwerking van boortunnels*, afstudeerverslag, TU Delft, november 1995
[21] ITM-D 50000-RE-004, *Beaming*, august 1997
[22] Betoniek, *Vezels*, 8/21, januari 1991
[23] Kooiman, A., *Staalvezelbeton in de linings van boortunnels, een state-of-the-art,* rapportnummer 25.5-96-10, TU Delft, december 1996
[24] Concrete technology and design, vol.2, *Fibre reinforced concretes*, New reinforced concretes 1984
[25] Stroband, J., Stevinlaboratorium: onderzoek treksterkte staalvezelbeton, COB-commissie M624
[26] ITM-D50000-RE-007, *Concrete strength required for removal* formwork, oktober 1997
[27] NEN 6702, *Loads and deformations*, (Voorschriften Beton TGB 1990)
[28] NEN 6740, *Geotechnics, basic requirements and loads*, (Voorschriften Beton TGB 1990)
[29] Werkgroep L550, *Betrouwbaarheidsaspecten van ontwerpmethoden en rekenmodellen voor boortunnels,* in het kader van de werkzaamheden van: Commissie L500, Tweede concept d.d. juni '97
[30] Schulze, H., & Duddeck, H., *Spannungen in schildvorgetriebenen Tunneln*, Berlin: Beton- und Stahlbetonbau nr. 8, 1964
[31] Erdmann, J., & Duddeck, H., *Statik der Tunnel in Lockergestein- Vergleich der Berechnungsmodelle*, Bauingenieur 58, pag. 407-414, 1983
[32] Bouma, A.L.., *Mechanica van constructies- Elasto-statica van slanke structuren*, TU Delft, Delft 1989

All rights reserved. Use of disclosure of this data is subject to the restriction stated on the first page of this document.

[33] Erdmann, J., *Vergleich Ebener und Entwickelung räumlicher Berechnungsverfahren für Tunnel*, TU Braunschweig
[34] Duddeck, H., *Zu den Berechnungsmethoden und zur Sicherheit von Tunnelbauten*, Der Bauingenieur (47), Heft 2, 1972
[35] Prof. drs. ir. J.K. Vrijling, ir. K.G. Bezuyen, *Waterbouwkundige kunstwerken B.O.*, collegedictaat f9c, TU Delft, mei 1997
[36] van Kinderen, S., *Risicoanalyse van een geboorde tunnel'*, afstudeerverslag, TU Delft, juni 1995
[37] A. van der Put, *Samenvatting berekeningen boortunnel 2e-Heinenoord*, Directoraat-Generaal Rijkswaterstaat, augustus 1996
[38] *Kunstwerk Sophia*, lijn 152 km 325.450 - 7.302 Document 2DS: Prestatiebestek Double Stack Boortunnel, NS Railinfrabeheer, Utrecht, mei 1996
[39] *Botlekspoortunnel*, km 950/413.000-414.575, Document 2: prestatiebestek, NS Railinfrabeheer, Utrecht, november 1995
[40] *Regulations for the calculations of building structures. General considerations and loading.* (Technische grondslagen voor de berekening van bouwconstructies - TGB 1972. Algemeen gedeelte en belastingen) NEN 3850, 1972/1974
[41] Eurocode 1, *Basis of design and actions on structures, Part I: basis of design,* Nederlands voornorm, NVN-ENV 1991-1, march 1995
[42] Werkgroep L550 "Betrouwbaarheid" in het kader van de werkzaamheden van: Commissie L500 "Ontwerpmethoden en rekenmodellen voor boortunnel" rapport 97-CON-R1528, tweede concept
[43] Koyama,-Y, Kishio,-T, Kobayashi,-T, *Design of linings for shield driven tunnels - A survey on Japanese shield tunnelling*, Underground construction in soft ground, Japanese Society of Soil Mechanics and Foundation Engineering, pag. 359-374, 1995.
[44] NEN 6770, *Basic requirements and basic rules for calculation of predominantly staticaly loaded structures,* (Staalconstructies, TGB 1990)
[45] Ahrens, H., Lux, K., Lindner, E.; Zur Dimensionierung von Tunnelausbauten nach den *'Empfehlungen zur Berechnung von Tunneln im Lockergestein (1980)'*, Die Bautechniek 1982 nr. 8 & 9.
[46] Windels, R.; *Spannungstheorie zweiter Ordnung für den teilweise gebetteten Kreisring,* Die Bautechniek 1966 nr. 8.
[47] Timoshenko & Gere, *Theory of elastic stability,* International Student Edition, second edition, 1982
[48] Prof. dr. ir. J.C. Walraven, *Gewapend beton,* collegedictaat g20A, TU Delft, september 1996.
[49] ir. C. Hartsuijker, *Stabiliteit van het evenwicht*, collegedictaat b11, TU Delft, september 1994.
[50] Duddeck, A., *Analysis of linings for shielddriven tunnels,* institut fur Statik, Technische Universität Braunschweig, in: Tunnelling in Soft and Water-Bearing Grounds, Boston, 1985.
[51] H. Hain, B. Falter, "Stabilität von biegesteifen oder durch Momentgelenke geschwächten und auf der Aussenseite elastisch gelbetteten Kreisringen under konstantem Aussendruck", Strasse Brücke Tunnel 4/1975 pp 98 - 105
[52] Windels R. "Spannungstheorie zweiter Ordnung für den teilweise gebetteten Kreisring. Die Bautechnik 43 (1966). H.8
[53] Prof. dr. ir. A. Verruijt, A., Grondmechanica, TU Delft, 1990
[54] dr. ir. R.A. Vonk, *Design of a lining of steelfibre reinforced concrete*, ITM-report, 1998
[55] CUR, *damwandconstructies*, publikatie 166, october 1993

All rights reserved. Use of disclosure of this data is subject to the restriction stated on the first page of this document.

Notations

R	= radius of the tunnel	[m]
D	= diameter of the tunnel	[m]
d, d_{lining}	= lining thickness	[m]
b	= section length or width	[-]
l	= construction length	[m]
A	= cross-sectional area	[m^2]
h_{tunnel}	= depth of the tunnel	[m]
h_{river}	= waterlevel of the river	[m]
h_{gw}	= phreatic surface	[m]
E_g	= modulus of elasticity of the soil	[MPa]
E_s, E_{oed}	= modulus of elasticity of the soil according to the oedometertest	[Mpa]
E, E_{lining}	= modulus of elasticity of the lining	[MPa]
$E_{fictitious}$	= fictitious modulus of elasticity of the lining	[MPa]
EI	= bending stiffness	[Nm^2]
$EI_{reduced}$	= reduced bending stiffness	[Nm^2]
I	= moment of inertia	[m^4]
φ	= creep coefficient	[-]
f'_{ck}	= compressive cube concrete strength	[N/mm^2]
$\sigma_{vertical}$	= vertical soil stresses	[kN/m^2]
g	= acceleration of gravity	[m/s^2]
$\sigma_{horizontal}$	= horizontal soil stresses	[kN/m^2]
$\sigma'_{vertical}$	= vertical effective stresses	[kN/m^2]
$\sigma'_{horizontal}$	= horizontal effective stresses	[kN/m^2]
ρ_k	= density of the grains	[kg/m^3]
ρ_{water}	= density of the water	[kg/m^3]
γ_{water}	= volume weight of the water	[kN/m^2]
γ_{wet}	= wet volume weight	[kN/m^2]
S_{wet}	= degree of saturation of the wet soil	[-]
S_{dry}	= degree of saturation of the 'dry' soil	[-]
γ_{dry}	= dry volume weight	[kN/m^2]
ν	= Poisson's ratio	[-]
K_0	= coefficient of lateral effective pressure	[-]
$K_{0,water}$	= coefficient of lateral water pressure	[-]
c	= cohesion	[kPa]
k_r	= bedding modulus	[kN/m]
R_Z	= resistance	[..]
S	= load	[..]
γ_S	= load factor	[-]
γ_R	= resistance factor	[-]
γ	= overall safety factor	[-]
$\Phi(..)$	= distribution function	
$P_b(..)$	= probability	
β	= reliability index	[-]
β_{AHRENS}	= stiffness ratio according to Ahrens (remark: $\alpha_{Duddedk} = \beta_{AHRENS}$)	[m^{-1}]
$\beta_{Duddeck}$	= coefficient that gives the lining-ground relationship in the Duddeck formulae	[m^{-1}]
β_R	= compressive concrete strength (i.e. steelfibre concrete)	[N/mm^2]
$\beta_{BZ,R}$	= tensile concrete strength (i.e. steelfibre concrete)	[N/mm^2]
μ	= mean value	[-]
σ	= standard deviation	[-]
V	= variation coefficient	[-]
m_b	= model factor for concrete	[-]
m_N	= model factor for the hoop force	[-]
m_M	= model factor for the bending moment	[-]

All rights reserved. Use of disclosure of this data is subject to the restriction stated on the first page of this document.

α_{AFDA}	= probabilistic influence coefficient	[-]
α_{SFRC}	= ratio of flexural strength and compressive concrete strength which depends on the amount of steelfibres	[-]
$\alpha_{Duddeck}$	= coefficient that gives the lining-ground relationship in the Duddeck formulae	[m^{-1}]
X_k	= characteristic value	[..]
X_{rep}	= representative value	[..]
X_d	= design value	[..]
X^*	= design point	[..]
q	= load	[kN/m^2]
p_v	= load at the top of the tunnel (used in the graphs of Ahrens)	[kN/m^2]
k	= subgrade factor	[kN/m^3]
w	= settlement	[m]
u	= displacement	[m]
F	= force in the spring as result of a displacement	[kN]
θ	= angle relative to the vertical axis through the hart of the tunnel	[^{0}]
n_{AHRENS}	= M_{II}/M_I = second order effect factor according to Ahrens	[-]
n_p	= porosity	[-]
n_{buc}	= N_{buc} / N	[-]
n	= hoop force	[-]
N	= hoop force	[kN]
N_{buc}	= buckling force	[kN]
N_{min}	= minimum hoop force	[kN]
N_{max}	= maximum hoop force	[kN]
N_u	= ultimate hoop force	[kN]
m	= bending moment	[-]
M	= bending moment	[kNm]
M_0,M_I	= first order bending moment	[kNm]
M_{linear}	= M_0 = M_I = bending moment according to the first order linear theory	[kNm]
M_{gnl}, M_{II}	= second order bending moment due to the geometrical non-linear effect	[kNm]
M_{fnl}	= second order bending moment due to the physical non-linear effect	[kNm]
$M_{gnl\text{-}fnl}$	= second order bending moment due the combined effect of geometrical and physical non-linearity	[kNm]
M_{max}	= maximum bending moment	[kNm]
M_u	= ultimate bending moment	[kNm]
$\mathbb{K}$	= curvature	[m^{-1}]
R_Z	= resistance	[..]
S	= load	[..]
Z	= reliability function	
C	= equation substituted in the reliability function Z = $-0,6\ \alpha^2 + 0,478\ \alpha + 0,0012$	
D	= equation substituted in the reliability function Z = $-0,56\ \alpha^2 + 0,852\ \alpha - 0,4812$	
E	= equation substituted in the reliability function Z = $0,18\ \alpha^2 + 0,478\ \alpha - 0,4876$	

All rights reserved. Use of disclosure of this data is subject to the restriction stated on the first page of this document.

Reliability analysis of a steel fibre reinforced concrete tunnel lining

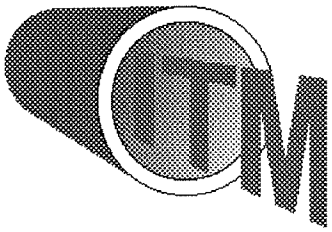

Industrial Tunnel building Method

Appendix

All rights reserved. Disclosure to third parties of this document or any part thereof, or the use of any information contained therin for purposes other than provided for by this document, is not permitted, except with the prior and express written permission of ITM cv.

Appendix

1. Design-equations of the analytical Duddeck method
2. Interpretation of the parameter K_0 of the analytical Duddeck method
3. Bending moments in the tunnel lining according to Duddeck
4. Equations of the Bouma-model
5. Definition of the design point
6. AFDA (level II, class 3)
7. Working procedure for a probabilistic analysis with the input of PLAXIS
8. Definition of the failure curves
9. Definition of Z in AFDA
10. Input of AFDA (linear model)
11. Output of AFDA (linear model; deep1)
12. Geometrical non-linearity according to Ahrens
13. Definition of the buckling force
14. Geometrical non-linear computation of the ITM-tunnel
15. NMK-diagram
15. Safety factors

All rights reserved. Use of disclosure of this data is subject to the restriction stated on the first page of this document.

1. Design-equations of the analytical Duddeck method

The design-equations of Duddeck are based on a continuum model.
Duddeck either takes into account the whole friction in tangential direction ('full bond') along the tunnel lining or neglects it partly or completely ('tangential slip'). He has published different equations for these two cases. In this appendix, only the equations of the case 'full bond' are given as ITM c.v. uses this approach.

Coefficients that give the interaction between the soil and the tunnel lining

$$\alpha_{Duddeck} = \frac{E_g R^3}{E_m I} \qquad \text{and} \qquad \beta_{Duddeck} = \frac{E_g R}{E_m A}$$

Hoop force

$$N_0(=const) = \sigma_{v,m}(1+K_0)R\frac{1}{2+1.54\beta_{Duddeck}}$$

$$N_2(\theta) = \sigma_{v,m}(1-K_0)R\frac{1+0.064\alpha_{Duddeck}}{2+0.171\alpha_{Duddeck}}\cos(2\theta)$$

$$N_{max} = N_0 + N_2(0)$$
$$N_{min} = N_0 - N_2(0)$$

Bending moment

$$M(\theta) = \sigma_{v,m}(1-K_0)R^2\frac{1}{4+0.342\alpha_{Duddeck}}\cos(2\theta)$$

Radial displacement

$$u(\theta) = -\sigma_{v,m}(1-K_0)\frac{\frac{R^4}{E_m I}}{12+1.03\alpha_{Duddeck}}\cos(2\theta)$$

The displacement as result of the shortening of the ring is negligible.

All rights reserved. Use of disclosure of this data is subject to the restriction stated on the first page of this document.

2. Interpretation of the K_0 of the analytical Duddeck method

The lateral earth pressure coefficient K_0 is the ratio between the horizontal and the vertical effective stresses. The analytical Duddeck method is based on *dry* soil, while the Dutch soil is wet due to the high phreatic surface. Consequently, the influence of the waterpressure has to be taken into account. The following alternatives are possible for the calculation of M and N in case of a high phreatic surface: (the calculation counts for soil profile deep1)

1. Calculation with Ko = σ'_h / σ'_v (this is the real interpretation of K_0 and is used in the reliability analysis)

effective stresses:

$\sigma'_v = \gamma_{dry} \cdot h_{groundwater} + (h_{tunnel} - h_{groundwater}) \cdot (\gamma_{wet} - \gamma_{water})$
$= 18 \cdot 1 + (22.5 - 1) \cdot (20 - 10) = 233\ kN/m^2$

$Ko = \lambda_n = 0.46$

cross-section forces according to Duddeck:

$M_{max,grain} = 309.9\ kNm$
$N_{min,grain} = 540\ kN$

water pressure:

$\sigma_w = \gamma_{water} \cdot (h_{tunnel} - h_{groundwater})$
$= 10 \cdot (22.5 - 1) = 215\ kN/m^2$

$Ko = \lambda_n = 1.0$

cross-section forces according to Duddeck:

$M_{max,water} = 0\ kNm$
$N_{min,water} = 1004\ kN$

total cross-section forces:

$M_{max,\ total} = M_{max,grain} + M_{max,water} =$ **309.9 kNm**
$N_{min,\ total} = N_{min,grain} + N_{min,water} = 540 + 1004 =$ **1544 kN**

2. Calculation with Ko = σ_h / σ_v (this definition does not correspond to the real interpretation, but does give the same results)

$\sigma_v = \gamma_{dry} \cdot h_{groundwater} + (h_{tunnel} - h_{groundwater}) \cdot \gamma_{wet}$
$= 18 \cdot 1 + (22.5 - 1) \cdot 20 = 448\ kN/m^2$

$\sigma'_v = \sigma_v - \gamma_{water} \cdot (h_{tunnel} - h_{groundwater})$
$= 448 - 10 \cdot (22.5 - 1) = 233\ kN/m^2$

$\sigma'_h = \sigma'_v \cdot \lambda_n = 233 \cdot 0.46 = 107.18\ kN/m^2$

$\sigma_h = \sigma'_h + (h_{tunnel} - h_{groundwater}) \cdot \gamma_{water}$
$= 107.18 + (22.5 - 1) \cdot 10 = 322.18\ kN/m^2$

$Ko = \sigma_h / \sigma_v = 322.18 / 448 = 0.719$

cross-section forces according to Duddeck:

$M_{max,1} =$ **310 kNm**
$N_{min,1} =$ **1544 kN**

All rights reserved. Use of disclosure of this data is subject to the restriction stated on the first page of this document.

3. Bending moments in the tunnel lining according to Duddeck

Remarks

- the graph shows that the bending moments decrease with d_{lining};
- clay profile: $\alpha = 3\ m^{-1}$
  sand profile: $\alpha = 20\ m^{-1}$
  in case of clay, M decreases more with decreasing lining thickness than in case of sand

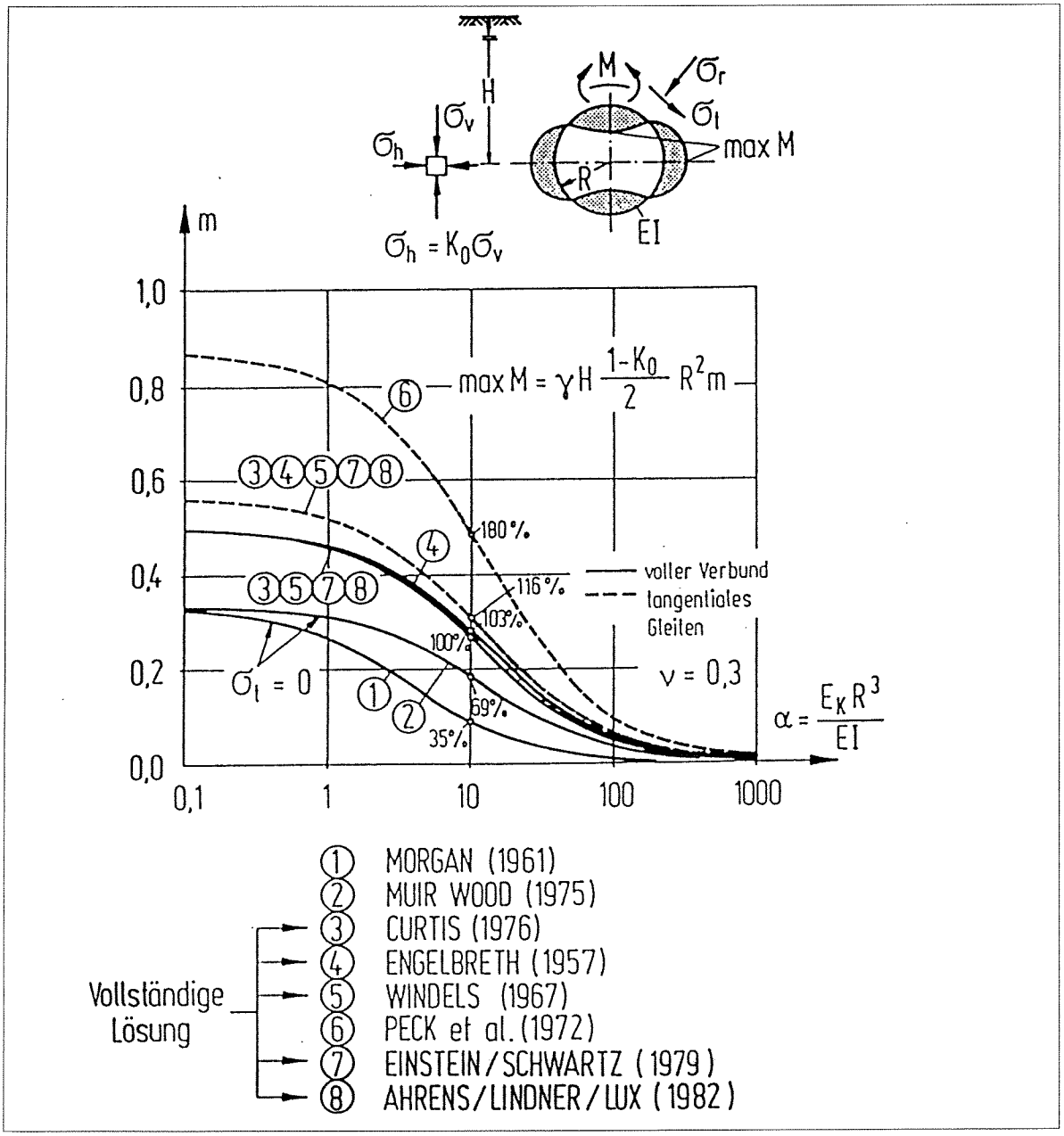

The models (1) to (8) are all models based on the Duddeck model.

All rights reserved. Use of disclosure of this data is subject to the restriction stated on the first page of this document.

4. Equations of the Bouma-model

Bouma has derived differential equations for hoop force and bending moment in circular rings. These differential equations are derived from equilibrium equations in tangential and radial direction of a ring-shaped segment.

Hoop force

$$N(\theta) = -\frac{1}{2}\cdot\sigma_{v,m}\cdot(1+K_o)\cdot R + \frac{1}{2}\cdot\sigma_{v,m}\cdot(1-K_o)\cdot R\cdot\cos(2\theta)$$

Bending moment

$$M(\theta) = -\frac{1}{4}\cdot\sigma_{v,m}\cdot(1-K_o)\cdot R^2\cdot\cos(2\theta)$$

Radial displacement

$$u(\theta) = -\frac{\sigma_{v,m}\cdot(1-K_o)}{12E_mI}\cdot R^4\cdot\cos(2\theta) - \frac{\frac{1}{2}\cdot\sigma_{v,m}\cdot(1+K_o)\cdot R^2}{E_mA}$$

All rights reserved. Use of disclosure of this data is subject to the restriction stated on the first page of this document.

5. Definition of the design point

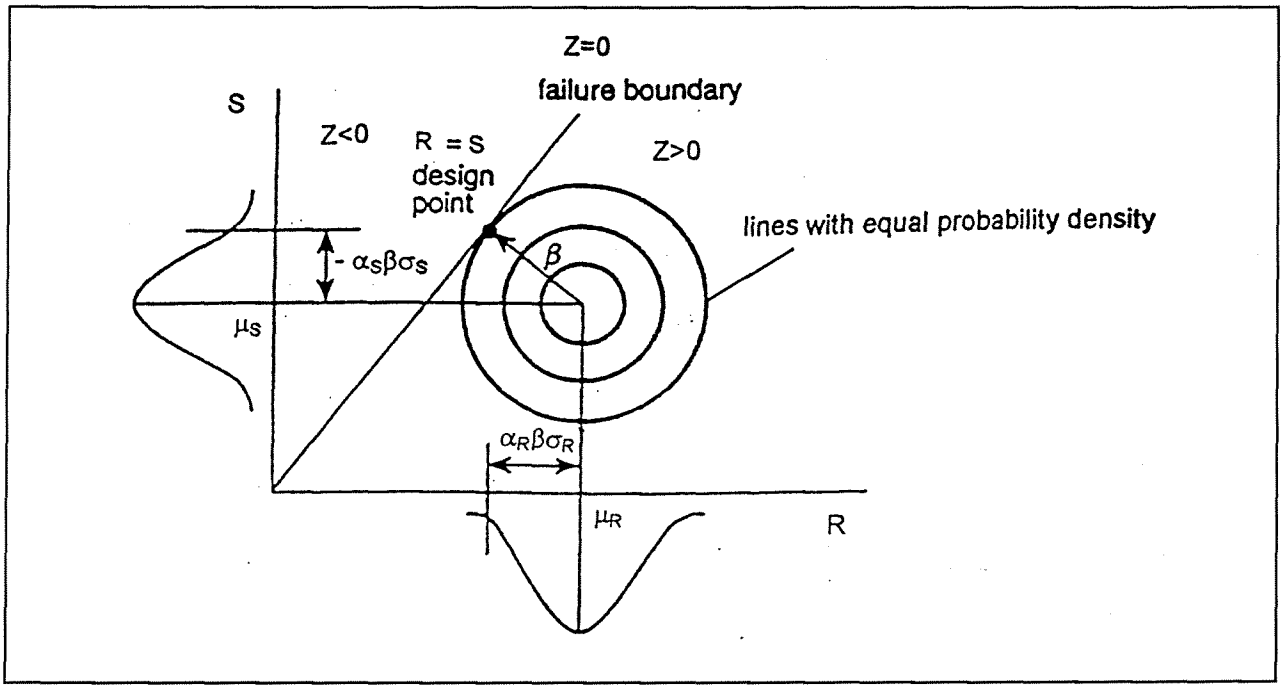

figure : design point definition [lit,41]

with:
S = action effect
R = resistance

design point:
R^* = $\mu_R - \alpha_R\beta\sigma_R$
S^* = $\mu_S - \alpha_S\beta\sigma_S$
(with $R^* = S^*$ when the design point is situated on the failure boundary R = S)

Z = 0 : failure boundary
Z < 0 : unsafe area
Z > 0 : safe area

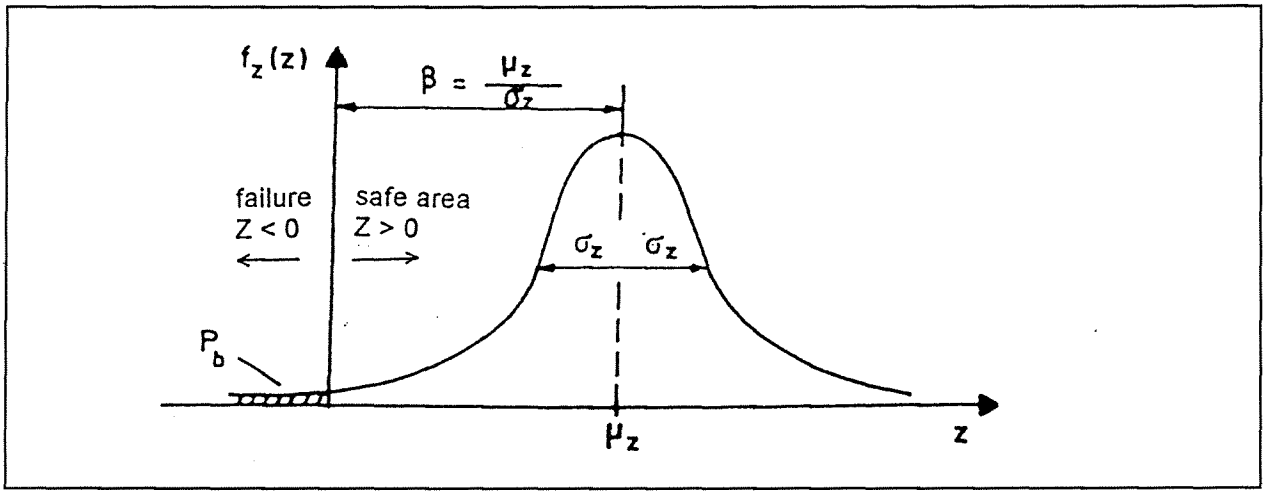

figure: probability density function of Z

All rights reserved. Use of disclosure of this data is subject to the restriction stated on the first page of this document.

6. AFDA (level II, class 3)

With this method the reliability function Z is linearised around the (design)point $\overline{X}^*$ (see appendix 5) of the failure boundary Z = 0 with the highest probability of occurrence. The function Z is linearised around the point $\overline{X}^*$ by means of the development of Taylor-series.
As first approximation of the unknown linearised failure boundary, the following is assumed:

$$Z \approx Z(X_1^*, X_2^*, \ldots, X_n^*) + \sum_{i=1}^{n} \frac{\delta Z}{\delta X_i}(X_i - X^*) = 0 \qquad (1)$$

wherein $\frac{\delta Z}{\delta X_i}$ is calculated in (X^*_1, X^*_2, ..., X^*_n)
this results in:

$$\mu_z = Z(X_1^*, X_2^*, \ldots, X_n^*) + \sum_{i=1}^{n} \frac{\delta Z}{\delta X_i}(\mu_{X_I} - X_i^*) \qquad (2)$$

and

$$\sigma_z = \left\{ \sum_{i=1}^{n} \left(\frac{\delta Z}{\delta X_i} \right)^2 \cdot \sigma_{X_i}^2 \right\}^{1/2} \qquad (3)$$

Equation (3) can be expressed as a linear function of the standard deviations:

$$\sigma_Z = \sum_{i=1}^{n} \alpha_i \frac{\delta Z}{\delta X_i} \sigma_{X_i} \qquad (4)$$

wherein:

$$\alpha_i = \frac{\frac{\delta Z}{\delta X_i} \cdot \sigma_{X_i}}{\left\{ \sum_{j=1}^{n} \left(\frac{\delta Z}{\delta X_j} \right)^2 \cdot \sigma_{X_j}^2 \right\}^{1/2}} \qquad (5)$$

As the point $\overline{X}^*$ has to lie on the failure boundary, the following equation has to be fulfilled:
Z = Z (X^*_1, X^*_2, ..., X^*_n) = 0
which gives:

$$\beta = \frac{\mu_Z}{\sigma_Z} = \frac{\sum_{i=1}^{n} (\mu_{X_i} - X_i^*) \cdot \frac{\delta Z}{\delta X_i}}{\sum_{i=1}^{n} \alpha_i \cdot \frac{\delta Z}{\delta X_i} \cdot \sigma_{X_i}} \qquad (6)$$

The result of this equation (6) gives a new estimate for the design point $\overline{X}^*$:
$X^*_i = \mu_{Xi} - \alpha_i \beta \sigma_{Xi}$ for all i (7)
The design-point corresponds to the point (X_1, X_2, ...,X_N) on the failure surface having the highest probability of occurrence, that satisfies:
Z(X^*_1, X^*_2, ..., X^*_N) = 0
The values of the partial derivatives, however, are determined in the 'old' point (X_{start}=X_{mean}). This means that the procedure has to be repeated until a stable value for $\overline{X}^*$ is found.

All rights reserved. Use of disclosure of this data is subject to the restriction stated on the first page of this document.

In equation (6) was assumed that Z(X*) = 0; this assumption was necessary in order to solve equation (7). As long as the right design point is not found, $Z(X^*) \neq 0$. This has to be taken into account when the best assumption of β has to be made:

$$\beta = \frac{\mu_Z}{\sigma_Z} = \frac{Z(\overline{X^*}) + \sum_{i=1}^{n} \frac{\delta Z}{\delta X_i} \cdot \left(\mu_{X_i} - X_i^*\right)}{\sum_{i=1}^{n} \alpha_i \cdot \frac{\delta Z}{\delta X_i} \cdot \sigma_{X_i}} \qquad (8)$$

The whole procedure has to be repeated for a new point $\overline{X}^*$, based on this new value of β (equation (8)), until Z(X*)=0.

Summarised, the correct solution is found by means of an iteration-procedure:

1. Estimate a value for β
2. Suppose $X^*_i = \mu_{Xi}$ for all i
3. Calculate $\delta Z/\delta Z(X_i)$ for all i in $X = \overline{X}^*_i$
4. Calculate α_i for all i
5. Calculate the new values of $\overline{X}^*_i$
6. Repeat step 3 to 5 until a stable value for $\overline{X}^*$ is found
7. Calculate $Z = (X^*_1, X^*_2, ..., X^*_N)$
8. Adapt β, if necessary, so that Z = 0 and repeat step 3 to 5
9. Determine the failure chance with $P_b = 1 - \phi_N(-\beta)$

All rights reserved. Use of disclosure of this data is subject to the restriction stated on the first page of this document.

7. Working procedure for a probabilistic analysis with input of PLAXIS

The following calculation strategy is used to perform the reliability analysis:

1. The AFDA calculation is executed manually as indicated in the following table:

X_i	$\delta Z/\delta X_i = \Delta Z(X_i)/\Delta X_i$	σ_{Xi}	$\Delta Z/\Delta X_i \cdot \sigma_{Xi}$	$(\Delta Z/\Delta X_i \cdot \sigma_{Xi})^2$	α_i
stochastic variables, start-value = mean value	$\frac{Z(Xi) - Z(Xi-\Delta X)}{\Delta X}$			$\frac{}{\pm \sigma^2_Z}$	$\frac{\frac{\delta Z}{\delta X_i} \cdot \sigma_{X_i}}{\left(\sum_{j=1}^{n} \left(\frac{\delta Z}{\delta X_j}\right)^2 \cdot \sigma^2_{x_j}\right)^{\frac{1}{2}}}$

Remarks

- As the partial derivatives are calculated as $\Delta Z/\Delta X_i$, the Z-function has to be linear. This linear Z-function shall be determined as the tangent line of the Z-curve;
- As the AFDA calculation has to be done manually, the amount of stochastic variables has to be reduced.

2. $\mu_Z = Z(\mu_{Xi})$
3. Calculation of the design point for each parameter X_i : $X_i^* = \mu_i - \alpha_i \beta \sigma_i$
4. The reliability function is calculated as function of X^*_i ; if $Z(X^*_1, X^*_2, \ldots X^*_n) \neq 0$, the calculation has To be iterated with the X_i^*-values as input until $Z(X^*_1, X^*_2, \ldots X^*_n) = 0$
5. Calculation of the reliability index $\beta = \mu_Z/\sigma_Z$
6. The failure probability can be calculated with β

All rights reserved. Use of disclosure of this data is subject to the restriction stated on the first page of this document.

8. Definition of the failure curves

Failure curve in case of $\alpha = 0.00$

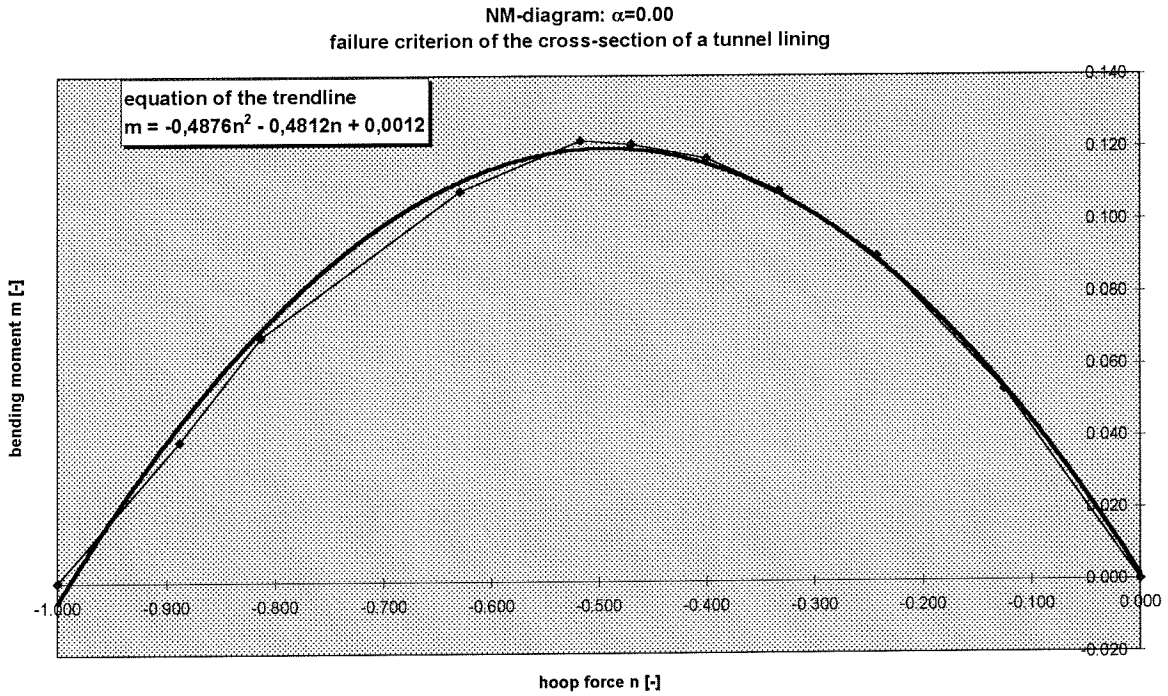

Failure curve in case of $\alpha = 0.05$

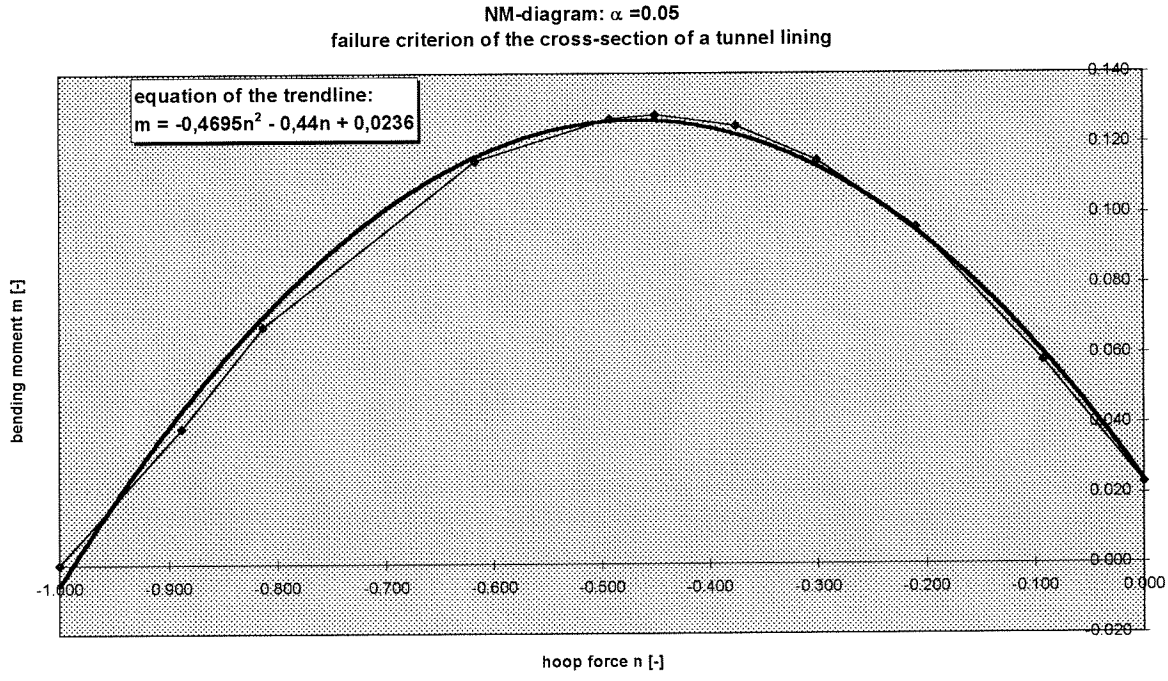

All rights reserved. Use of disclosure of this data is subject to the restriction stated on the first page of this document.

Failure curve in case of α = 0.10

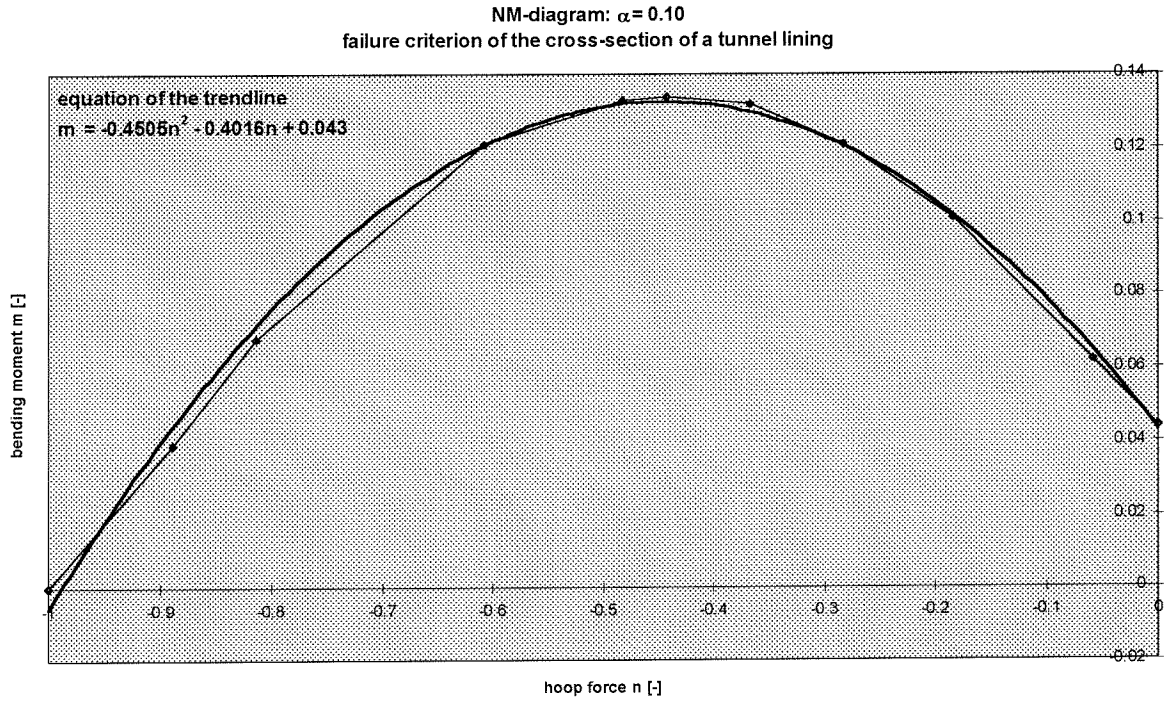

All rights reserved. Use of disclosure of this data is subject to the restriction stated on the first page of this document.

9. Definition of Z in AFDA

9.1 Linear model

(deep profile)

```
FUNCTION Z (X:ARY): REAL;
CONST
  g       = 9.81;    { acceleration of gravity [m/s2]}
  br      = 1.00;    { sectionlength [m] }
  htunnel= 22.5;     { depth of the tunnel-axis [m]}

VAR
  Gdry    ,     { volume weight of the dry soil [kN/m3] }
  Gwet    ,     { volume weight of the wet soil [kN/m3] }
  Gwater  ,     { volume weight of water [kN/m3] }
  R       ,     { radius [m] }
  dlining,      { thickness of the lining [m] }
  hgw     ,     { groundwaterlevel [m] }
  Eg      ,     { modulus of elasticity of the soil [MPa] }
  Eoed    ,     { modulus of elasticity of the soil according to the oedometertest [MPa]}
  Elining,      { modulus of elasticity of the lining (short term) [MPa]}
  Elong   ,     { modulus of elasticity of the lining (long term) [MPa]}
  poisson,      { Poisson's ratio [-]}
  creep   ,     { creep coefficient [-]}
  Swet    ,     { degree of saturation of the wet soil [-]}
  Sdry    ,     { degree of saturation of the dry soil [-]}
  n       ,     { porosity [-] }
  Rgrain  ,     { density of the grains [kg/m3]}
  Rwater  ,     { density of the water [kg/m3]}
  Sv      ,     { vertical soilstress [kN/m2] }
  Sw      ,     { waterpressure [kN/m2] }
  kn      ,     { coefficient of lateral effective pressure [-] }
  phi     ,     { angle of internal friction [rad] }
  K0      ,     { coefficient of lateral earth pressure [-] }
  K0water,      { coefficient of lateral pressure of the water [-]}
  I       ,     { moment of inertia [m3] }
  O       ,     { cross sectional area [m2] }
  A       ,     { interaction coefficient, alpha factor [-] }
  B       ,     { interaction coefficient, beta factor [-] }
  Mmax    ,     { maximum bending moment [kNm] }
  Nmin    ,     { minimum hoop force [kN] }
  N0      ,     { first term of the fourierseries of the hoop force [kN] }
  N2      ,     { second term of the fourierseries of the hoop force [kN] }
  Nmingrain,    { minimum hoop force with respect to the grains [kN]}
  Nmaxgrain,    { maximum hoop force with respect to the grains [kN]}
  Nminwater,    { minimum hoop force with respect to the water [kN]}
  Nmaxwater,    { maximum hoop force with respect to the water [kN]}
  N0grain,      { first term of the fourier series of the hoop force (grains) [kN]}
  N2grain,      { second term of the fourier series of the hoop force (grains) [kN]}
  N0water,      { first term of the fourier series of the hoop force (water) [kN]}
  N2water,      { second term of the fourier series of the hoop force (water) [kN]}
  f       ,     { compresion strength of concrete [N/mm^2]}
  al      ,     { alpha factor = Sbz / f [-]}
  C       ,     { first coefficient of the Z-function}
  D       ,     { second coefficient of the Z-function}
  E       ,     { third coefficient of the Z-function }
  mb      ,     { modelfactor of concrete [-] }
  mN      ,     { modelfactor of the hoop force [-] }
  mM      ,     { modelfactor of the bending moment [-] }
  Nu      ,     { ultimate hoop force determined with the N&M diagram [kN] }
  Mu            { bending moment [kNm] }
          : extended;
```


All rights reserved. Use of disclosure of this data is subject to the restriction stated on the first page of this document.

```
PROCEDURE INTERF;
    BEGIN
      K0water     := X[1];
      K0          := X[2];
      Swet        := X[3];
      Sdry        := X[4];
      n           := X[5];
      Rgrain      := X[6];
      Rwater      := X[7];
      hgw         := X[8];
      Gwater      := X[9];
      R           := X[10];
      dlining     := X[11];
      Eg          := X[12];
      poisson     := X[13];
      Elining     := X[14];
      creep       := X[15];
      f           := X[16];
      mb          := X[17];
      mN          := X[18];
      mM          := X[19];
      al          := X[20];
      C           := -0.6*al*al+0.478*al+0.0012;
      D           := -0.56*al*al+0.852*al-0.4812;
      E           := 0.18*al*al+0.353*al-0.4876;
      Elong       := (1/(1+0.75*creep))*Elining;
      Eoed        := ((1-poisson)/((1+poisson)*(1-2*poisson)))*Eg;
      I           := (1/12)*br*dlining*dlining*dlining;
      A           := (Eoed*R*R*R)/(Elong*I);
      O           := br*dlining;
      B           := (Eoed*R)/(Elong*O);
      Gwet        := (Swet*n*Rwater*g+(1-n)*Rgrain*g)/1000;
      Gdry        := (Sdry*n*Rwater*g+(1-n)*Rgrain*g)/1000;
      Sv          := Gdry*hgw+(Gwet-Gwater)*(htunnel-hgw);
      N0grain     := (Sv*(1+K0)*R)/(2+1.54*B);
      N2grain     := ((Sv*(1-K0)*R)*(1+0.064*A))/(2+0.171*A);
      Nmingrain   := mN*(N0grain-N2grain);
      Sw          := Gwater*(htunnel-hgw);
      N0water     := (Sw*(1+K0water)*R)/(2+1.54*B);
      N2water     := ((Sw*(1-K0water)*R)*(1+0.064*A))/(2+0.171*A);
      Nminwater   := mN*(N0water-N2water);
      Nmin        := Nmingrain+Nminwater;
      Mmax        := mM*((Sv*(1-K0)*R*R)/(4+0.342*A));
      Nu          := -mb*f*br*dlining*1000;
      Mu          := mb*f*br*dlining*dlining*1000;
          END;

{ *************************
  ****** MAIN PROGRAM ******
  ************************* }
  BEGIN
      Interf;
      Z:=Mu*(C+D*(Nmin/Nu)+E*((Nmin*Nmin)/(Nu*Nu)))-Mmax    {z-functie}
  END;
```


All rights reserved. Use of disclosure of this data is subject to the restriction stated on the first page of this document.

9.2 Non-linear model

(deep profile)

```
FUNCTION Z (X:ARY): REAL;
CONST
  g       = 9.81;    { acceleration of gravity [m/s2]}
  br      = 1.00;    { sectionlength [m] }
  htunnel= 22.5;     { depth of the tunnel-axis [m]}

VAR
  Gdry    ,     { volume weight of the dry soil [kN/m3] }
  Gwet    ,     { volume weight of the wet soil [kN/m3] }
  Gwater ,      { volume weight of water [kN/m3] }
  R       ,     { radius [m] }
  dlining,      { thickness of the lining [m] }
  hgw     ,     { groundwaterlevel [m] }
  Eg      ,     { modulus of elasticity of the soil [MPa] }
  Eoed    ,     { modulus of elasticity of the soil according to the oedometertest [MPa]}
  Efict   ,     { fictitious modulus of elasticity of the lining [MPa]}
  poisson,      { Poisson's ratio [-]}
  Swet    ,     { degree of saturation of the wet soil [-]}
  Sdry    ,     { degree of saturation of the dry soil [-]}
  n       ,     { porosity [-] }
  Rgrain ,      { density of the grains [kg/m3]}
  Rwater ,      { density of the water [kg/m3]}
  Sv      ,     { vertical soilstress [kN/m2] }
  Sw      ,     { waterpressure [kN/m2] }
  kn      ,     { coefficient of lateral effective pressure [-] }
  phi     ,     { angle of internal friction [rad] }
  K0      ,     { coefficient of lateral earth pressure [-] }
  K0water,      { coefficient of lateral pressure of the water [-]}
  I       ,     { moment of inertia [m3] }
  O       ,     { cross sectional area [m2] }
  A       ,     { interaction coefficient, alpha factor [-] }
  B       ,     { interaction coefficient, beta factor [-] }
  Mmax1   ,     { maximum first order moment [kNm]}
  Mmax2   ,     { max.second order moment including physical and geometrical non-linearitykNm]}
  Nmin    ,     { minimum hoop force [kN] }
  Nmax    ,     { maximum hoop force [kN] }
  N0      ,     { first term of the fourierseries of the hoop force [kN] }
  N2      ,     { second term of the fourierseries of the hoop force [kN] }
  Nbuc    ,     { buckling force [kN] }
  Nmingrain,    { minimum hoop force with respect to the grains [kN]}
  Nmaxgrain,    { maximum hoop force with respect to the grains [kN]}
  Nminwater,    { minimum hoop force with respect to the water [kN]}
  Nmaxwater,    { maximum hoop force with respect to the water [kN]}
  N0grain,      { first term of the fourier series of the hoop force (grains) [kN]}
  N2grain,      { second term of the fourier series of the hoop force (grains) [kN]}
  N0water,      { first term of the fourier series of the hoop force (water) [kN]}
  N2water,      { second term of the fourier series of the hoop force (water) [kN]}
  u       ,     { displacements [m] }
  f       ,     { compresion strength of concrete [N/mm^2]}
  al      ,     { alpha factor = Sbz / f [-]}
  C       ,     { first coefficient of the Z-function}
  D       ,     { second coefficient of the Z-function}
  E       ,     { third coefficient of the Z-function }
  mb      ,     { modelfactor of concrete [-] }
  mN      ,     { modelfactor of the hoop force [-] }
  mM      ,     { modelfactor of the bending moment [-] }
  Nu      ,     { ultimate hoop force determined with the N&M diagram [kN] }
  Mu            { bending moment [kNm] }
            : extended;
```


All rights reserved. Use of disclosure of this data is subject to the restriction stated on the first page of this document.

```
PROCEDURE INTERF;
   BEGIN
     K0water     := X[1];
     K0          := X[2];
     Swet        := X[3];
     Sdry        := X[4];
     n           := X[5];
     Rgrain      := X[6];
     Rwater      := X[7];
     hgw         := X[8];
     Gwater      := X[9];
     R           := X[10];
     dlining     := X[11];
     Eg          := X[12];
     poisson     := X[13];
     Efict       := X[14];
     f           := X[15];
     mb          := X[16];
     mN          := X[17];
     mM          := X[18];
     al          := X[19];
     C           := -0.6*al*al+0.478*al+0.0012;
     D           := -0.56*al*al+0.852*al-0.4812;
     E           := 0.18*al*al+0.353*al-0.4876;
     Eoed        := ((1-poisson)/((1+poisson)*(1-2*poisson)))*Eg;
     I           := (1/12)*br*dlining*dlining*dlining;
     A           := (Eoed*R*R*R)/(Efict*I);
     O           := br*dlining;
     B           := (Eoed*R)/(Efict*O);
     Gwet        := (Swet*n*Rwater*g+(1-n)*Rgrain*g)/1000;
     Gdry        := (Sdry*n*Rwater*g+(1-n)*Rgrain*g)/1000;
     Sv          := Gdry*hgw+(Gwet-Gwater)*(htunnel-hgw);
     N0grain     := (Sv*(1+K0)*R)/(2+1.54*B);
     N2grain     := ((Sv*(1-K0)*R)*(1+0.064*A))/(2+0.171*A);
     Nmingrain   := mN*(N0grain-N2grain);
     Nmaxgrain   := mN*(N0grain+N2grain);
     Sw          := Gwater*(htunnel-hgw);
     N0water     := (Sw*(1+K0water)*R)/(2+1.54*B);
     N2water     := ((Sw*(1-K0water)*R)*(1+0.064*A))/(2+0.171*A);
     Nminwater   := mN*(N0water-N2water);
     Nmaxwater   := mN*(N0water+N2water);
     Nmin        := Nmingrain+Nminwater;
     Nmax        := Nmaxgrain+Nmaxwater;
     Mmax1       := mM*((Sv*(1-K0)*R*R)/(4+0.342*A));
     Nbuc        := (3*Efict*1000*I)/(R*R);
     n           := Nbuc/Nmax;
     u           := (Sv*(1-K0)*R*R*R*R)/(Efict*1000*I*(12+1.03*A));
     Mmax2       := Mmax1+Nmin*u*(n/(n-1));
     Nu          := -mb*f*br*dlining*1000;
     Mu          := mb*f*br*dlining*dlining*1000;
         END;

{ *************************
  ****** MAIN PROGRAM ******
  ************************* }
  BEGIN
      Interf;
      Z:=Mu*(C+D*(Nmin/Nu)+E*((Nmin*Nmin)/(Nu*Nu)))-Mmax2    {z-functie}
  END;
```


All rights reserved. Use of disclosure of this data is subject to the restriction stated on the first page of this document.

10. Input of AFDA (linear model)

Input of soil profile deep 1

datad11.dta N = normal distribution ; L = lognormal distribution

20		μ	σ		Xstart
K0water	N	1.0	0.01	0.00	1.00
K0	N	0.46	0.046	0.00	0.46
Swet	N	1.0	0.01	0.00	1.0
Sdry	N	0.4	0.004	0.00	0.4
n	N	0.36	0.011	0.00	0.36
Rgrain	N	2650	26.5	0.00	2650
Rwater	N	1000	10.0	0.00	1000
hgw	N	1.00	0.50	0.00	1.00
Gwater	N	10.0	0.10	0.00	10.0
R	N	4.70	0.05	0.00	4.70
dlining	N	0.4	0.02	0.00	0.40
Eg	L	25.0	6.25	0.00	25.0
poisson	N	0.3	0.06	0.00	0.3
Elining	N	33500	3350	0.00	33500
creep	N	1.5	0.30	0.00	1.5
f	L	43.2	6.48	0.00	43.2
mb	L	1.00	0.10	0.00	1.00
mN	L	1.00	0.10	0.00	1.00
mM	L	1.00	0.20	0.00	1.00
al	N	0.05	0.0025	0.00	0.05

Input of soil profile deep 2

datad21.dta N = normal distribution ; L = lognormal distribution

20		μ	σ		Xstart
K0water	N	1.0	0.01	0.00	1.00
K0	N	0.70	0.07	0.00	0.70
Swet	N	1.0	0.01	0.00	1.0
Sdry	N	0.8	0.008	0.00	0.8
n	N	0.55	0.017	0.00	0.55
Rgrain	N	2650	26.5	0.00	2650
Rwater	N	1000	10.0	0.00	1000
hgw	N	1.00	0.50	0.00	1.00
Gwater	N	10.0	0.10	0.00	10.0
R	N	4.70	0.05	0.00	4.70
dlining	N	0.40	0.02	0.00	0.40
Eg	L	4.00	1.00	0.00	4.00
poisson	N	0.3	0.06	0.00	0.3
Elining	N	33500	3350	0.00	33500
creep	N	1.5	0.3	0.00	1.5
f	L	43.2	6.48	0.00	43.2
mb	L	1.00	0.10	0.00	1.00
mN	L	1.00	0.10	0.00	1.00
mM	L	1.00	0.20	0.00	1.00
al	N	0.05	0.0025	0.00	0.05

Input of soil profile shallow 1

datas11.dta N = normal distribution ; L = lognormal distribution

19		μ	σ		Xstart
K0water	N	1.0	0.01	0.00	1.00
K0	N	0.46	0.046	0.00	0.46
Swet	N	1.0	0.01	0.00	1.0
n	N	0.36	0.011	0.00	0.36
Rgrain	N	2650	26.5	0.00	2650
Rwater	N	1000	10.0	0.00	1000
hriver	N	9.00	0.50	0.00	9.00
Gwater	N	10.0	0.10	0.00	10.0
R	N	4.70	0.05	0.00	4.70
dlining	N	0.40	0.02	0.00	0.40
Eg	L	25.0	6.25	0.00	25.0
poisson	N	0.3	0.06	0.00	0.3
Elining	N	33500	3350	0.00	33500
creep	N	1.5	0.3	0.00	1.5
f	L	43.2	6.48	0.00	43.2
mb	L	1.00	0.10	0.00	1.00
mN	L	1.00	0.10	0.00	1.00
mM	L	1.00	0.20	0.00	1.00
al	N	0.05	0.0025	0.00	0.05

All rights reserved. Use of disclosure of this data is subject to the restriction stated on the first page of this document.

Input of soil profile shallow 2

datas21.dta N = normal distribution ; L = lognormal distribution

19		μ	σ		Xstart
K0water	N	1.0	0.01	0.00	1.00
K0	N	0.70	0.07	0.00	0.70
Swet	N	1.0	0.01	0.00	1.0
n	N	0.55	0.017	0.00	0.55
Rgrain	N	2650	26.5	0.00	2650
Rwater	N	1000	10.0	0.00	1000
hriver	N	9.00	0.50	0.00	9.00
Gwater	N	10.0	0.10	0.00	10.0
R	N	4.70	0.05	0.00	4.70
dlining	N	0.40	0.02	0.00	0.40
Eg	L	4.00	1.00	0.00	4.00
poisson	N	0.3	0.06	0.00	0.3
Elining	N	33500	3350	0.00	33500
creep	N	1.5	0.3	0.00	1.5
f	L	43.2	6.48	0.00	43.2
mb	L	1.00	0.10	0.00	1.00
mN	L	1.00	0.10	0.00	1.00
mM	L	1.00	0.20	0.00	1.00
al	N	0.05	0.0025	0.00	0.05

All rights reserved. Use of disclosure of this data is subject to the restriction stated on the first page of this document.

11. Output of AFDA

(linear model - geotechnical profile deep 1 - α = 0.05)

zfd1.fun - datad11.dta

Datum: 12/ 5/1998 Tijd: 21/38/8.30

Design point uitvoer
Iteratie 9. Verschil Beta met vorige iteratie 1.3E-0009
Grootte van Z 2.7E-0008

Beta = 2.858
Faalkans = 2.1E-0003
BTF = 2.681E-0008

Naam	Type	A[I]	B[I]	C[I]	Mu[I]	Si[I]	Xstart[I]
K0water	N	1.000E+0000	1.000E-0002	0.000E+0000	1.000E+0000	1.000E-0002	1.000E+0000
K0	N	4.600E-0001	4.600E-0002	0.000E+0000	4.600E-0001	4.600E-0002	4.600E-0001
Swet	N	1.000E+0000	1.000E-0002	0.000E+0000	1.000E+0000	1.000E-0002	1.000E+0000
Sdry	N	4.000E-0001	4.000E-0003	0.000E+0000	4.000E-0001	4.000E-0003	4.000E-0001
n	N	3.600E-0001	1.100E-0002	0.000E+0000	3.600E-0001	1.100E-0002	3.600E-0001
Rgrain	N	2.650E+0003	2.650E+0000	0.000E+0000	2.650E+0003	2.650E+0000	2.650E+0003
Rwater	N	1.000E+0003	1.000E+0001	0.000E+0000	1.000E+0003	1.000E+0001	1.000E+0003
hgw	N	1.000E+0000	5.000E-0001	0.000E+0000	1.000E+0000	5.000E-0001	1.000E+0000
Gwater	N	1.000E+0001	1.000E-0001	0.000E+0000	1.000E+0001	1.000E-0001	1.000E+0001
R	N	4.700E+0000	5.000E-0002	0.000E+0000	4.700E+0000	5.000E-0002	4.700E+0000
dlining	N	4.000E-0001	2.000E-0002	0.000E+0000	4.000E-0001	2.000E-0002	4.000E-0001
Eg	L	2.500E+0001	6.250E+0000	0.000E+0000	2.304E+0001	4.187E+0000	2.500E+0001
poisson	N	3.000E-0001	6.000E-0002	0.000E+0000	3.000E-0001	6.000E-0002	3.000E-0001
Elining	N	3.350E+0004	3.350E+0003	0.000E+0000	3.350E+0004	3.350E+0003	3.350E+0004
creep	N	1.500E+0000	3.000E-0001	0.000E+0000	1.500E+0000	3.000E-0001	1.500E+0000
f	L	4.320E+0001	6.480E+0000	0.000E+0000	4.256E+0001	5.819E+0000	4.320E+0001
mb	L	1.000E+0000	1.000E-0001	0.000E+0000	9.942E-0001	9.530E-0002	1.000E+0000
mN	L	1.000E+0000	1.000E-0001	0.000E+0000	9.939E-0001	9.452E-0002	1.000E+0000
mM	L	1.000E+0000	2.000E-0001	0.000E+0000	9.030E-0001	2.764E-0001	1.000E+0000
al	N	5.000E-0002	2.500E-0003	0.000E+0000	5.000E-0002	2.500E-0003	5.000E-0002

NAAM	X*	dZ/dXi*Si	(dZ/dXi*Si)**2	ALPHA**2	Alpha
K0water	9.99701E-0001	1.23458E+0000	1.52418E+0000	1.09313E-0004	1.04553E-0002
K0	4.20105E-0001	3.58366E+0001	1.28426E+0003	9.21062E-0002	3.03490E-0001
Swet	1.00023E+0000	-9.56805E-0001	9.15477E-0001	6.56573E-0005	-8.10292E-0003
Sdry	4.00002E-0001	-1.96421E-0002	3.85812E-0004	2.76702E-0008	-1.66344E-0004
n	3.58621E-0001	5.17882E+0000	2.68202E+0001	1.92352E-0003	4.38580E-0002
Rgrain	2.65003E+0003	-4.76630E-0001	2.27176E-0001	1.62929E-0005	-4.03644E-0003
Rwater	1.00024E+0003	-9.76438E-0001	9.53432E-0001	6.83794E-0005	-8.26919E-0003
hgw	1.09838E+0000	-8.12999E+0000	6.60967E+0001	4.74041E-0003	-6.88506E-0002
Gwater	9.99018E+0000	4.05819E+0000	1.64689E+0001	1.18114E-0003	3.43677E-0002
R	4.69755E+0000	2.02129E+0000	4.08560E+0000	2.93016E-0004	1.71177E-0002
dlining	4.04544E-0001	-9.38844E+0000	8.81429E+0001	6.32154E-0003	-7.95081E-0002
Eg	1.70060E+0001	5.95750E+0001	3.54919E+0003	2.54545E-0001	5.04524E-0001
poisson	2.58045E-0001	2.88936E+0001	8.34840E+0002	5.98741E-0002	2.44692E-0001
Elining	3.53585E+0004	-2.29240E+0001	5.25510E+0002	3.76892E-0002	-1.94137E-0001
creep	1.29986E+0000	2.75663E+0001	7.59900E+0002	5.44995E-0002	2.33451E-0001
f	3.90083E+0001	2.51915E+0001	6.34612E+0002	4.55139E-0002	2.13340E-0001
mb	9.55383E-0001	1.68462E+0001	2.83794E+0002	2.03535E-0002	1.42666E-0001
mN	9.47538E-0001	2.02613E+0001	4.10522E+0002	2.94423E-0002	1.71588E-0001
mM	1.39583E+0000	-7.36718E+0001	5.42753E+0003	3.89258E-0001	-6.23906E-0001
al	4.96806E-0002	5.27879E+0000	2.78656E+0001	1.99850E-0003	4.47046E-0002

---------- +

1.394325518E+0004

SigmaZ = 1.181E+0002; MuZ = 3.374E+0002

Aantal iteraties = 9 Rekenduur =8850.000083 ms

All rights reserved. Use of disclosure of this data is subject to the restriction stated on the first page of this document.

12. Geometrical non-linearity according to Ahrens

12.1 Graphs

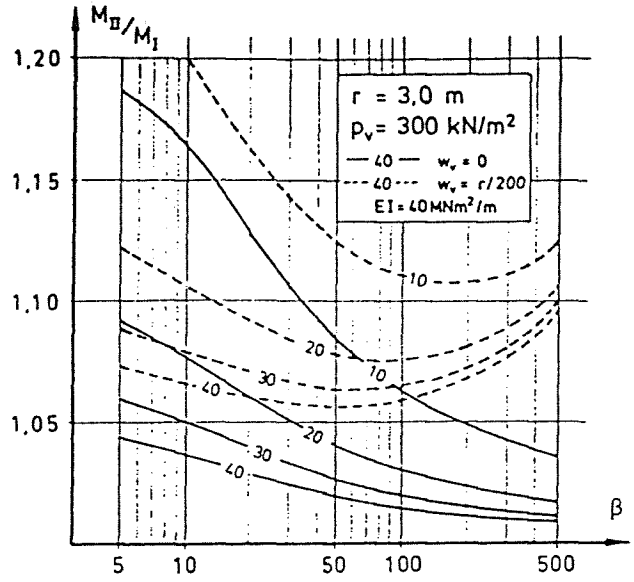

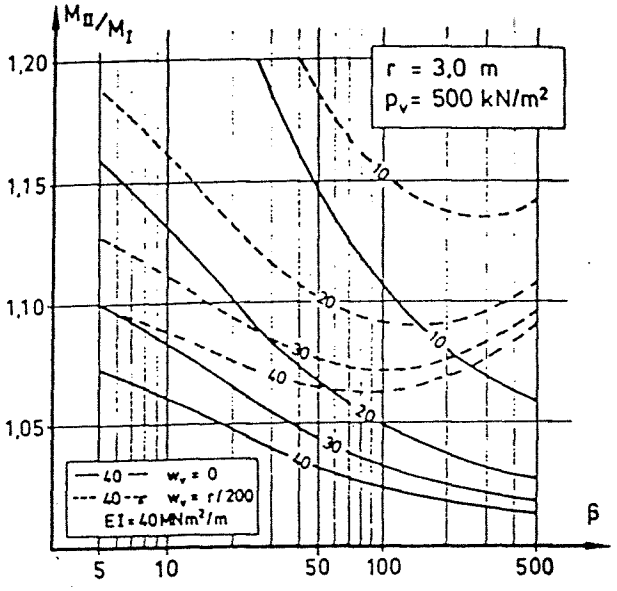

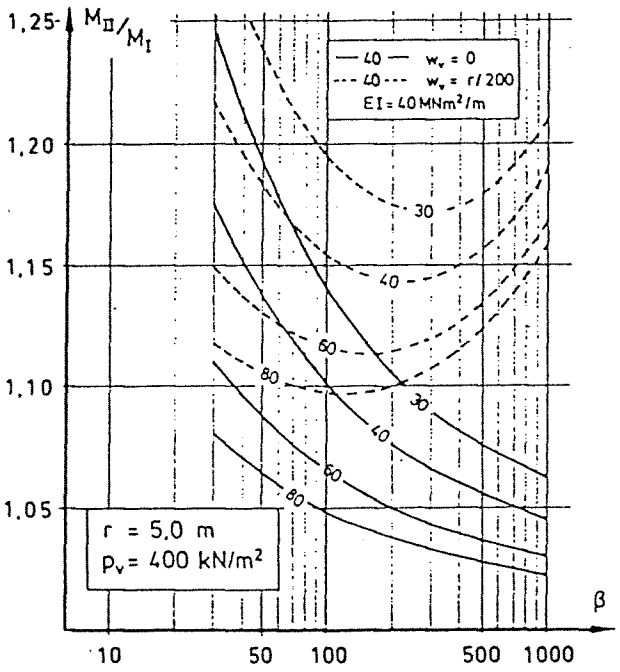

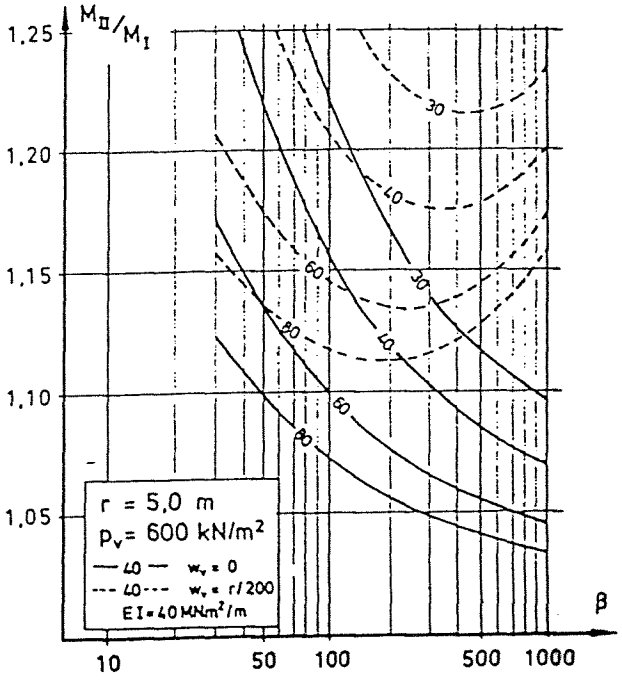

All rights reserved. Use of disclosure of this data is subject to the restriction stated on the first page of this document.

12.2 Calculation of the geometrical non-linearity according to Ahrens

(soil profile deep1; short term)

effective stress σ' and soil stress σ

γ_{wet} [kN/m²]	20.0	h_{gw} [m]	1.0
γ_{dry} [kN/m²]	18.0	λ_n [-]	0.46
h_{tunnel} [m]	22.5	γ_{water} [kN/m²]	10
$h_{top\ tunnel}$ [m]	17.80		
$\sigma'_{top\ tunnel}$ [kN/m²]	196	Ko (effective stresses)	0.46
$\sigma_{top\ tunnel}$ [kN/m²]	374	Ko (earth stresses)	0.717

β [-]

d_{lining} [m]	0.4	**necessary input-values for design graphs**	
I [m⁴]	0.0053	(no measure deviations)	
f'_{ck} [N/mm²]	45	σ' = p_v	196
E_{lining} [N/mm²]	33500	r [m]	4.70
Eg [MPa]	25	EI [MNm²]	178.67
ν [-]	0.3	EI_{00} [MNm²]	**89.33**
Es [MPa]	33.65		
r [m]	4.70		n = M_{II}/M_I
β [-]	**19.56**	reading from graph	1.09
		after inter/extrapolation	1.044
EI'=EI+No(1+W)r²/3	167.65	factor	1.036
Wo=r/200	0.00	eventual n = n*factor	**1.08**
W=Wo/W1	0.00		
No [MN/m]	-1.50		
EI'_{00}	78.90 = 80		
creep coefficient	1.5		

factor in behalf of the inclusion of the waterpressures

cross-section forces according to Duddeck (at top of the tunnel)

$N_{without\ water}$ [kN] = N1	456.8
$N_{with\ water}$ [kN] = N2	1285.9
$M_{with\ water}$= $M_{without\ water}$ [kNm]	218.7
displacements u1 [m]	0.009
displacements u2 [m]	0.009

FACTOR =(M+n2/(n2-1)*N2*u) / (M+n1/(n1-1)*N1*u)

Nbuc [kN]	24264
n1	53.12
n2	18.870
n1/(n1-1)	1.019
n2/(n2-1)	1.06
(M+n2/(n2-1)*N2*u2)	230.92
(M+n1/(n1-1)*N1*u1)	222.89
Factor	1.04

All rights reserved. Use of disclosure of this data is subject to the restriction stated on the first page of this document.

13. Definition of the buckling force

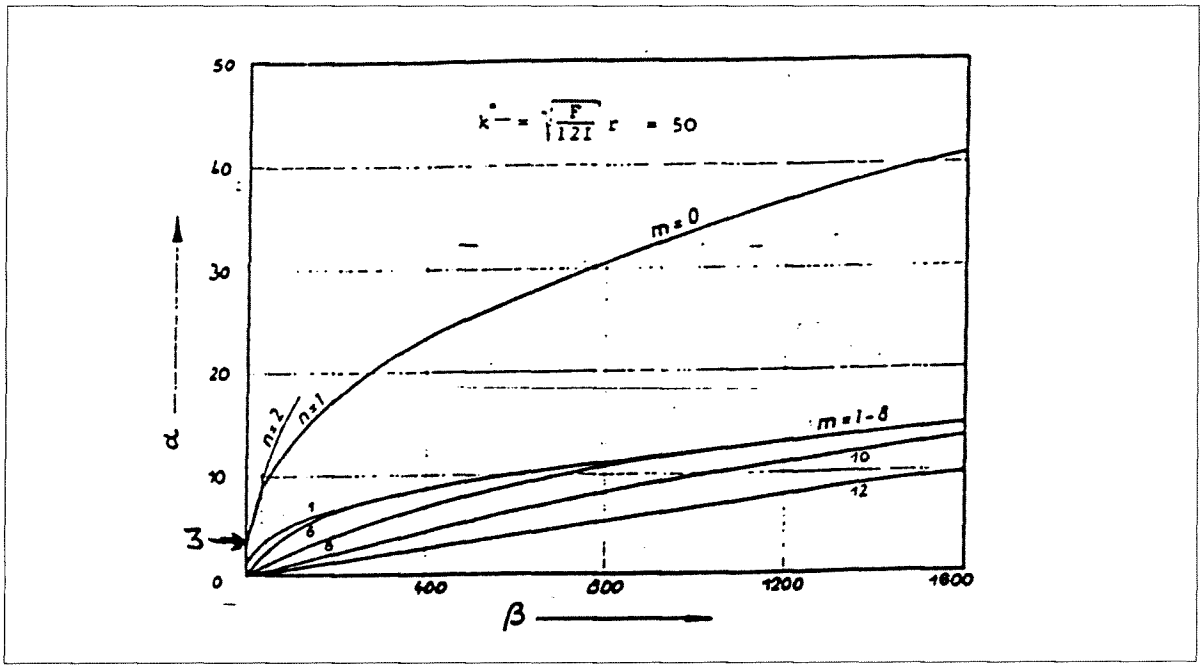

figure: critical load as function of the bending stiffness [lit, 51]

with:

$$\alpha = \frac{p \cdot R^3}{EI}$$

$$\beta = \frac{k_r \cdot R^4}{EI}$$

p	= critical radial pressure	[N/mm^2];
R	= radius	[m] ;
m	= amount of hinges	[-];
k_r	= bedding modulus	[N/mm^2];
EI	= bending stiffness	[Nmm^2].

remarks:

- the presence of hinges (m), like in the segmented tunnel, reduces the buckling load;
- buckling pressure:
  with m = 0 and β = 0 (i.e. no bedding, so this is an approach of the real situation):

  $$\alpha = 3 = \frac{p \cdot R^3}{EI} \Rightarrow p = \frac{3 \cdot EI}{R^3}$$

- buckling force: $N_{buc} = \frac{3 \cdot EI}{R^2}$ [lit,47]

All rights reserved. Use of disclosure of this data is subject to the restriction stated on the first page of this document.

14. Geometrical non-linear computation of the ITM-tunnel

Failure criterion: buckling

Parameter study with respect to d_{lining} (E_{lining} = 33500 N/mm^2 = constant)

Computation geometrical non-linearity **deep1**

D [m]	9				
d_{lining} [m]	0.4	h_{gw} [m]	1.0	Nbuc [kN]	24264
I [m^4]	0.0053	λ_n [-]	0.46		
f'_{ck} [N/mm^2]	45	γ_{water} [kN/m^2]	10	σ_v [kN/m^2]	448
E_{lining} [N/mm^2]	33500			σ'_v [kN/m^2]	233
Eg [MPa]	25			Ko [-]	0.719
ν [-]	0.3				
Es [MPa]	33.65			n = Nbuc / N_{max}	
r [m]	4.70			$M_{II} = M_I + n / (n-1) * u * N_{min}$	
γ_{wet} [kN/m^2]	20.0				
γ_{dry} [kN/m^2]	18.0				
h_{tunnel} [m]	22.5				

parameterstudy with respect to dlining

d lining [m]	r [m]	α [m^{-1}]	N_{min} [kN]	N_{max} [kN]	M_I [kNm]	u [m]	Nbuc [kN]	n [-]	n/(n-1) [-]	M_{II} [kNm]	M_{II} / M_I	% EI_0
0.50	4.75	10.34	1552.26	2079.40	376.76	0.0081	46399	22.314	1.047	389.93	1.03	195.31
0.45	4.73	13.96	1548.31	2061.48	320.20	0.0093	34184	16.582	1.064	335.60	1.05	142.38
0.40	4.70	19.56	1544.47	2042.77	260.04	0.0107	24264	11.878	1.092	278.07	1.07	100.00
0.35	4.68	28.73	1540.34	2023.43	198.90	0.0121	16430	8.120	1.140	220.11	1.11	66.99
0.30	4.65	44.89	1535.28	2003.63	140.57	0.0134	10458	5.219	1.237	166.02	1.18	42.19
0.25	4.63	76.33	1528.40	1983.43	89.40	0.0146	6118	3.084	1.480	122.34	1.37	24.41
0.20	4.60	146.67	1518.46	1962.44	49.15	0.0155	3166	1.613	2.630	110.93	2.26	12.50
0.19	4.60	170.52	1515.95	1958.04	42.63	0.0156	2721	1.389	3.568	127.06	2.98	10.72
0.18	4.59	199.89	1513.21	1953.53	36.63	0.0157	2318	1.187	6.355	188.02	5.13	9.11
0.17	4.59	236.51	1510.23	1948.88	31.16	0.0159	1957	**1.004**	233.083	5614.41	**180.18**	7.68
0.16	4.58	282.75	1506.95	1944.06	26.21	0.0160	1635	0.841	-5.298	-101.26	-3.86	6.40

conclusion:
buckling: d_{lining} = 0.17m , as n = 1

Parameter study with respect to E_{lining} (d_{lining} = 0.40 m = constant)

factor * E	%(EI_0)	EI [kNm^2]	E [N/mm^2]	α [m^{-1}]	N_{min} [kN]	N_{max} [kN]	M_I [kNm]	u [m]	Nbuc [kN]	n [-]	n/(n-1) [-]	M_{II} [kNm]	M_{II} / M_I
* E	100	178666.7	33500	19.6	1544.47	2042.77	260.04	0.0107	24264	11.878	1.092	278.07	1.07
0.9	90	160800.0	30150	21.7	1544.49	2039.17	243.13	0.0111	21838	10.709	1.103	262.05	1.08
0.8	80	142933.3	26800	24.4	1544.20	2034.98	224.86	0.0116	19411	9.539	1.117	244.79	1.09
0.7	70	125066.7	23450	27.9	1543.46	2029.99	205.05	0.0120	16985	8.367	1.136	226.15	1.10
0.6	60	107200.0	20100	32.6	1541.95	2023.87	183.49	0.0126	14559	7.193	1.161	206.00	1.12
0.5	50	89333.3	16750	39.1	1539.17	2016.05	159.95	0.0131	12132	6.018	1.199	184.21	1.15
0.4	40	71466.7	13400	48.9	1534.03	2005.39	134.14	0.0138	9706	4.840	1.260	160.77	1.20
0.3	30	53600.0	10050	65.2	1524.06	1989.34	105.70	0.0145	7279	3.659	1.376	136.06	1.29
0.2	20	35733.3	6700	97.8	1501.98	1960.51	74.23	0.0152	4853	2.475	1.678	112.65	1.52
0.1	10	17866.7	3350	195.6	1433.60	1884.65	39.21	0.0161	2426	1.287	4.479	142.58	3.64

conclusion: no buckling

All rights reserved. Use of disclosure of this data is subject to the restriction stated on the first page of this document.

Parameter study with respect to EI

parameterstudy with respect to EI (dlining= 0,4 m) r = 4.7

factor	%(EI)$_0$	EI [kNm^2]	E [N/mm^2]	α [m^{-1}]	N_{min} [kN]	N_{max} [kN]	M_I [kNm]	u [m]	Nbuc [kN]	n [-]	n/(n-1) [-]	M_{II} [kNm]	M_{II} / M_I
* E	100	178666.7	33500	19.6	1544.47	2042.77	260.04	0.0107	24264	11.878	1.092	278.07	1.07
0.9	90	160800.0	30150	21.7	1544.49	2039.17	243.13	0.0111	21838	10.709	1.103	262.05	1.08
0.8	80	142933.3	26800	24.4	1544.20	2034.98	224.86	0.0116	19411	9.539	1.117	244.79	1.09
0.7	70	125066.7	23450	27.9	1543.46	2029.99	205.05	0.0120	16985	8.367	1.136	226.15	1.10
0.6	60	107200.0	20100	32.6	1541.95	2023.87	183.49	0.0126	14559	7.193	1.161	206.00	1.12
0.5	50	89333.3	16750	39.1	1539.17	2016.05	159.95	0.0131	12132	6.018	1.199	184.21	1.15
0.4	40	71466.7	13400	48.9	1534.03	2005.39	134.14	0.0138	9706	4.840	1.260	160.77	1.20
0.3	30	53600.0	10050	65.2	1524.06	1989.34	105.70	0.0145	7279	3.659	1.376	136.06	1.29
0.2	20	35733.3	6700	97.8	1501.98	1960.51	74.23	0.0152	4853	2.475	1.678	112.65	1.52
0.1	10	17866.7	3350	195.6	1433.60	1884.65	39.21	0.0161	2426	1.287	4.479	142.58	3.64

parameterstudy with respect to EI (dlining= 0,35 m)

r = 2.525 d_{lining} = 0.35

factor	%(EI)$_0$	EI [kNm^2]	E [N/mm^2]	α [m^{-1}]	N_{min} [kN]	N_{max} [kN]	M_I [kNm]	u [m]	Nbuc [kN]	n [-]	n/(n-1) [-]	M_{II} [kNm]	M_{II} / M_I
* E	67	119692.7	33500	28.7	1540.34	2023.43	198.90	0.0121	16430	8.120	1.140	220.11	1.11
0.9	60	107723.4	30150.0	31.9	1539.88	2019.84	184.35	0.0124	14787	7.321	1.158	206.52	1.12
0.8	54	95754.2	26800.0	35.9	1539.02	2015.66	168.90	0.0128	13144	6.521	1.181	192.19	1.14
0.7	47	83784.9	23450.0	41.0	1537.56	2010.66	152.47	0.0132	11501	5.720	1.212	177.09	1.16
0.6	40	71815.6	20100.0	47.9	1535.15	2004.49	134.96	0.0136	9858	4.918	1.255	161.26	1.19
0.5	33	59846.4	16750.0	57.5	1531.19	1996.50	116.27	0.0141	8215	4.115	1.321	144.81	1.25
0.4	27	47877.1	13400.0	71.8	1524.46	1985.47	96.27	0.0146	6572	3.310	1.433	128.17	1.33
0.3	20	35907.8	10050.0	95.8	1512.16	1968.55	74.83	0.0151	4929	2.504	1.665	112.92	1.51
0.2	13	23938.5	6700.0	143.6	1486.14	1937.58	51.76	0.0157	3286	1.696	2.437	108.61	2.10
0.1	7	11969.3	3350.0	287.3	1408.66	1854.75	26.89	0.0163	1643	0.886	-7.757	-151.31	-5.63 **buckling**

parameterstudy with respect to EI (dlining= 0,3 m)

r = 4.65 d_{lining} = 0.3

factor	%(EI)$_0$	EI [kNm^2]	E [N/mm^2]	α [m^{-1}]	N_{min} [kN]	N_{max} [kN]	M_I [kNm]	u [m]	Nbuc [kN]	n [-]	n/(n-1) [-]	M_{II} [kNm]	M_{II} / M_I
* E	42	75375.0	33500	44.9	1535.28	2003.63	140.57	0.0134	10458	5.219	1.237	166.02	1.18
0.9	38	67837.5	30150.0	49.9	1534.18	2000.07	129.19	0.0137	9412	4.706	1.270	155.84	1.21
0.8	34	60300.0	26800.0	56.1	1532.57	1995.89	117.31	0.0140	8366	4.192	1.313	145.44	1.24
0.7	30	52762.5	23450.0	64.1	1530.20	1990.83	104.91	0.0143	7320	3.677	1.374	134.93	1.29
0.6	25	45225.0	20100.0	74.8	1526.67	1984.50	91.95	0.0146	6275	3.162	1.463	124.56	1.35
0.5	21	37687.5	16750.0	89.8	1521.29	1976.18	78.39	0.0149	5229	2.646	1.608	114.92	1.47
0.4	17	30150.0	13400.0	112.2	1512.64	1964.47	64.19	0.0153	4183	2.129	1.885	107.80	1.68
0.3	13	22612.5	10050.0	149.6	1497.55	1946.16	49.31	0.0157	3137	1.612	2.634	111.07	2.25
0.2	8	15075.0	6700.0	224.5	1466.78	1912.01	33.68	0.0160	2092	1.094	11.648	307.82	9.14
0.1	4	7537.5	3350.0	448.9	1378.12	1819.80	17.27	0.0165	1046	0.575	-1.351	-13.36	-0.77 **buckling**

parameterstudy with respect to EI (dlining= 0,25 m)

r = 4.625 d_{lining} = 0.25

factor	%(EI)$_0$	EI [MNm^2]	E [N/mm^2]	α [m^{-1}]	N_{min} [kN]	N_{max} [kN]	M_I [kNm]	u [m]	Nbuc [kN]	n [-]	n/(n-1) [-]	M_{II} [kNm]	M_{II} / M_I
* E	24	43619.8	33500.0	76.3	1528.40	1983.43	89.40	0.0146	6118	3.084	1.480	122.34	1.37
0.9	22	39257.8	30150.0	84.8	1526.50	1979.83	81.54	0.0148	5506	2.781	1.561	116.73	1.43
0.8	20	34895.8	26800.0	95.4	1523.96	1975.53	73.47	0.0150	4894	2.477	1.677	111.71	1.52
0.7	17	30533.9	23450.0	109.0	1520.48	1970.24	65.18	0.0152	4282	2.174	1.852	107.89	1.66
0.6	15	26171.9	20100.0	127.2	1515.60	1963.51	56.65	0.0154	3671	1.869	2.150	106.77	1.88
0.5	12	21809.9	16750.0	152.7	1508.48	1954.49	47.88	0.0156	3059	1.565	2.770	113.05	2.36
0.4	10	17447.9	13400.0	190.8	1497.50	1941.54	38.86	0.0158	2447	1.260	4.841	153.55	3.95
0.3	7	13085.9	10050.0	254.4	1478.94	1920.96	29.57	0.0161	1835	0.955	-21.420	-478.97	-16.20 **buckling**

All rights reserved. Use of disclosure of this data is subject to the restriction stated on the first page of this document.

parameterstudy with respect to EI (dlining= 0,20 m)

					r = 4.6		d_{lining} = 0.2							
factor	$\%(EI)_0$	EI [MNm^2]	E [N/mm^2]	α [m^{-1}]	N_{min} [kN]	N_{max} [kN]	M_I [kNm]	u [m]	Nbuc [kN]	n [-]	n/(n-1) [-]	M_{II} [kNm]	M_{II} / M_I	
* E	13	22333.3	33500.0	146.67	1518.46	1962.44	49.15	0.0155	3166	1.613	2.630	110.93	2.26	
0.9	11	20100.0	30150.0	162.97	1515.59	1958.56	44.57	0.0156	2850	1.455	3.198	120.09	2.69	
0.8	10	17866.7	26800.0	183.34	1511.90	1953.86	39.91	0.0157	2533	1.296	4.373	143.71	3.60	
0.7	9	15633.3	23450.0	209.54	1507.04	1947.97	35.19	0.0158	2216	1.138	8.256	231.98	6.59	
0.6	8	13400.0	20100.0	244.46	1500.46	1940.34	30.39	0.0159	1900	0.979	-46.876	-1090.57	-35.89	**buckling**

parameterstudy with respect to EI (dlining= 0,15 m)

					r = 4.575		d_{lining} = 0.15						
factor	$\%(EI)_0$	EI [MNm^2]	E [N/mm^2]	α [m^{-1}]	N_{min} [kN]	N_{max} [kN]	M_I [kNm]	u [m]	Nbuc [kN]	n [-]	n/(n-1) [-]	M_{II} [kNm]	M_{II} / M_I
* E	5	9421.9	33500.0	342.04	1503.35	1939.01	21.77	0.0161	1350	0.696	-2.294	-33.63	-1.54 **buckling**
0.9	5	8479.7	30150.0	380.04	1499.18	1934.38	19.66	0.0161	1215	0.628	-1.690	-21.18	-1.08

parameterstudy with respect to EI (dlining= 0,10 m)

					r = 4.55		d_{lining} = 0.1						
factor	$\%(EI)_0$	EI [MNm^2]	E [N/mm^2]	α [m^{-1}]	N_{min} [kN]	N_{max} [kN]	M_I [kNm]	u [m]	Nbuc [kN]	n [-]	n/(n-1) [-]	M_{II} [kNm]	M_{II} / M_I
* E	2	2791.7	33500.0	1135.5	1477.59	1907.58	6.64	0.0163	405	0.212	-0.269	0.14	0.02 **buckling**
0.9	1	2512.5	30150.0	1261.7	1471.29	1901.14	5.98	0.0164	364	0.192	-0.237	0.28	0.05

All rights reserved. Use of disclosure of this data is subject to the restriction stated on the first page of this document.

Failure of the compression mode

Failure criterion: failure curve based on a combination of N&M (see appendix 8)

Parameter study with respect to d_{lining} (E_{lining} = 33500 N/mm^2 = constant)

chart input (α = **0.00**)				**gnl point**	
				N_{min} [kN]	M_{II} [kNm]
f'ck	45			-1544.47	278.07
d lining =	0.4				
		failure boundary			
n	m	N_{min} [kN]	M [kNm]	M_{II} [kNm]	M_I [kNm]
0.000	0.000	0	0.0		
		-1544.47	261.9	278.07	260.04 **collapse**
-0.125	0.053	-2250	381.6		
-0.242	0.090	-4356	648.0		
-0.333	0.108	-5994	777.6		
-0.400	0.117	-7200	842.4		
-0.470	0.121	-8460	871.2		
-0.517	0.122	-9306	878.4		
-0.629	0.108	-11322	777.6		
-0.813	0.068	-14634	489.6		
-0.888	0.039	-15984	280.8		
-1.000	0.000	-18000	0.0		
d = 0,40m : collapse due to M_{II}					
d > 0,45 : collapse due to M_I , not due to the geometrical effect					

chart input (α = **0.0**)				**gnl point**	
				N_{min} [kN]	M_{II} [kNm]
f'ck	45			-1515.95	127.06
d lining =	0.19				
		failure boundary			
n	m	N_{min} [kN]	M_{II} [kNm]	M_{II} [kNm]	M_I [kNm]
0.000	0.000	0	0.0		
-0.125	0.053	-1068.75	86.1		
		-1515.95	112.97	127.06	42.63
-0.242	0.090	-2069.1	146.2		
-0.333	0.108	-2847.15	175.4		
-0.400	0.117	-3420	190.1		
-0.470	0.121	-4018.5	196.6		
-0.517	0.122	-4420.35	198.2		
-0.629	0.108	-5377.95	175.4		
-0.813	0.068	-6951.15	110.5		
-0.888	0.039	-7592.4	63.4		
-1.000	0.000	-8550	0.0		

All rights reserved. Use of disclosure of this data is subject to the restriction stated on the first page of this document.

chart input (α = **0.05**)				**gnl point**	
				N_{min} [kN]	M_{II} [kNm]
f'ck	45			-1513.21	188.02
d lining =	0.18				
		failure boundary			
n	m	N_{min} [kN]	M_{II} [kNm]	M_{II} [kNm]	M_I [kNm]
0.000	0.023	0	33.5		
-0.092	0.058	-745.2	84.6		
		-1513.21	129.46	188.02	36.63 **collapse**
-0.209	0.096	-1692.9	140.0		
-0.300	0.115	-2430	167.7		
-0.375	0.125	-3037.5	182.3		
-0.450	0.128	-3645	186.6		
-0.492	0.127	-3985.2	185.2		
-0.617	0.115	-4997.7	167.7		
-0.813	0.068	-6585.3	99.1		
-0.888	0.039	-7192.8	56.9		
-1.000	0.000	-8100	0.0		

The failure curve and geometric non linear point given in the table above are shown in the following graph.

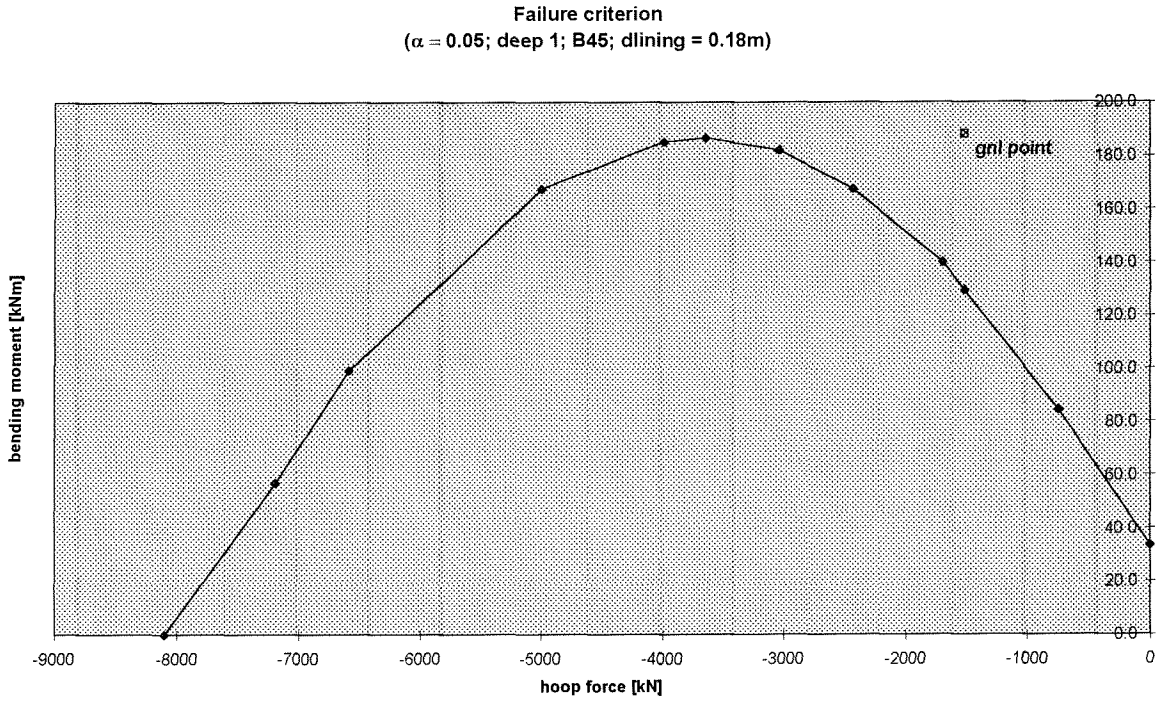

All rights reserved. Use of disclosure of this data is subject to the restriction stated on the first page of this document.

Parameter study with respect to E_{lining} (d_{lining} = 0.40m = constant)

chart input (α = **0.00**)		**gnl point**		
			N_{min} [kN]	M_{II} [kNm]
f'ck	45	100% EI	-1544.47	278.07
d lining =	0.4	90% EI	-1544.49	262.05

		failure boundary			
n	m	N_{min} [kN]	M [kNm]	M_{II} [kNm]	M_I [kNm]
0.000	0.000	0	0.0		
		-1544.47	261.9	278.07	260.04 **collapse**
		-1544.49	261.9	262.05	243.13 **collapse**
-0.125	0.053	-2250	381.6		
-0.242	0.090	-4356	648.0		
-0.333	0.108	-5994	777.6		
-0.400	0.117	-7200	842.4		
-0.470	0.121	-8460	871.2		
-0.517	0.122	-9306	878.4		
-0.629	0.108	-11322	777.6		
-0.813	0.068	-14634	489.6		
-0.888	0.039	-15984	280.8		
-1.000	0.000	-18000	0.0		

α = **0,05** : no failure

All rights reserved. Use of disclosure of this data is subject to the restriction stated on the first page of this document.

Parameter study with respect to EI (E_{lining} and d_{lining} are varied)

chart input (α = 0.0)				**gnl point**		
				N_{min} [kN]	M_{II} [kNm]	M_I [kNm]
f'ck	45			-1515.59	120.09	44.57
d lining =	**0.2**			-1511.90	143.71	39.91
		failure boundary				
n	m	N_{min} [kN]	M_{II} [kNm]	M_{II} [kNm]		
0.000	0.000	0	0.0			
-0.125	0.053	-1125	95.4			
		-1515.59	120.1	120.09 **90% EI_0**		
		-1511.90	119.9	143.71 **80% EI_0**		**collapse**
-0.242	0.090	-2178	162.0			
-0.333	0.108	-2997	194.4			
-0.400	0.117	-3600	210.6			
-0.470	0.121	-4230	217.8			
-0.517	0.122	-4653	219.6			
-0.629	0.108	-5661	194.4			
-0.813	0.068	-7317	122.4			
-0.888	0.039	-7992	70.2			
-1.000	0.000	-9000	0.0			

chart input (α = **0.05**)				**gnl point**		
70% EI				N_{min} [kN]	M_{II} [kNm]	M_I [kNm]
f'ck	45			-1507.04	231.98	35.19
d lining =	**0.2**					
		failure boundary				
n	m	N_{min} [kN]	M_{II} [kNm]	M_{II} [kNm]	M_I [kNm]	
0.000	0.023	0	41.4			
-0.092	0.058	-828	104.4			
		-1507.04	148.51	231.98	35.19	**collapse**
-0.209	0.096	-1881	172.8			
-0.300	0.115	-2700	207.0			
-0.375	0.125	-3375	225.0			
-0.450	0.128	-4050	230.4			
-0.492	0.127	-4428	228.6			
-0.617	0.115	-5553	207.0			
-0.813	0.068	-7317	122.4			
-0.888	0.039	-7992	70.2			
-1.000	0.000	-9000	0.0			

All rights reserved. Use of disclosure of this data is subject to the restriction stated on the first page of this document.

15. NMK-diagram

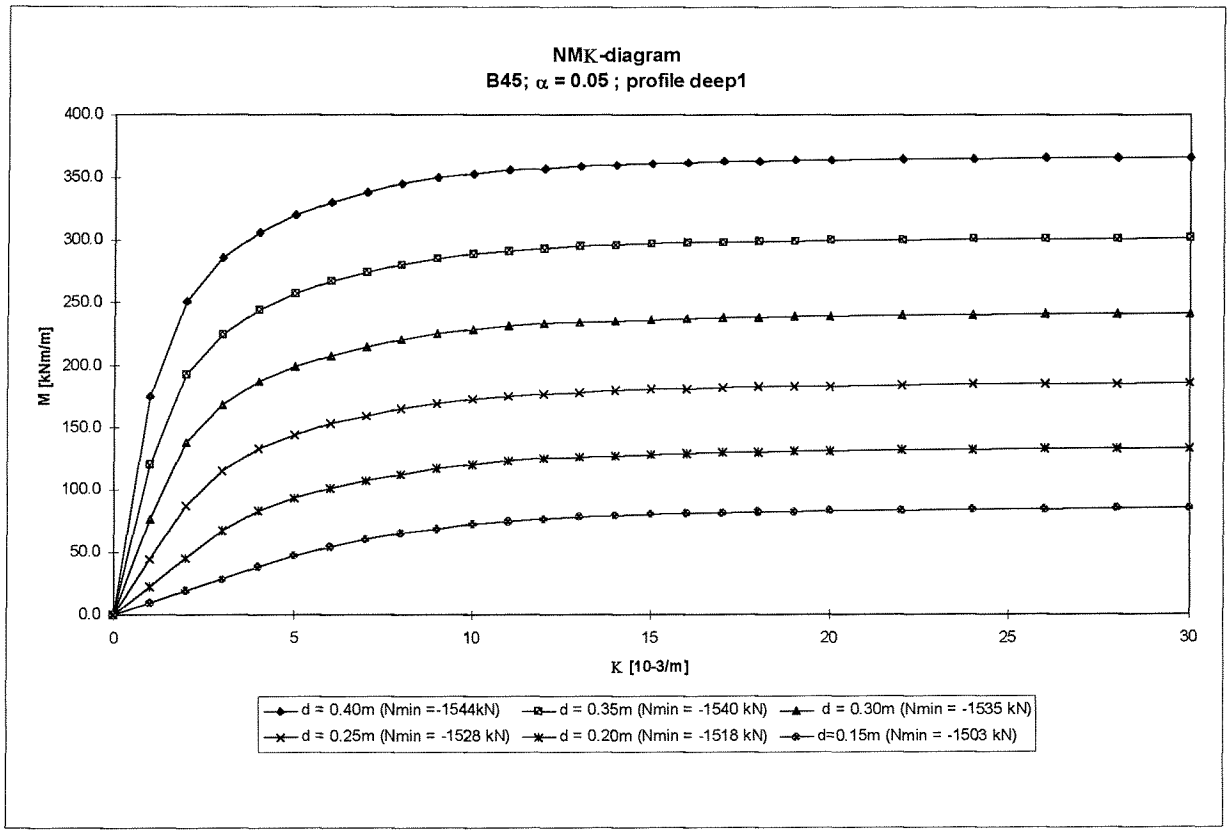

figure: NMK-diagrams as function of different d_{lining}

All rights reserved. Use of disclosure of this data is subject to the restriction stated on the first page of this document.

16. Safety factors

(partial) safety factors of the geotechnical profile deep1

safety factors	zfunction zfd1 - data deep 1 (zfd1.fun - datad11.dta)						
β	2.9	μ	σ	X*	Xkar	γ_R	γ_S
K_{0water}	resistance	1	0.01	1.00	0.9836	0.983894	
K_0	resistance	0.46	0.046	0.42	0.46	1.094964	
S_{wet}	load	1	0.01	1.00	1.0164		0.984091
S_{dry}	load	0.4	0.004	0.40	0.40656		0.98387
n	resistance	0.36	0.011	0.36	0.34196	0.953541	
γ_{wet}	load			20.19352	20.852849		0.968382
γ_{dry}	load			18.08137	18.773512		0.963132
ρ_k	load	2650	26.5	2650.03	2693.46		0.983876
ρ_{water}	load	1000	10	1000.24	1016.4		0.984101
h_{gw}	load	1	0.5	1.10	1		1.09838
γ_{water}	resistance	10	0.1	9.99	9.836	0.984567	
R	resistance	4.7	0.05	4.70	4.618	0.983066	
d_{lining}	resistance	0.4	0.02	0.40	0.4	0.988768	
E_g	resistance	25	6.25	17.01	25	1.470069	
υ	resistance	0.3	0.06	0.26	0.3	1.162588	
E_{lining}	load	33500	3350	35358.50	33500		1.055478
ϕ_{creep}	resistance	1.5	0.3	1.30	1.5	1.15397	
f	resistance	43.2	6.48	39.01	43.2	1.107457	
m_b	resistance	1	0.1	0.96	1	1.046701	
m_N	resistance	1	0.1	0.95	1	1.055367	
m_M	load	1	0.2	1.40	1.328		1.051077
α	resistance	0.05	0.0025	0.05	0.05	1.006429	

		Safety criterion:			
M_{max}* [kNm]	372.0007	Z = R* - S* > 0			
N_{min}* [kN]	1429.699	Z =	-0.00117		
γ_R	**1.095094**	S_k	223.6365	R_k	407.3745
γ_S	**1.663416**	S*	372.0007	R*	371.9995
γ	**1.821597**				

All rights reserved. Use of disclosure of this data is subject to the restriction stated on the first page of this document.

(partial) safety factors of the geotechnical profile deep2

safety factors		zfunction zfd1 - data deep 2 (zfd1.fun - datad21.dta)					
β	2.5	μ	σ	X*	Xkar	γ_R	γ_S
K_{0water}	resistance	1	0.01	1.00	0.9836	0.98388	
K_0	resistance	0.7	0.07	0.59	0.5852	0.988584	
S_{wet}	load	1	0.01	1.00	1.0164		0.984298
S_{dry}	load	0.8	0.008	0.80	0.81312		0.983883
n	resistance	0.55	0.017	0.55	0.52212	0.956416	
γ_{wet}	load			17.16503	17.73496		0.967864
γ_{dry}	load			16.09118	16.67668		0.964891
ρ_k	load	2650	2.65	2650.03	2654.346		0.998374
ρ_{water}	load	1000	10	1000.46	1016.4		0.984317
h_{gw}	load	1	0.5	1.12	1		1.12066
γ_{water}	resistance	10	0.1	9.99	9.836	0.984705	
R	resistance	4.7	0.05	4.70	4.618	0.982081	
d_{lining}	resistance	0.4	0.02	0.40	0.4	1.010869	
E_g	resistance	4	1	3.34	4	1.198175	
υ	resistance	0.3	0.06	0.28	0.3	1.07545	
E_{lining}	load	33500	3350	34311.90	33500		1.024236
ϕ_{creep}	resistance	1.5	0.3	1.42	1.5	1.057217	
f	resistance	43.2	6.48	39.38	43.2	1.097009	
m_b	resistance	1	0.1	0.96	1	1.042274	
m_N	resistance	1	0.1	0.95	1	1.049991	
m_M	load	1	0.2	1.35	1		1.34535
α	resistance	0.05	0.0025	0.05	0.05	1.005749	

M_{max}* [kNm]	361.0739	Safety criterion			
N_{min}* [kN]	1419.0352	Z = R* - S* > 0			
		Z =	-0.00101		
γ_R	**1.1056691**	S_k	267.956	R_k	399.2271
γ_S	**1.3475119**	S*	361.0739	R*	361.0729
γ	**1.4899022**				

All rights reserved. Use of disclosure of this data is subject to the restriction stated on the first page of this document.

(partial) safety factors of the geotechnical profile shallow1

safety factors		zfunction zfs1 - data shallow 1 (zfs1.fun - datas11.dta)					
β	**4.4**	μ	σ	X*	Xkar	γ_R	γ_S
K_{0water}	resistance	1	0.01	1.00	0.9836	0.984166	
K_0	resistance	0.46	0.046	0.40	0.38456	0.959292	
S_{wet}	load	1	0.01	1.00	1.0164		0.984301
n	resistance	0.36	0.011	0.36	0.34196	0.956461	
γ_{wet}	load			20.21291	20.60035		0.981193
ρ_k	load	2650	2.65	2650.06	2654.346		0.998385
ρ_{water}	load	1000	10	1000.45	1016.4		0.984307
h_{river}	resistance	9	0.5	8.93	9	1.007763	
γ_{water}	resistance	10	0.1	9.98	9.836	0.985466	
R	resistance	4.7	0.05	4.70	4.618	0.983068	
d_{lining}	resistance	0.4	0.02	0.40	0.4	0.988685	
E_g	resistance	25	6.25	14.35	14.75	1.027946	
υ	resistance	0.3	0.06	0.24	0.3	1.227647	
E_{lining}	load	33500	3350	36185.20	33500		1.080155
ϕ_{creep}	resistance	1.5	0.3	1.19	1.5	1.259065	
f	resistance	43.2	6.48	36.74	43.2	1.175888	
m_b	resistance	1	0.1	0.93	1	1.075145	
m_N	resistance	1	0.1	0.92	1	1.087401	
m_M	load	1	0.2	1.75	1.328		1.314375
α	resistance	0.05	0.0025	0.05	0.05	1.011135	

M_{max}* [kNm]	327.6316	Safety criterion:			
N_{min}* [kN]	1221.25	Z = R* - S* > 0			
		Z =	0.193341		
γ_R	**0.99941**	S_k	211.8835	R_k	327.6316
γ_S	**1.751092**	S*	371.0276	R*	327.825
γ	**1.75006**				

All rights reserved. Use of disclosure of this data is subject to the restriction stated on the first page of this document.

(partial) safety factors of the geotechnical profile shallow2

safety factors		zfunction zfs1 - data shallow 2 (zfs1.fun - datas21.dta)					
β	**4.2**	μ	σ	X*	Xkar	γ_R	γ_S
K_{0water}	resistance	1	0.01	1.00	0.9836	0.984191	
K_0	resistance	0.7	0.07	0.54	0.5852	1.091504	
S_{wet}	load	1	0.01	1.00	1.0164		0.984789
n	resistance	0.55	0.017	0.54	0.52212	0.963728	
γ_{wet}	load			17.23739	17.73496		0.971944
ρ_k	load	2650	2.65	2650.06	2654.346		0.998385
ρ_{water}	load	1000	10	1000.94	1016.4		0.984789
h_{river}	resistance	9	0.5	8.93	9	1.007755	
γ_{water}	resistance	10	0.1	9.98	9.836	0.985951	
R	resistance	4.7	0.05	4.70	4.618	0.981588	
d_{lining}	resistance	0.4	0.02	0.39	0.4	1.022738	
E_g	resistance	4	1	3.04	4	1.317284	
υ	resistance	0.3	0.06	0.27	0.3	1.117389	
E_{lining}	load	33500	3350	34804.50	33500		1.03894
ϕ_{creep}	resistance	1.5	0.3	1.37	1.5	1.098845	
f	resistance	43.2	6.48	36.91	43.2	1.170468	
m_b	resistance	1	0.1	0.93	1	1.072926	
m_N	resistance	1	0.1	0.92	1	1.085206	
m_M	load	1	0.2	1.72	1.328		1.293373
α	resistance	0.05	0.0025	0.05	0.05	1.01073	

M_{max}* [kNm]	310.2985	Safety criterion:	
N_{min}* [kN]	1201.8	Z = R* - S* > 0	
		Z =	0.00677

γ_R	**0.999978**	S_k	203.4587	R_k	310.2985
γ_S	**1.83524**	S*	373.3956	R*	310.3053
γ	**1.8352**				

All rights reserved. Use of disclosure of this data is subject to the restriction stated on the first page of this document.